

**THE ROLE OF FLOW-SENSITIVE MIRNAS AND UBE2C-
DEPENDENT HIF1A PATHWAY IN CALCIFIC AORTIC VALVE
DISEASE**

A Dissertation

Presented to

The Academic Faculty

by

Joan Fernández Esmerats

In Partial Fulfillment

of the Requirements for the Degree

Doctor of Philosophy in the

Wallace H. Coulter Department of Biomedical Engineering

Georgia Institute of Technology and Emory University

December 2018

COPYRIGHT © 2018 BY Joan Fernández Esmerats

**THE ROLE OF FLOW-SENSITIVE MIRNAS AND UBE2C-
DEPENDENT HIF1A PATHWAY IN CALCIFIC AORTIC VALVE
DISEASE**

Approved by:

Dr. Hanjoong Jo, Advisor

Department of Biomedical Engineering
*Georgia Institute of Technology and Emory
University*

Dr. Ajit Yoganathan

Department of Biomedical Engineering
Georgia Institute of Technology

Dr. Robert Nerem

Parker H. Petit Institute for Bioengineering
and Bioscience
Georgia Institute of Technology

Dr. Robert W. Taylor

School of Medicine, Division of
Cardiology
Emory University

Dr. Andres J. Garcia

School of Mechanical Engineering
Georgia Institute of Technology

Dr. Keith D. Wilkinson

Department of Biochemistry
Emory University

Date Approved: 08/27/2018

To my family and friends.

Acknowledgements

First, I would like to thank my parents, Miguel and Ana, and my siblings, Andreu and Anna, for their support throughout all my education career and for encouraging me to take the leap and conduct my PhD outside of Spain. They were always there to help me keep going and always trusted I would achieve my goals. Second, I really need to thank my wife Alicia, she has been with me through all my college and graduate school years and has always supported me all my decisions. No matter how bad the day was, she was always there for me and I cannot wait to what lies after graduate school next to her. I cannot forget to mention my two cats, Garfield and Petit, they have been with us nearly since the start of my PhD path and they have always been next to me whenever I had to study or do work at home. Thanks to them, I have not been late to work a single day throughout my PhD, there is no better alarm clock than the cats meowing at 6AM for food.

I also want to thank my advisor, Dr. Hanjoong Jo, for some reason, he decided that having a mechanical engineer without previous experience on any biological work would be a good fit for a cell biology lab. Working in his lab allowed me to learn about a new field of research I had never worked on and I cannot thank him enough as this new knowledge will be really useful for my future career. I need to thank all the members from the Jo lab, and the labs around us, who have made my work days so much fun and enjoyable: Jess, Rachel, Salim, Jack, Nico, Cat, Darian, Sandra, Aline, Natasha, Sanjoli, Sandeep, Dong-Won, Sunkum, Colleen, Lina, Tasha and Rithika among others. No matter if we were discussing a lab experiment that went wrong or the latest show on Netflix, coming every day to the lab has never been a hassle for me. Apart from the Jo lab members, there are lots of amazing people from my department that I need to thank for helping me whenever needed: Lisa, Shannon, Leita, Elizabeth, Steven, Robert, and Maurice.

I have also met a lot of wonderful people in Atlanta who rapidly became friends and made my time outside of the lab such a fun experience. It all started with the day I moved

to my apartment and I found out that one of my undergraduate fellows, Ignacio, lived right across the street from me. Through him I met a lot of wonderful people which have made my time out-of-work extremely fun: Andrew, Jess, Vanessa, Victor, Maarten, and Janae.

Last, I would like to thank my PhD committee: Dr. Nerem, Dr. Yoganthan, Dr. Garcia, Dr. Taylor, Dr. Wilkinson and Dr. Thourani. Meeting with them and discussing my research has been really beneficial and has been really useful to make sure I was always on the right track to complete my PhD and to conduct good and meaningful research.

Table of Contents

Acknowledgements.....	iv
LIST OF TABLES.....	x
LIST OF FIGURES.....	xi
LIST OF ABBREVIATIONS.....	xiii
SUMMARY.....	xiv
1 INTRODUCTION.....	1
1.1 Aortic valve anatomy structure.....	3
1.2 Aortic valve disease.....	5
1.3 Aortic valve hemodynamics.....	7
1.4 Mechanosensors in the aortic valve endothelium.....	12
1.5 Mechanosensitive genes in flow-mediated valve biology and dysfunction.....	16
1.6 <i>In vitro</i> and <i>in vivo</i> models to study CAVD.....	28
1.6.1 In vitro and ex vivo models of CAVD.....	28
1.6.2 In vivo models of CAVD.....	29
1.6.3 Computational Models of CAVD.....	33
1.7 MicroRNAs and CAVD.....	34
1.7.1 Biogenesis of miRNAs.....	34
1.7.2 Role of miRNAs in CAVD.....	35
1.7.3 miRNAs in the Clinic.....	38
1.8 MiR-181b in CAVD.....	40
1.9 ECM degradation and TIMP3 in CAVD.....	41
1.10 MicroRNA miR-483 in CAVD.....	42
1.11 Role of UBE2C and HIF1 α in CAVD.....	43
2 SPECIFIC AIMS AND HYPOTHESES.....	46
2.1 Significance and Impact.....	46
2.2 Rationale.....	47
2.3 Innovation.....	48
2.4 Project Objective.....	48
2.5 Overall Hypothesis.....	49
2.6 Specific Aim I: Demonstrate the mechanosensitivity of miR-181b in HAVECs and its role in ECM remodeling.....	50

2.7	Specific Aim II: Determine the shear-sensitivity of miR-483, its targets and their function in endothelial dysfunction and AV calcification	50
2.8	Specific Aim III: Develop an accelerated <i>in vivo</i> animal model for CAVD.....	51
3	METHODS.....	53
3.1	Cell Culture and Shear Experiments	53
3.1.1	HAVECs	53
3.1.2	Human embryonic kidney cells 293 (HEK).....	53
3.2	Shear Stress experiments.....	54
3.2.1	Cone and Plate Viscometer.....	54
3.2.2	Ibidi shear stress experiments	54
3.3	Quantitative real-time PCR (qPCR) for validation of miRNAs.....	55
3.4	Quantitative real-time PCR (qPCR) for validation of mRNAs.....	56
3.5	RNA Extraction from organs and qPCR	58
3.6	Transfection of Nucleic Acids.....	58
3.7	PX478 treatment.....	59
3.8	Gelatinase assay	59
3.9	In vitro MMP inhibition	60
3.10	Monocyte Adhesion Assay.....	60
3.11	Protein assay and Western Blotting for Inflammatory Markers	60
3.12	pVHL and HIF1 α staining in shear stress conditions.....	62
3.13	<i>In silico</i> analysis	62
3.14	3'UTR Luciferase assay.....	62
3.15	Scratch migration assay.....	63
3.16	Tunel assay for apoptosis quantification.....	63
3.17	Immunofluorescence Staining.....	63
3.18	Mouse De-paraffinization and Immunostaining	64
3.19	Hematoxylin and Eosin Staining.....	64
3.20	Alizarin red staining.....	65
3.21	Statistical Analysis	65
4	Role of miR-181b in extracellular matrix remodeling in CAVD.....	66
4.1	Introduction	66
4.2	Results	69
4.2.1	miR-181b is side-specific and shear-sensitive in valvular endothelium.....	69

4.2.2	TIMP3 is a potential shear-sensitive target of miR-181b	69
4.2.3	miR-181b regulates TIMP3 expression	72
4.2.4	miR-181b regulates ECM degradation via silencing of TIMP3	74
4.2.5	miR-181b regulates shear -regulated ECM degradation in HAVECs	76
4.3	Discussion and future directions	77
5	Role of miR-483 in HAVEC biology and AV calcification.....	81
5.1	Introduction	81
5.2	Results	82
5.2.1	miR-483 is side-specific and shear-sensitive in valvular endothelium.....	82
5.2.2	miR-483 regulates inflammation, EndMT, proliferation and apoptosis in HAVECs.....	83
5.2.3	KLF2 regulates expression of IGF2 and miR-483.....	88
5.2.4	miR-483 regulates shear-dependent expression of UBE2C and ASH2L ...	89
5.2.5	miR-483 exerts its anti-inflammatory role via silencing of UBE2C	92
5.2.6	UBE2C mediates OS-induced endothelial inflammation and EndMT	93
5.2.7	pVHL and HIF1 α are shear-sensitive in HAVECs and are regulated by UBE2C	94
5.2.8	UBE2C binds and ubiquitinates pVHL, leading to its degradation.	97
5.2.9	pVHL and HIF1 α mediate UBE2C-dependent inflammation and EndMT in HAVECs.....	101
5.2.10	MiR-483 mimic and HIF1 α chemical inhibitor PX478 inhibit calcification in porcine aortic valves.....	103
5.3	Summary and discussion.....	105
6	Development of an accelerated animal model of CAVD using GATA5 mice	109
6.1	Introduction	109
6.2	Results	110
6.2.1	Injection of PCSK9 induces hypercholesterolemia in GATA5 knockout mice	110
6.2.2	GATA5 $^{-/-}$ bicuspid AV mice develop sclerosis and calcification.....	112
6.2.3	Ube2c levels are increased in BAVs of GATA5 mice	113
6.2.4	SubQ injection of fluorescently labeled siRNA is delivered to the AV. ..	114
6.3	Summary and discussion.....	115
7	DISCUSSION.....	117
7.1	Summary	117

7.2	Conclusions	120
7.3	Future Directions.....	121
REFERENCES		125

LIST OF TABLES

Table 3.1 Primer sequences for qPCR for human samples.....	57
Table 3.2 Primer sequences for qPCR for pig samples	58
Table 3.3 List of Antibodies used for Western blotting and Immunostaining.....	61

LIST OF FIGURES

Figure 1.1 Aortic valve anatomy and structure.....	5
Figure 1.2 Healthy and diseased aortic valve	7
Figure 1.3 Forces affecting the aortic valve in systole and diastole.	12
Figure 1.4 Major mechanosensors in valvular endothelial cells.....	16
Figure 1.1.5 Mechanosensitive genes in the aortic valve endothelium	27
Figure 1.1.6 Models of flow and shear stress.	29
Figure 1.7 Echocardiogram of healthy and diseased mouse aortic valve.	33
Figure 1.8 Biogenesis of miRNAs	35
Figure 1.9 Shear-sensitive miRNAs in HAVECs and side-specific miRNAs in Porcine AVs	36
Figure 1.10 Target genes of HIF1 α	44
Figure 1.11 Regulatory mechanism of HIF1 α	44
Figure 3.1 LS aligns endothelial cells.....	54
Figure 3.2 Ibidi shear system aligns HAVEC in LS conditions	55
Figure 4.1 miR-181b induces endothelial ECM degradation by targeting TIMP3	68
Figure 4.2 miR-181b is side-specific and shear-sensitive in valvular endothelium	69
Figure 4.3 TIMP3 is shear-sensitive in HAVECs.....	70
Figure 4.4 OS induces MMP activity in HAVECs.....	71
Figure 4.5 miR-181b upregulation decreases GATA6, TIMP3 and SIRT1 expression ...	72
Figure 4.6 MiR-181b inhibition upregulates GATA6, TIMP3 and SIRT1	73
Figure 4.7 MiR-181b directly binds to the 3'UTR of TIMP3	74
Figure 4.8 MiR-181b regulates ECM degradation in HAVECs.....	75
Figure 4.9 miR-181b regulates ECM degradation by silencing TIMP3	76
Figure 4.10 miR-181b is responsible for shear-dependent ECM degradation.....	77
Figure 5.1 Regulation of miR-483 in HAVECs.....	83
Figure 5.2 Regulation of miR-483 in HAVECs.....	84
Figure 5.3 miR-483 regulates inflammation in static HAVECs	84
Figure 5.4 miR-483 regulates shear-induced inflammation in HAVECs	85
Figure 5.5 miR-483 regulates shear-induced EndMT.....	86
Figure 5.6 miR-483 regulates proliferation and apoptosis but has no effect in cell migration.	87
Figure 5.7 miR-483 is an intronic miRNA in IGF2 regulated by KLF2	88
Figure 5.8 In silico analysis to identify potential shear-sensitive targets of miR-483.....	89
Figure 5.9 ASH2L, UBE2C and PSAT1 are regulated by miR-483 in static HAVECs... 90	90
Figure 5.10 UBE2C and ASH2L are shear-sensitive targets of miR-483 in HAVECs.... 91	91
Figure 5.11 UBE2C is side-specific and is regulated by miR-483 in OS conditions	92
Figure 5.12 UBE2C regulates miR-483 dependent anti-inflammatory effect in HAVECs	93
Figure 5.13 UBE2C regulates OS-induced endothelial inflammation and EndMT	94
Figure 5.14 pVHL and HIF1 α are shear-sensitive in HAVECs	95
Figure 5.15 UBE2C mediates shear-dependent expression of pVHL and HIF1 α	96

Figure 5.16 UBE2C, pVHL and HIF1 α are expressed in a side-dependent manner in human AV leaflet.....	97
Figure 5.17 UBE2C regulates pVHL ubiquitination in HAVECs.....	98
Figure 5.18 UBE2C binds and ubiquitinates pVHL.....	99
Figure 5.19 Degradation of pVHL by UBE2C requires pVHL ubiquitination sites.....	100
Figure 5.20 UBE2C degrades pVHL in a lysine-dependent manner.....	100
Figure 5.21 Silencing of pVHL leads to increased endothelial inflammation.....	101
Figure 5.22 pVHL and HIF1 α mediate UBE2C-induced endothelial inflammation and EndMT.....	102
Figure 5.23 The miR-483-mimic reduces AV calcification by silencing of Ube2c.....	103
Figure 5.24 HIF1 α inhibitor PX478 reduces AV calcification.....	104
Figure 5.25 Working hypothesis.....	107
Figure 6.1 GATA5 ^{-/-} mice with bicuspid AV present higher AV velocity by ultrasound.....	110
Figure 6.2 GATA5 ^{-/-} mice develop BAV and AV sclerosis.....	111
Figure 6.3 . Hypercholesterolemic BAV GATA5 ^{-/-} mice develop AV sclerosis.....	112
Figure 6.4 Hypercholesterolemic BAV GATA5 ^{-/-} mice develop AV calcification.....	113
Figure 6.5 BAVs have higher Ube2c expression compared to TAV in GATA5 ^{-/-} mice as shown by.....	113
Figure 6.6 SiRNA delivery to the AV by using SubQ injection.....	115

LIST OF ABBREVIATIONS

d-flow	Disturbed flow
OS	Oscillatory shear stress
miRNA	MicroRNA
HAVECs	Human Aortic Valve Endothelial Cells
ECs	Endothelial Cells
LS	Unidirectional shear stress
S-flow	Stable, unidirectional flow
TIMP3	Tissue inhibitor of metalloproteinases 3
UBE2C	Ubiquitin-conjugating enzyme E2 C
HIF1 α	Hypoxia-inducible factor 1-alpha
pVHL	Von Hippel Lindau protein
KLF2	Kruppel Like Factor 2
VCAM1	Vascular Cell Adhesion Molecule
ICAM1	Intercellular Adhesion Molecule 1
MMP	Matrix Metalloproteinase
ECM	Extracellular Matrix
UTR	Untranslatable Region
EndMT	Endothelial-to-Mesenchymal Transition

SUMMARY

Calcific Aortic Valve Disease (CAVD), characterized by aortic valve (AV) stenosis and insufficiency (regurgitation), is a major cause of cardiac-related deaths worldwide, especially in the aging population in advanced countries [6-8]. Once developed, it is treated mainly with AV repair or replacement by surgical or transcatheter methods [9, 10]; however, there are currently no pharmacological treatment options for these patients. This is largely due to a relative paucity in molecular mechanistic understanding of the disease. CAVD was once thought to be a passive degenerative disease, but overwhelming evidence demonstrates that it is actively regulated by cellular and molecular pathways that lead to AV inflammation, sclerosis (thickening and fibrosis), and calcific lesions [11-13].

MicroRNAs (miRNAs) are a large class of evolutionarily conserved, noncoding RNAs which function as post-transcriptional regulators by interacting with the 3' untranslated region (3'UTR) of specific target mRNAs in a sequence-specific manner. A single miRNA can typically target hundreds of mRNAs. These miRNAs negatively regulate gene expression through translational repression or mRNA cleavage, depending on the degree of complementarity. Flow-sensitive miRNAs have been mostly characterized *in vitro* however, their role in human disease has not been fully studied.

Previous work in our laboratory has focused on identifying shear-sensitive and side-specific (ventricularis compared to fibrosa layers of the AV) miRNAs relevant to CAVD. To this end, we conducted two independent microRNA array studies. First, we isolated human aortic valve endothelial cells (HAVECs) from each side of the leaflet and exposed them to high-magnitude unidirectional laminar shear stress (LS) or low-magnitude oscillatory shear stress (OS) conditions for 24 hours to discover shear-sensitive miRNAs [14]. Second, we isolated endothelial-enriched total RNAs from each side of the leaflet from porcine AVs to discover side-specific miRNAs [15]. These studies allowed us to identify miR-181b and miR-483 as potential miRNAs for further studies.

In Aim 1, we focused on studying shear-sensitive miR-181b. We showed that miR-181b was upregulated in OS conditions and that it regulates matrix metalloproteinases (MMP) activity in valvular endothelium. We conducted an *in silico* analysis combining predicted gene targets of miR-181b and shear-sensitive target genes from our *in vitro* HAVEC array and identified tissue inhibitor of metalloproteinases 3 (TIMP3) as a shear-sensitive target of miR-181b responsible for the role of miR-181b in extracellular matrix (ECM) degradation. Therefore, we showed that ECM degradation, a critical step in CAVD, might be mediated by the miR-181b/TIMP3 pathway.

In Aim 2, we focused on studying the novel shear-sensitive miR-483-3p. We discovered that it regulated inflammation and endothelial-to-mesenchymal transition (EndMT) in HAVECs. In HAVECs we identified UBE2C as a novel shear-sensitive gene targeted by miR-483; which regulates endothelial inflammation and EndMT. Additionally, UBE2C exerts its function by silencing pVHL, which allows the upregulation and stabilization of HIF1 α . Therapeutic studies were conducted in porcine AVs, and we showed that the miR-483 mimic as well as PX478, a HIF1 α inhibitor, can inhibit AV calcification. These studies identified two potential therapeutic targets for CAVD and identified a novel mechanistic pathway for CAVD involving the miR-483/UBE2C/pVHL/HIF1 α pathway.

In Aim 3, we are developing a novel accelerated *in vivo* model for CAVD by combining hypercholesterolemia (via AAV-PCSK9) and mice with bicuspid AV phenotype (via GATA5 knockout mice). This animal model appears to generate severe sclerosis and microcalcifications in AVs in just four months after PCSK9 injection, allowing for accelerated testing of therapeutics for CAVD in an *in vivo* setting.

1 INTRODUCTION

Calcific aortic valve disease (CAVD), is a highly prevalent disease among the adult population and is associated with significant mortality and morbidity; once it is fully developed, the only available treatment is aortic valve (AV) repair or replacement by surgical or transcatheter methods [6-8]. Due in part to limited knowledge on the molecular pathways of CAVD, there are no pharmacological treatments available for CAVD. Originally CAVD was thought to be a passive degenerative disease; however, recent studies have demonstrated that CAVD is an actively-regulated disease characterized by AV inflammation, sclerosis (thickening and fibrosis), and calcific lesions [11-13].

MicroRNAs (miRNAs) are conserved, noncoding RNAs that regulate mRNAs at the post-transcriptional level by interacting with the 3' untranslated region (3'UTR) in a sequence-specific manner. Potential targets of miRNAs can be identified computationally, and most miRNAs can target hundreds of mRNAs. Once the miRNA is bound to the 3'UTR of the mRNA, it negatively regulates mRNA expression either by translational repression or by mRNA cleavage (depending on the degree of complementarity). Several flow-sensitive miRNAs have been characterized *in vitro*; however, more research needs to be conducted to better understand the role of shear stress in miRNA function in the valvular endothelium.

Previous work in our laboratory has identified shear-sensitive and side-specific miRNAs relevant to CAVD. Two independent miRNA array studies were conducted. First, in order to discover shear-sensitive miRNAs human aortic valve endothelial cells (HAECs) from each side of the leaflet were isolated and exposed to high magnitude-unidirectional shear stress (LS) or low magnitude-oscillatory shear stress (OS) conditions for 24 hours. Second, endothelial-enriched total RNAs from each side of the leaflet from

porcine AVs were isolated to discover side-specific miRNAs. From these studies, we have been able to identify miR-181b and miR-483 as potential miRNAs for further studies.

In Aim 1, we studied the role of shear-sensitive miR-181b in valvular endothelial biology. miR-181b was upregulated in OS conditions, and it regulated matrix metalloproteinases (MMP) activity in AV endothelium. After identifying TIMP3 in an *in silico* analysis, we validated that TIMP3 is regulated by miR-181b in a shear-dependent manner. Additionally, we discovered that miR-181b regulated MMP activity by silencing TIMP3. Anti-miR-181b also prevented OS-induced MMP activity upregulation in HAVECs and can be used as a potential therapeutic to decrease ECM degradation.

In Aim 2, we centered our attention on studying the role of the novel shear-sensitive miR-483-3p (miR-483). We found that in both HAVECs and the ventricularis of porcine AVs, miR-483 is upregulated in stable flow conditions. In HAVECs, UBE2C was identified as a novel shear-sensitive target regulated in a miR-483 dependent manner. miR-483 regulated inflammation and EndMT in HAVECs by silencing UBE2C. Furthermore, UBE2C silenced pVHL, which lead to upregulation and stabilization of HIF1 α . We conducted therapeutic studies in porcine AVs and showed that the miR-483 mimic, as well as PX478, a HIF1 α inhibitor, can inhibit AV calcification. In this aim, we identified two potential therapeutic targets for CAVD and identified a novel pathway for CAVD involving the miR-483/UBE2C/pVHL/HIF1 α pathway.

Lastly, in Aim 3 we established a new accelerated animal for CAVD by combining hypercholesterolemia (via AAV-PCSK9) and mice with bicuspid AV phenotype (via GATA5 knockout mice). This model induces severe sclerotic and calcific lesions in the AV in four months after PCSK9 injection, allowing for accelerated testing of CAVD therapeutics in an *in vivo* setting.

1.1 Aortic valve anatomy structure

The aortic valve is a complex, heterogeneous tissue with three layers that define its function and behavior. The aortic valve is normally composed of three leaflets (Fig. 1.1); in humans, the leaflets have a thickness between 0.6 and one millimeter and are composed of three separate, interacting layers (as shown in Fig. 1.1):

1. *Fibrosa*: This layer faces the aortic side of the valve and is comprised of valvular endothelial cells (VECs, in direct contact with the blood), valvular interstitial cells (VICs, residing below the endothelial cells), a small amount of elastin fibers, and circumferential type I and type III fibrillar collagen, which serves as the load-bearing layer. The collagen fibers are aligned along the circumference of the valve (circumferential) to allow for high strain under low loads and for a higher elastic modulus when more load is applied during the cardiac cycle[16]. In porcine aortic valves, the tissue is six times stiffer in the circumferential direction than the radial direction (along the radius of the circumference) [17, 18]; the aortic valve stretches considerably in the radial direction to ensure good coaptation and to avoid regurgitation during the diastolic phase. In diseased AVs, calcification normally occurs in the fibrosa (Fig. 1.1C).
2. *Spongiosa*: This layer is placed between fibrosa and ventricularis and is comprised of VICs, a small amount of elastin fibers, glycosaminoglycans, and proteoglycans. These last two components serve as lubricant for the fibrosa and ventricularis layers when they deform during the cardiac cycle. The main component of the extracellular matrix in this layer is hyaluronan, which binds large amounts of water to form a foam-like

structure. During compression of the aortic valve, this layer absorbs energy and helps arrange elastin fibers on the ventricularis and collagen fibers on the fibrosa [18, 19].

3. *Ventricularis*: This layer faces the ventricular side of the aortic valve and is comprised of valvular endothelial cells (VECs), VICs, collagen, and radially oriented elastin fibers [18, 20, 21]. Collagen fibers are stretched during the diastolic phase and relaxed during the systolic phase as the valve compresses. Elastin fibers in this layer aid in fast compression during the opening phase to ensure the valve opens and closes in a fast and consistent manner [19].

The unique structure of the valve (Fig. 1.1) allows for consistent, long-term physiological movement due to the presence of elastin fibers throughout the tissue structure. The amount of collagen and elastin in the valve is 55% and 13% (dry weight), respectively [22]. Although collagen fibrils are stiff and have a maximum strain of 2% before yielding [23], they possess a crimped and wavy configuration that allows for strain of up to 40% without yielding [17]. Elastin serves as a scaffold between the different layers and helps intertwine collagen fibers between the spongiosa and fibrosa; a “honeycomb” arrangement of elastin surrounds collagen fibers and links them within the tissue [24]. Without this interconnection, the aortic valve would be at risk of delamination and separation of its different layers, as a consequence of the dynamic mechanical environment experienced throughout a cardiac cycle [25].

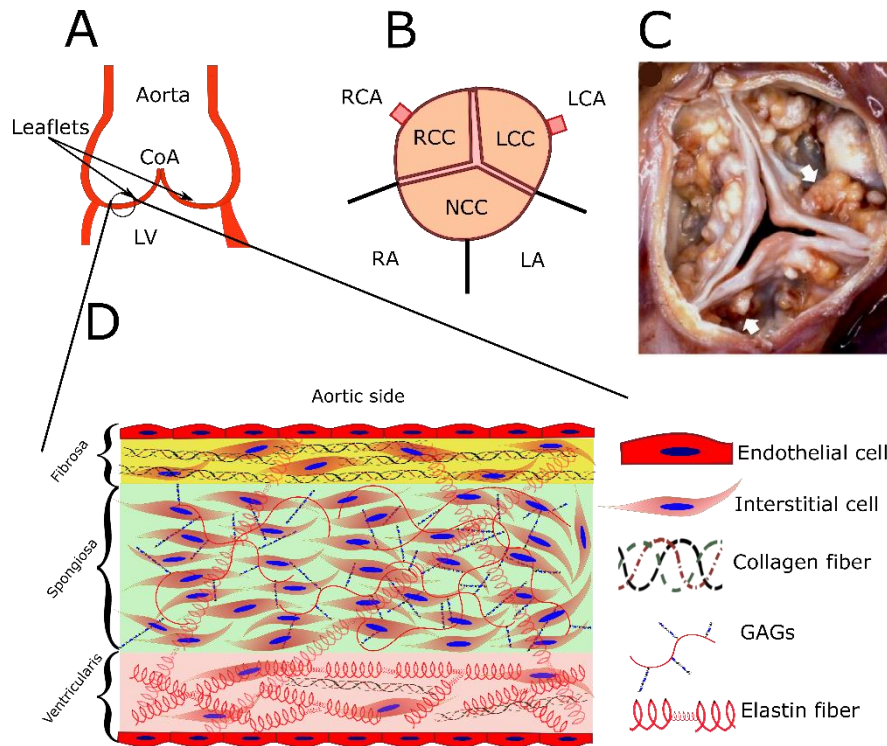


Figure 1.1 Aortic valve anatomy and structure.

A) The aortic valve is located between the left ventricle (LV) and the aorta, and it regulates systemic blood delivery from the heart. The coaptation area (CoA) denotes the joining of the three leaflets to result in a tight seal. **B)** Valve leaflet nomenclature. The right coronary cusp (RCC) is the leaflet nearest to the right main coronary artery (RCA). The left coronary cusp (LCC) is proximal to the left main coronary artery (LCA). The noncoronary cusp (NCC) is the third leaflet, adjacent to the right (RA) and left atria (LA). **C)** Calcified nodules (white arrows) deposited on the fibrosa of the aortic valve (image borrowed from [1]). This widespread calcification is usually not observed until later stages of CAVD. **D)** Layers of the aortic valve. The fibrosa layer faces the aorta and contains less elastin and more collagen fibers. Interstitial cells are dispersed throughout the layers of the valve excluding the endothelium. The middle layer, the spongiosa, contains most of the interstitial cells, as well as glycosaminoglycans (GAGs) and a small amount of elastin. That elastin spans the spongiosa and the ventricularis, which is the side of the valve facing the left ventricle of the heart. The ventricularis contains a greater amount of elastin than the other layers and a small amount of collagen.

1.2 Aortic valve disease

A normally-functioning AV ensures the unidirectionality of blood flow from the left ventricle to the aorta. Abnormalities of the valve arise due to a variety of risk factors

such as hypertension, high low-density lipoprotein (LDL) content, old age, hyperphosphatemia, diabetes, obesity, smoking, and others [26]. These valve abnormalities range from mild thickening to severe calcification that causes impaired leaflet motion (Fig. 1.2). AV stenosis is a major disease characterized by the narrowing of the AV opening during systole, which leads to a greater pressure gradient across the valve and increased transvalvular velocity [27]. The classic symptoms of the AS are syncope, angina, and congestive heart failure. AV stenosis is a progressive disease found in the aging population; however, it is found in earlier ages in patients with bicuspid AV (BAV), a congenital condition occurring in 1-2% of all live births [28]. BAV presents elevated levels of turbulence downstream of the stenosed valve which causes mechanical damage to the endothelial layer of ascending aorta and leads to aortic aneurisms [29].

Aortic regurgitation (AR) is a condition characterized by the AV not fully closing in diastole, causing a backflow of the blood from the aorta into the left ventricle. Around 50% of the cases of AR are due to dilatation of the aortic root, which is idiopathic in most instances. In about 15% of regurgitation cases, the cause is innate BAV; another 15% of the cases are due to retraction of the cusps as part of the post-inflammatory processes of endocarditis in rheumatic fever and various collagen vascular diseases [30].

Calcific AV disease is a strong risk factor for cardiovascular related deaths [12, 31, 32] and is a significant source of mortality worldwide, with the number of patients requiring AV surgery expected to triple from 250,000 to 850,000 by 2050 [33]. The most common forms of the AV disease can be distinguished clinically by their characteristic echocardiographic findings. Currently, the treatment for AV calcification is to surgically replace the diseased valve with a mechanical or biological valve or repair. Recent

developments are aimed towards the use of transcatheter AV replacement of the diseased valve, especially in elderly patients who do not qualify for a surgery. **However, as of now, no proven medical therapies exist for the treatment of calcified AV leaflets.**

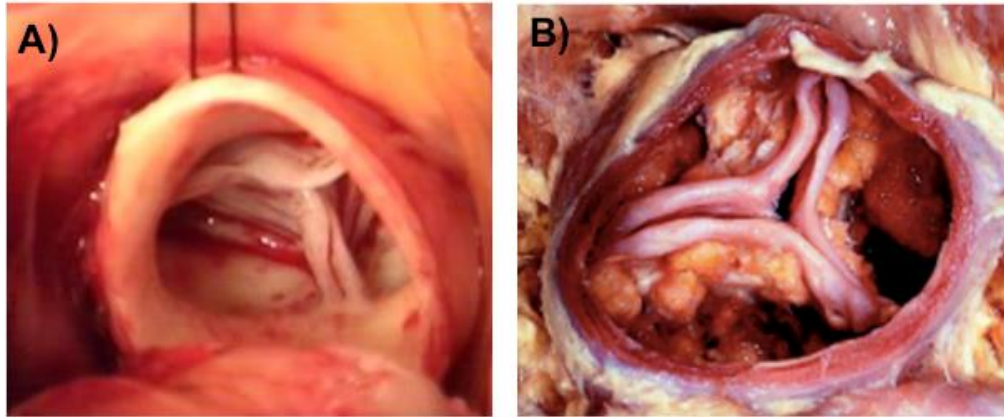


Figure 1.2 Healthy and diseased aortic valve

On the left panel (A) a healthy tricuspid valve is shown while on the right panel (B) a calcified tricuspid valve is observed (adapted from deptmed.queensu.ca).

1.3 Aortic valve hemodynamics

As discussed previously, the aortic valve is in constant motion, resulting in an ever-changing mechanical environment. Understanding of the dynamic mechanics of the valve is crucial for the study of the biological pathways that regulate CAVD. Four types of forces, summarized in Figure 1.3, are exerted upon the aortic valve:

1. *Pressure*: The two faces of the valve are subjected to contrasting pressures as the valve opens and closes, which affect the tissue shape and geometry [34]. During diastole, pressure in the ventricle rapidly drops while pressure in the aorta remains stable. Under physiological conditions this transvalvular pressure, defined as the difference between the aortic and left ventricular pressure during diastole, ranges between 80 and 120 mmHg. In hypertensive patients, the systemic blood pressure is increased, and the transvalvular pressure can reach values greater than 180 mmHg [35]. The second manifestations of arterial disease study (SMART) found

that systolic blood pressure has a 9% correlation with total cardiovascular calcifications (including aortic valve calcification) indicating that systemic changes in the cardiovascular system can affect the aortic valve [36]. Another study conducted on elderly patients found that increased ambulatory diastolic blood pressure was the most significant independent factor contributing to advanced aortic valve calcification [37]; this increase in pressure enhances the effect of low shear stress and cyclic stretch, accelerating the progression of aortic valve calcification. These two studies and others [38-40] reflect the importance of systemic pressure to the onset and progression of aortic valve calcification. In the future, specific animal studies, using models described later in this chapter, should be performed to better understand the effect of increased pressure on the molecular mechanisms of CAVD.

2. *Bending stress*: Bending stress is defined as the stress generated on a solid when it is deformed. In the valve, bending stress causes the concave fibrosa layer to be compressed while the convex ventricularis layer is under tension [41]. The most precise model of bending stress is by Corden et al [42], who tested trileaflet polyurethane valves (used in ventricular assist devices and artificial hearts) under pulsatile flow. With this system, the group found that the bending stress for the polymeric valves ranges between 0.4 and 0.7 MPa, with a bending strain ranging from 4.7 to 8.5% at peak systole compared to the diastolic position.

In the search for clearer models of aortic valve function, the examination of the bicuspid aortic valve has been invaluable. BAV is the most common congenital heart defect; it has a prevalence of 0.5% to 2% and a male predominance of 3 to 1 [43]. BAV patients develop symptomatic aortic stenosis at the age of 50-60 years old [44] while patients with tricuspid valves normally develop symptomatic AS at the age of 70-80 years old [45, 46]. Because patients with BAV develop faster and more severe AV stenosis, this condition is useful in studying aortic

valve calcification and can be used to develop an accelerated *in vivo* model of CAVD. Katayama et al [47] studied the bending strain, defined as deformation of the tissue caused by bending stress, in stenotic and non-stenotic tricuspid and bicuspid aortic valves using a computational model and concluded two findings: bending strain increased in stenotic tricuspid and bicuspid valves compared to nonstenotic valves, and a greater increase was observed in bicuspid valves, with strain concentrations at the midline of the leaflets. The group hypothesized that excessive bending strain on the bicuspid leaflets could be responsible for the rapid progression of calcification in bicuspid versus tricuspid valves. Another study by Conti et al [48] found that bicuspid aortic valves experience an eight-fold increase in strain compared to tricuspid valves. Thus bending stress is clearly a critical factor in the valve environment, and it may be important to control the bending stress to prevent valve dysfunction.

3. *Axial stress*: Valves change their shape and length throughout the cardiac cycle to adapt to the mechanical environment. Axial stress, defined as tension that the valve experiences perpendicular to the valve face, is paramount in creating a tight seal to prevent regurgitation of blood into the ventricle [41]. Axial stress is separated into two categories in the valve: circumferential and radial (Fig. 1.3A). In the aortic valve of many different species—ovine, porcine and human—the circumferential direction presents a higher elastic modulus than the radial direction [49]. In canine aortic valves, leaflets elongate from diastole to systole by 11% in the circumferential direction and by 31% in the radial direction [50]. This behavior is expected because the leaflets need to stretch in the radial direction to form a tight seal and prevent regurgitation. Maximum axial stress in the aging valve is at the area where the valve leaflet attaches to the aortic root; this region is also where calcification is first observed [51]. This increase in stress is associated with development and progression of valve calcification. Furthermore, disease

progression leads to increased axial stress, generating a “vicious cycle” that accelerates valve dysfunction.

4. *Shear stress*: Shear stress is exerted on the valve by blood flowing across the face of the valve tissue. In basic terms, shear stress is defined as the component of the stress parallel to the surface of interest. Each side of the leaflet in the the aortic valve experiences completely different shear profiles correlating with the preferential calcification of the fibrosa [52, 53]. Due to the blood flow during the typical cardiac cycle, shear stress at the leaflet surface is experienced in a cyclical manner. As blood is ejected from the ventricle to the aorta, the ventricularis is subjected to unidirectional shear stress while the fibrosa experiences oscillatory shear stress. Oscillatory shear stress at the fibrosa has been directly associated with valve dysfunction and CAVD [52-54]. Interestingly, these disturbed conditions in the fibrosa side were firstly described by Leonardo da Vinci where he built a replica of the aortic valve and using some grass seeds he was able to demonstrate that the disturbed flow conditions observed in the fibrosa helped to close the valve to prevent backflow [55]. His work was validated in 1968 by Bellhouse et al [56]. Aboelkassem et al [57] derived a mathematical model combining aortic valve dynamics, systemic vascular resistance and sinus vortex local pressure to describe shear stress during systole. The model uses a Hill’s classical semi-spherical vortex model and an aortic pressure–area compliance constitutive relationship to effectively mimic the oscillatory flow experienced at the fibrosa, with a change in flow direction between the opening and closing sequence of the valve. This model nicely shows the flow forces on the valve during systole as well as the relationship between the blood flow and the deformation of the valve during the cardiac cycle. In agreement with the mathematical model, the peak shear stresses have been measured by another group using laser Doppler velocimetry: 20 dyn/cm² on the aortic side and 64-71 dyn/cm² on the ventricular side [58]. The results from this

study corroborate the theory that the fibrosa layer preferentially calcifies due to the low and oscillatory shear stress. Likewise, atherosclerosis presents similar mechanisms of disease onset such as endothelial dysfunction and inflammation [59] and also shows preferential development in regions of low and oscillatory flow [60, 61].

Because endothelial cells are in direct contact with blood flow, shear stress is a key regulator of endothelial cell function, and can communicate systemic changes in the body to the valvular tissue. Laminar shear stress, as observed at the ventricularis, regulates cell shape and microfilament structure as cells align in the direction of flow [62], correlating with synthesis of endothelial nitric oxide synthase and production of nitric oxide, a potent vasodilator. Further discussion of the biological pathways altered by differential shear stresses is discussed later in the chapter.

A study conducted by Saikrishnan et al [63] utilizing bicuspid aortic valves constructed from porcine tricuspid valves showed reduced wall shear stress and increased turbulence in bicuspid valves. The study concluded that these differences in hemodynamics may play a key role in amplifying the biological responses of the valvular leaflets, which may be one of the key components in the accelerated progression of calcification in bicuspid aortic valves. Another valve computational model examined bicuspid aortic valves in a fluid-structure computational model, and showed that the fused leaflets of the bicuspid valve exhibited strong abnormalities in shear stress compared to the tricuspid controls [64]. The same group studied these abnormalities in *ex vivo* porcine aortic valve leaflets and found that abnormal shear stress increased endothelial inflammation [65]. These functional studies emphasize the importance of endothelial shear stress in tissue function.

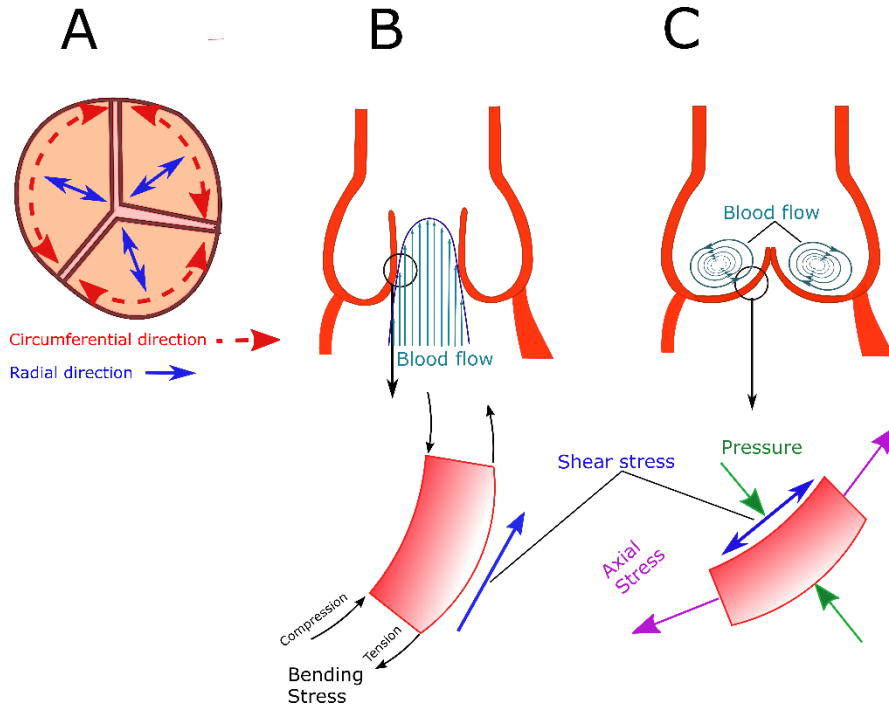


Figure 1.3 Forces affecting the aortic valve in systole and diastole.

A) A cross-section of the aortic valve is shown indicating the circumferential (red dashed arrows) and radial direction (blue solid arrows) of the valve. **B)** The main forces acting on the valve during systole (when the valve is open) are shown. The fibrosa is compressed while the ventricularis is stretched and subjected to tensile bending stress. The ejection of blood from the ventricle exerts unidirectional laminar shear stress on the ventricularis (represented by the parallel blue arrows in the top panel and the single blue arrow in the lower panel). **C)** The main forces acting during diastole (valve is closed) are shown. Pressure (green arrows) exerted from cycling blood flow pulls the valve shut, and axial stress (purple arrows) seals the valve to prevent regurgitation. The fibrosa, the aortic side of the valve, experiences oscillatory shear stress (represented by the blue circling arrows in the top panel and the double-headed blue arrow in the lower panel).

1.4 Mechanosensors in the aortic valve endothelium

Endothelial cells utilize a variety of sensing mechanisms to respond to the extracellular mechanical environment. Numerous studies have been carried out to further understand mechanosensors in the vascular endothelium [66]. However, a relatively small body of work has focused on the mechanical sensing of the valvular endothelial cells. In the following subsections, we describe the current state of research into valvular endothelial mechanosensing and the major players at the cell surface, including integrins, GPCR, and the glycocalyx are described (Fig. 1.4).

Integrins, focal adhesion complexes, and the cytoskeleton

Integrins are a superfamily of transmembrane cell adhesion receptors that have traditionally been known to bind to ligands at the cell surface, within the extracellular matrix, and within the cytoplasm. Integrins transduce signals from the extracellular environment to the cell interior; through this process, changes in the concentrations of key signaling molecules in the plasma are communicated to the cell. In addition, integrins have more recently been recognized as sensors of the mechanical environment surrounding the cell, which can result in changes in intracellular signal transduction pathways [67, 68]. Furthermore, integrins receive intracellular signals that regulate their ligand-binding affinity, fine-tuning the communication between the cell membrane and other cellular compartments [69]. By coordinating cues from the extracellular environment with intracellular signaling, integrins play an important role in cell adhesion, migration, proliferation, and survival.

The mechanism by which integrins transmit signals to the cell is dependent on their binding to the cytoskeleton [70]. Along with cytoskeletal proteins such as actin, many binding partners colocalize with integrins near the cell surface, forming complexes known as focal adhesion complexes [71, 72]. Focal adhesion proteins in these complexes mediate bidirectional mechanical transduction among integrins, external stimuli, and the cell [73]. Extensive research has found that integrin-focal adhesion complexes have the ability to sense forces important to the aortic valve, including cyclic stretch [74], shear stress [75], and hypotonic stress [76]. Integrin-focal adhesion complexes are also critical in signaling changes in the cell phenotype in response to mechanical stimuli and other cues, such as signals for cell and tissue remodeling [77, 78], cell proliferation and apoptosis [78, 79], and cell migration and angiogenesis [75, 80]. Integrins encompass only one of the families of mechanosensors, but the signals they transmit through focal adhesion complexes are critical for cell phenotype.

G protein-coupled receptors (GPCR)

Similar to the other transmembrane proteins discussed above, GPCR bind to a variety of extracellular ligands to activate downstream signaling, namely through G-protein activated signal transduction pathways [81]. These receptors have also been shown to be strongly sensitive to changes in flow across the surface of the endothelium [82]. Some research has demonstrated the specific methods of subunit recruitment utilized by the GPCR to become activated under mechanical stimuli [83], but the role of GPCR in the endothelium has not been fully realized in the vasculature or in the valve. Studies by Anger et al. showed that statins may partially inhibit inflammation in the aortic valve is through GPCR and their downstream effectors [84]. This work also demonstrated via array analysis that the extracellular regulated kinase (ERK) activation regulated by GPCR is highly upregulated in calcified human aortic valve tissue [84]. In addition, although the mechanism is unclear, statin therapy inhibits valvular expression of the GPCR regulatory proteins (RGS) [84]. While this initial data offer exciting directions for future targeted therapies, new insights have not been discovered. GPCR have known functions in many disease models [85], but their potential importance in the valve is not fully clear. More work must be conducted in this field to integrate these mechanical receptors into the lexicon of valvular mechanobiology.

Glycocalyx

The large network of sugars embedded into the cell membrane consists of proteoglycans and glycoproteins, bound to long chains of carbohydrates called glycosaminoglycans (GAGs). These sugars provide a physical barrier between the blood and the endothelial cells [86, 87] and act as a “trap” where ions and other molecules in the blood may interact with membrane proteins [88]. The endothelial glycocalyx significantly changes in shape and height as a result of disturbed flow, possibly leading to changes in its function as a scaffold for signaling molecules [89]. Inflammation also plays a role in the deformation of the glycocalyx, possibly indicating a positive feedback between the

oscillatory flow and inflammation, which leads to upregulation of pro-inflammatory signaling pathways [90]. Specific studies of the glycocalyx in the valve endothelium show that pro-inflammatory mediators such as low-density lipoprotein (LDL) and immunoglobulins are more tightly bound to the sugar network in the valves of rabbits fed a high-cholesterol diet [91, 92]. The binding of these molecules to the glycocalyx is increased on the fibrosa endothelium, the aortic side of the valve more vulnerable to interstitial calcification. Investigative work by Sarphie [92] shows a the link between shear stress and the composition of the glycocalyx, which may alter the affinity of LDL particles for the cell surface and lead to infiltration and lesion formation. Of note, these studies have not been confirmed or improved for over a quarter century, leaving a significant gap in our understanding of the glycocalyx and its role in the valve. New technologies may prove useful in understanding this role and developing future therapies which may change glycocalyx stability and composition. In addition, although the characterization of the glycocalyx has not recently been studied in the valve, its extensive characterization in the vasculature may be easily translated to the valvular environment. With more work focused on this exciting area, we may discover a wide assortment of targets for therapeutic intervention in early stages of valve dysfunction in the future.

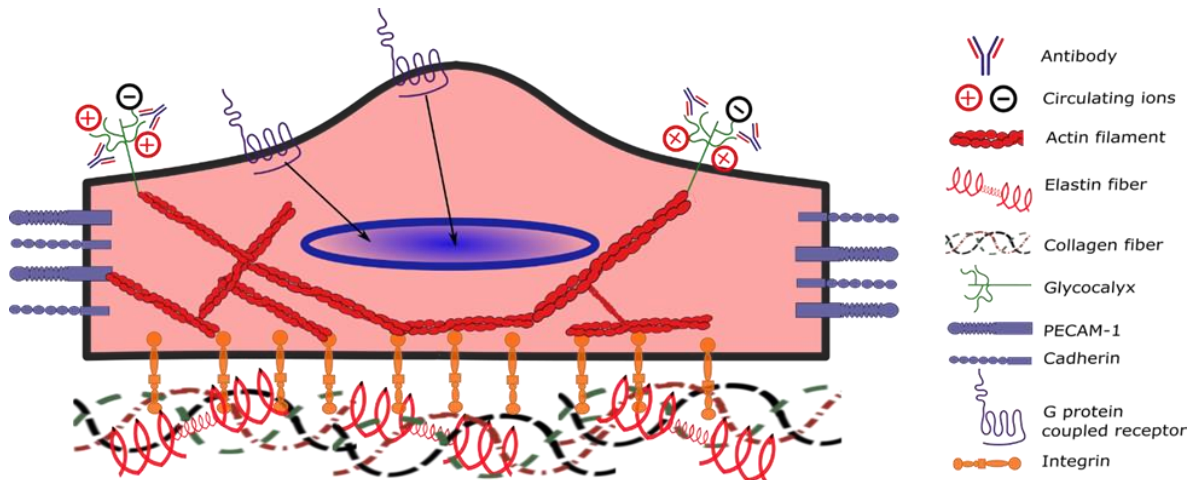


Figure 1.4 Major mechanosensors in valvular endothelial cells

Integrins bind to the extracellular matrix to sense the dynamic mechanical environment surrounding the endothelial cell. Ions and antibodies are trapped by the glycocalyx in the surface of the cell, which translates to various downstream signal transduction pathways. Cell adhesion molecules (CAMs), such as cadherins or PECAM-1, sense changes in the mechanical environment between cells due to shear stress or other mechanical stimuli. These mechanosensors transduce the changes sensed through diverse signaling cascades (represented by black arrows) and through the actin cytoskeleton, which ultimately leads to transcriptional changes. The function of G protein coupled receptors is not fully known in the valve but their role in vascular endothelium suggests that they play a role in sensing the cellular mechanical environment and causing transcriptional changes in the nucleus.

1.5 Mechanosensitive genes in flow-mediated valve biology and dysfunction

Shear stress is an important regulator of endothelial cell function. The vascular endothelium has been widely studied in the context of shear stress, and a variety of vascular mechanosensitive genes have been discovered [66, 93-95]. However, little is known about the role of these mechanosensitive genes in the valvular endothelium. In this section, we review the genes that have been studied in valvular endothelial cells, including some exciting new opportunities in valve research based on findings in the vasculature. For reference, Figure 1.5 shows a summary of valvular mechanosensitive genes in both disturbed flow, as seen at the calcifying fibrosa, and laminar flow, as observed at the ventricularis.

Transforming growth factor- β (TGF- β) ligand and receptors

The TGF- β family of growth factors regulate a wide variety of cellular response such as growth, development, immune system regulation, and tissue homeostasis [96]. TGF- β signaling is initiated by the binding of TGF- β to TGF- β receptors type I and type II. These two receptors form a receptor heterocomplex that recruits and phosphorylates R-Smad proteins. Different signal transduction pathways can be activated depending on the Smad protein complexes phosphorylated [97]. TGF- β activity increases more than 100-fold in bovine aortic endothelial cells under shear conditions compared to static condition [98], suggesting that TGF- β plays a role in flow-induced vascular remodeling driven by fluid shear stress in the endothelium.

Villar et al [99] found that in patients with aortic stenosis circulating plasma levels of TGF- $\beta 1$, the most abundant isoform of the TGF- β family, were nearly three-fold higher than in healthy controls. Yetkin et al [100] studied patients with tricuspid calcified and stenotic aortic valves and found that the calcified valves presented similarly increased expression of TGF- $\beta 1$. Furthermore, this work suggested a link between TGF- $\beta 1$ and cysteine C, a cysteine protease inhibitor highly expressed in mature osteoblasts that inhibits bone resorption and appears in osteoblast differentiation [101, 102]. These findings show that high levels of the TGF- β cytokine in blood induce an endothelial cell inflammatory phenotype; thus, TGF- β and its receptors may play an important role in aortic valve calcification and in regulating AV endothelium function . TGF- β has also been found to promote endothelial-mesenchymal transition (EndMT); ovine aortic valve endothelial cells grown in the presence of TGF- β exhibited decreased levels of CD31 (an endothelial cell marker) and increased levels of α -smooth muscle actin [103].

The combined evidence from these studies illustrates the importance of TGF- β in the events leading to CAVD. Matrix production and endothelial phenotypic transformation are critical for the events leading to CAVD, and TGF- β is a critical regulator of these pathologies.

Bone morphogenetic proteins (BMPs)

BMPs are multi-functional growth factors that belong to TGF- β superfamily [104]. These proteins are physiologically observed in bone and initiate bone formation during development and in injury [105]. In vascular endothelium, bone morphogenetic protein 4 (BMP4) is upregulated by disturbed flow, leading to endothelial inflammation and ultimately dysfunction [105-107]. Additionally, in human atherosclerotic vasculature, both BMP2 and BMP4 expression are upregulated [105, 108]. Endothelial dysfunction and hypertension in mice infused with BMP4 has been observed [109], and BMP antagonist treatment protects against atherosclerosis [110, 111]. Endothelial cells in the aortic valve may secrete BMPs in response to changes in shear stress [112], and BMP expression of interstitial cells may be linked with age-related valvular degeneration [106]. Smad 1, 5, and 8 are downstream molecules in the BMP signaling pathway and have been associated with the onset of aortic stenosis [113]. Sucosky et al [65] studied porcine aortic valve leaflets exposed to physiological and altered shear-stress conditions for 48 hours *ex vivo* and found that BMP-4 and TGF- β were increased in pathologically altered conditions; these conditions stimulated endothelial inflammatory response demonstrated by an increase in adhesion molecule expression. These results were validated by Ankeny et al [54] in human calcified aortic valves and non-calcified AVs; calcified fibrosa presented higher Smad 1/5/8 phosphorylation and lower BMP antagonists (crossviesless-2/BMPER

and noggin). This data, in the valve and in other vascular tissues, strongly suggests the importance of the BMP signaling pathway in aortic valve calcification.

Wnt/ β -catenin

Wnt proteins are a family of secreted signaling glycoproteins used for short- or long- range signaling. They bind to receptors of the Frizzled family to regulate a wide variety of cellular processes such as cell fate determination, motility, stem cell renewal, and cell migration [114-116]. The Wnt/ β -catenin pathway (also known as the canonical Wnt pathway) is widely known to regulate aortic valve formation and disease [117]. β -catenin is a cytosolic protein that is bound to Wnt receptors in the cytosol and is degraded via ubiquitination in the absence of Wnt [118]. When Wnt binds to Wnt receptors, β -catenin is stabilized and released to the cytosol, where it accumulates and translocates to the nucleus to activate the transcription of specific genes [114]. Shear stress has been found to regulate the canonical Wnt pathway in endothelial cells, leading to the increased expression of angiopoietin-2, a protein involved in vascular development and repair, in human aortic endothelial cells (HAECs) [119]. In patients with symptomatic aortic valve stenosis, modulators of the Wnt signaling pathway, including WIF-1, DKK-1, and sFRP-3, exhibit increased expression in calcified aortic valves. Some modulators also positively correlate with valvular calcification, indicating their potential role as biomarkers of aortic valve stenosis [120]. Additionally, total levels of Wnt binding protein β -catenin have been found to be upregulated in human calcified aortic valves [121], calcified valves in a hypercholesterolemic rabbit model [122], and calcified valves in a hypercholesterolemic mouse model [123]. This evidence shows the importance of the Wnt canonical pathway in CAVD. No evidence directly linking the Wnt/ β -catenin pathway and valvular shear stress has been found; however, the data obtained from HAECs indicates that the abnormal shear stress profile in the fibrosa may regulate this pathway and lead to CAVD.

Notch signaling pathways

Notch is a single transmembrane protein that, upon activation, releases a soluble Notch intracellular domain; this domain translocates to the nucleus and binds to specific sequences in the DNA to regulate gene transcription [124, 125]. The Notch signaling pathway plays a critical role in the development and homeostasis of the cardiovascular system [126]. While not directly working with the valve endothelium, Theodoris et al [127] studied the effect of shear stress in Notch1 (a single transmembrane protein of the Notch family) in endothelial cells. Notch1 haploinsufficient (Notch1^{+/-}) and wild-type (Notch1^{+/+}) iPSC-derived ECs were exposed to hemodynamic shear stress. The expression of more than 1,000 genes involved in osteogenesis, oxidative stress, and inflammation was dysregulated in the Notch1^{+/-} cells, causing an osteogenic and inflammatory phenotype. Interestingly, in the aortic valve, overrepresentation of Notch1 missense variants correlates with increased prevalence of bicuspid aortic valve disease in human patients [128]. Notch1 in the aortic valve interstitium has been found to repress the activity of Runx2, a transcription regulator of osteoblast cell fate [129]; therefore, decreased expression of Notch1 in the aortic valve may lead to accelerated valve calcification. While no known direct link relates the disturbed shear stress profile observed at the fibrosa with calcification, hemodynamic shear stress at the ventricularis may promote Notch1 activity, leading to an anti-osteogenic and anti-inflammatory endothelial phenotype that protects the ventricularis endothelium from dysfunction and calcification.

Nitric oxide (NO) signaling and endothelial nitric oxide synthase (eNOS)

Nitric oxide (NO) is a soluble gas with a short half-life (up to 30 seconds) that is synthesized from the amino acid L-arginine by the constitutive calcium calmodulin-dependent enzyme nitric oxide synthase (NOS) [130]. It is considered one of the most

important substances produced in the endothelium and plays a key role in inflammation, vasodilation, and oxidative stress [131]. Decreased NO biosynthesis facilitates vascular inflammation through an increase in lipoprotein oxidation [132]. Endothelial nitric oxide synthase (eNOS) is a shear-sensitive gene that is upregulated in laminar shear conditions (physiological conditions) and downregulated in low and oscillatory shear conditions (pathophysiological conditions) [133]. Bosse et al [134] studied the role of NO in aortic valve calcification using a co-culture system of endothelial cells and aortic valve interstitial cells (AVICs). The authors found that endothelial cells secrete NO which is absorbed by AVICs, preventing calcification through regulation of the Notch1 signaling pathway in AVICs. Richards et al [53] found that, in both calcified and non-calcified human aortic valves, the ventricularis side exhibited three-fold higher expression of eNOS compared to the fibrosa. Interestingly, the calcified valves presented lower values of eNOS expression on both sides compared to healthy aortic valves. In the same study, *in vitro* experiments determined that endothelial secretion of NO decreases myofibroblastic activation, osteoblastic differentiation, and matrix calcification of valvular interstitial cells. El Accaoui et al [135] developed a mice model of aortic valve stenosis by knocking down eNOS. They found that 30% of these mice had bicuspid aortic valves and that these mice presented fibrosis and calcification at six and eighteen months of age. To further validate their work, El Accoui et al co-cultured porcine VICs with or without valvular endothelial cells, and they found that the endothelial cells inhibited profibrotic processes in VICs.

This VIC study shows the importance of eNOS in valvular calcification and provides a clear mechanism linking decreased NO bioavailability to endothelial dysfunction and increased fibrosis and calcification. While NO has been investigated

previously as a therapeutic agent, stimulation of endothelial NO production and exogenous NO treatment in the valve still offers an avenue for potential therapy in aortic valve disease.

Reactive oxygen species (ROS)

ROS are partially reduced metabolites of oxygen that possess high oxidizing capabilities and act by damaging DNA and oxidizing lipid and cellular constituents [136]. They regulate cell growth, apoptosis, senescence, cell adhesion, and differentiation and are considered a key component in inflammatory diseases [137, 138]. One of the most important mechanisms in ROS production is the NADPH oxidase complex, which donates an electron to oxygen species in the cell to generate superoxide [139]. Both gene expression and protein levels of NADPH are increased four-fold in oscillatory flow in bovine aortic endothelial cells; this correlates with an increase of oxidized LDL through superoxide ($O_2^{\cdot-}$) modification [140]. Under laminar shear stress, the ROS production in human umbilical vein endothelial cells (HUVECs) increases initially but decreases back to baseline levels over time, demonstrating the complexity of ROS signaling in the endothelium [141]. Both superoxide and hydrogen peroxide expression are significantly increased in calcified regions of the valves; however, non-calcified regions, even in stenosed valves, present similar levels of superoxide and hydrogen peroxide as the tissue of healthy valves [142]. Finding key components in these pathways may be critical in creating a full picture of the pathological degeneration of the valve.

ROS play a role further downstream of the endothelium; even in early stages of CAVD, valvular interstitial cells exhibit an accumulation of ROS, suggesting the role of ROS in disease development [143-145]. Branchetti et al [146] collected VICs from patients with and without CAVD and found that cells from stenosed patients had ROS-induced DNA damage and impaired DNA repair ability, which could be rescued with antioxidant

enzyme treatment. In a thorough study showing the direct role of ROS in the interstitium, Das et al [147] found that treatments decreasing ROS formation, specifically via decreases in the MAPK-TGF- β pathway, resulted in decreased calcium nodule formation. Throughout the valve, ROS are important contributors to CAVD both at the endothelial and interstitial cell layer, and changes in the oxidative state of the valve and the valvular endothelium may contribute significantly to pathological degeneration of the valve.

Interleukins

Interleukins are important inflammatory cytokines released from T lymphocytes, macrophages, monocytes, and endothelial cells; they bind to specific cell receptors and play a role in communication with leukocytes, cell growth, and differentiation [148, 149]. Interleukins produced in the endothelium play an important role in several diseases such as atherosclerosis, tumor development, and chronic infections [148, 150]. Pathological low shear stress facilitates the increased expression of interleukin-6 (IL-6) and interleukin-1 (IL-1) from the endothelium, causing vascular smooth muscle cells to proliferate in early atherosclerotic plaques [151]. Interleukins also play a role in the valve: IL-6 has been found to be involved in the development and progression of aortic valve disease by affecting EndMT [152]. In innovative studies, Mahler et al [153] utilized a three-dimensional collagen gel to culture porcine aortic valve endothelial cells (PAVECs); they found that PAVECs underwent EndMT via the Akt/nuclear factor- $\kappa\beta$ -dependent pathway when treated with IL-6 in a dose-dependent manner. Thus, IL-6 is a potent regulator of EndMT, which is a critical step in tissue dysfunction and ultimately valve calcification [154]. Moura et al [155] conducted a study in patients with asymptomatic moderate to severe aortic stenosis treated with or without rosuvastatin, a statin used to reduce total and LDL cholesterol [156]; the expression of IL-6 was measured in the patients before and

after the statin treatment. Patients treated with rosuvastatin exhibited a slowed progression of aortic valve stenosis and a five-fold decrease in the serum levels of IL-6, indicating reduced inflammation at the endothelial level. Interleukin-1 is expressed in the endothelium of atherosclerotic plaque and may be linked to atherogenic inflammation [157]. In the frame of aortic valve disease, IL-1 receptor antagonist deficient mouse were studied. These mice presented an increase in aortic valve thickness compared to wild type mice. T cells of the IL-1 receptor deficient mouse were analyzed and found to express much higher levels of tumor necrosis factor (TNF)- α compared to T-cells of wild-type mice. This finding suggests that IL-1 may induce inflammation in aortic valve endothelial cells through TNF- α signaling pathway and that this inflammation may play a critical role in development of aortic stenosis [158]. These studies, in combination with those *in vitro*, show that abnormal shear stress, as experienced at the fibrosa, increases IL-6 and this interleukin, possibly coupled with others, promotes valve calcification.

Kruppel-like factors (KLF)

Kruppel-like factors (KLF) are members of the zinc-finger family of transcription factors which bind to DNA sequences including CACC-, GC- or GT- box elements in promoter and enhancer regions [159]. In the vascular endothelium, KLF2 has been widely studied; it is upregulated in high laminar unidirectional shear stress (physiological conditions) and downregulated in low oscillatory shear stress (pathophysiological conditions) [160-162]. In extensive *in vitro* experiments, human aortic valve endothelial cells (HAVECs) from non-calcified aortic valves exhibited higher KLF2 expression in high unidirectional shear stress (20 dynes/cm², conditions similar to ventricularis) and lower expression in low oscillatory shear stress (\pm 5 dynes/cm², conditions similar to fibrosa); these studies support the idea that the ventricularis side shows higher KLF2 expression and

an anti-inflammatory phenotype [14]. To study inflammatory markers such as KLF2 in detail, Weinberg et al [163] created a computational model of aortic valve hemodynamics to mimic the exact shear profile experienced by the aortic valve. The simulated shear profiles were then applied to HUVECs, and the expression of KLF2 was found to be significantly higher in the cells that experienced the ventricularis shear profile. In microarray studies by our group, porcine aortic valve fibrosa showed decreased expression of KLF2 and KLF4, indicating the importance of KLF2 and KLF4 in valvular endothelium [14]. These initial studies may lead to important discoveries for these anti-inflammatory markers in valvular function and endothelial cell phenotype.

KLF4 is another member of the KLF family that, when overexpressed, induces anti-inflammatory and anti-thrombotic factors such as thrombomodulin and endothelial nitric-oxide synthase; conversely, when knocked down, KLF4 induces inflammation [164, 165]. More importantly, KLF4 is known to be upregulated in vascular endothelial cells in laminar shear stress compared to oscillatory shear stress [166, 167]. So far, the role of this KLF protein in aortic valve calcification is unknown; however, a study conducted by Maleki et al [168] analyzed patients with bicuspid aortic valve (BAV), who are known to develop aortic valvular stenosis more rapidly than patients with tricuspid aortic valve (TAV), and found a significant decrease in KLF4 expression in the aortic region near the valve in BAV patients compared to TAV patients. The authors postulate that the disturbed flow generated by BAV is the primary contributor to this decreased KLF4 expression. Therefore, we expect that the same abnormal shear profile will be experienced by the valve and will cause a decrease of KLF4 and an increase in inflammatory endothelial response.

YAP/TAZ pathway

YAP and TAZ are effectors of the Hippo signaling cascade known to regulate several transcription factors that are key players in CAVD such as Runx2, SMADs, and PPAR [169]. These effectors have been studied in aortic valve interstitial cells where they have been correlated with osteoblastic differentiation [170]. Interestingly, changes in matrix stiffness, such as the ones observed during AV fibrosis, have been shown to affect translocation and activation of YAP which indicates a potential link between ECM degradation and osteoblastic differentiation [171]. This pathway has also been found to be flow-sensitive in the vascular endothelium where it was upregulated in disturbed flow conditions and its inhibition lead to decreased atherogenesis [172, 173]. However, the flow-sensitive role of these effectors in the valvular endothelium is yet to be studied.

Endothelial-to-mesenchymal transition (EndMT)

EndMT is defined as the process by which endothelial cells lose a portion of their cellular features and obtain characteristics of mesenchymal cells such as loss of tight junctions, increased motility and increased ECM secretion [174]. EndMT has been widely studied in the vascular endothelium and atherosclerosis where it has been shown that disturbed flow promoted EndMT and its inhibition reduced atherosclerosis progression [175]. Regarding EndMT in the aortic valve endothelium, changes in matrix stiffness, such as the ones observed in AV fibrosis, can induce EndMT [176]. Another study demonstrated that treatment of TNF α to valvular endothelial cells promoted EndMT [177]. Aikawa et al [178] studied the interplay between interstitial cells and endothelial cells demonstrating that VICs can help mitigate EndMT when in contact with VECs which reinforces the notion that the interplay between VECs and VICs is crucial for CAVD. The role of shear stress in EndMT in the aortic has not been fully studied however there has been a study by Butcher et al [179] that demonstrated that oscillatory shear stress increased markers of EndMT

(ACTA2, SMA, Snail and TGF β 1) in valvular endothelial cells while steady flow did not. This study does not delve in the mechanism by which EndMT is regulated by shear stress and opens interesting avenues for future studies to better understanding such a key step in CAVD pathogenesis.

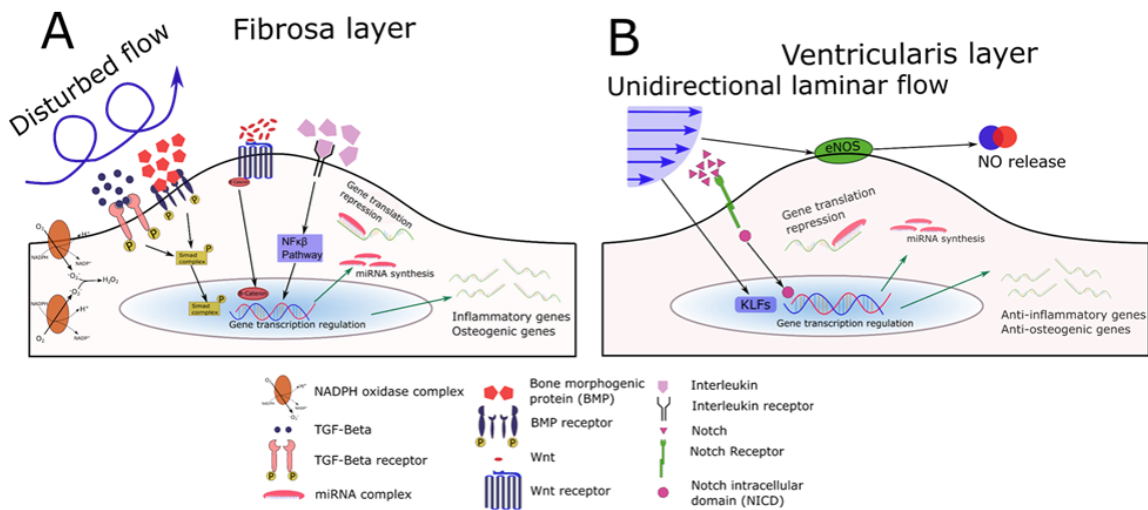


Figure 1.1.5 Mechanosensitive genes in the aortic valve endothelium

A) TGF- β and BMP are mechanosensitive molecules that bind to their respective receptors and activate the SMAD signaling cascade by phosphorylating SMAD molecules, which ultimately translocate to the nucleus. Wnt molecules bind to frizzled Wnt receptors and cause the release of β -catenin (Wnt canonical pathway) which leads to cytosolic β -catenin accumulation and translocation to the nucleus. Interleukins bind to interleukin receptors and regulate the NF- κ B signaling cascade that alters gene transcription. All these pathways induce inflammatory and osteogenic gene transcription, leading to endothelial dysfunction. Inflammatory miRNAs are also upregulated in disturbed flow, causing gene translation repression of anti-inflammatory genes. NADPH is upregulated in disturbed flow, which induces the generation of ROS. **B)** KLFs are mechanosensitive genes upregulated in laminar flow that translocate to the nucleus and induce anti-inflammatory gene transcription. Notch1 binds to Notch receptors and causes NICD to be released and translocate to the nucleus, thereby promoting gene transcription. Anti-inflammatory miRNAs are upregulated in laminar flow, repressing translation of inflammatory genes. eNOS is upregulated in laminar flow and induces nitric oxide generation and release outside of the cell [5].

1.6 *In vitro* and *in vivo* models to study CAVD

1.6.1 *In vitro* and *ex vivo* models of CAVD

One of the first and most characterized *in vitro* models of shear stress is the cone-and-plate viscometer [180, 181]. In this system, shear stress is applied to cultured cells in a stationary plate by a rotating cone. A modified version including a speed-controlled motor with variable rotational velocities was later introduced [182]. More recently, our lab has developed a modified cone-and-plate which is housed in a standard incubator; in this system, programmed shear stress profiles can be controlled by using a computer [183, 184]. Furthermore, in collaboration with Dr. Nerem and Dr. Yoganathan, we have developed a modified cone-and-plate viscometer that can be used with porcine AVs and can apply different shear stress profiles using a computer [15, 65, 185]. Another relevant porcine model for aortic valve calcification has been developed by Balachandran et al [71]. In this model, the effects of cyclic stretch were studied using porcine aortic valve leaflets in a unidirectional stretch bioreactor. Calcification increased significantly under higher stretch conditions, along with bone marker expression, cellular apoptosis, total calcium content, and alkaline phosphatase activity. These results correlate with those observed in human valve calcification and prove the utility of this model for the study of CAVD mechanisms and treatments.

Another *in vitro* model of shear stress is the parallel-plate flow chamber, developed originally by Frangos, McIntire, and colleagues [186, 187]. In this system, a flow chamber consisting of a polycarbonate plate, a rectangular Silastic gasket, and a glass slide (or cover slip) with the attached EC monolayer is held together by a vacuum maintained at the periphery of the slide. Additionally, novel shear stress system developed by Ibbidi ® consists of two syringes connected to a slide with a channel where cells are plated; by applying different pressure to the syringes the system can generate various shear stress profiles. This system allows for long-term experiments in sterile conditions and for live

imaging as the only part of the system that needs to be in the microscope is the slide. Although these shear stress systems are the most commonly used *in vitro* shear systems, microfluidic chambers are being used because they allow for high throughput experiments. This method was pioneered and commercialized by Schaff et al. [188-190]. More recently there have been new bioreactors that allow for more precise control of shear stress profiles and matrix composition and that have been used to study shear profiles in valvular endothelial cells such as the one developed by Butcher et al [179].

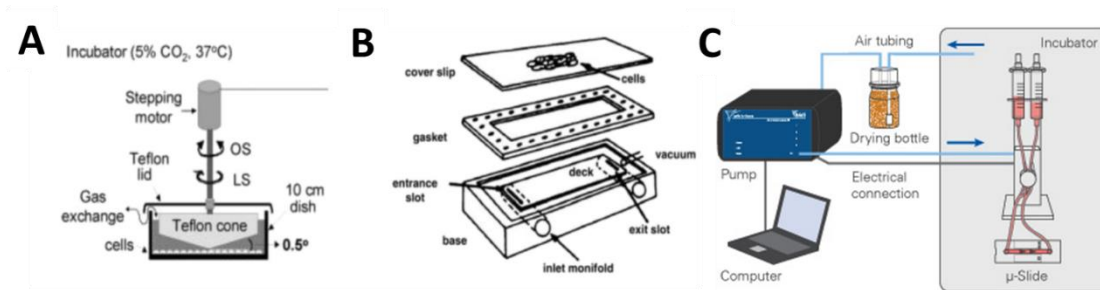


Figure 1.1.6 Models of flow and shear stress.

A) Cone-and-plate viscometer. Adapted from Jo et al. (1991). **B)** Parallel plate flow chamber. Adapted from Lawrence et al. (1987). **C)** Ibidi shear stress system.

1.6.2 *In vivo* models of CAVD

To study CAVD in a controlled system, animal models of valvular dysfunction are utilized in a laboratory setting. The same principles used to diagnose CAVD in humans may be used to study the progression of the disease in animal models. Valvular cells extracted from bovine sources have been widely used because they are easy to extract and because the structure of the bovine aortic valve is similar to the human aortic valve [65-67]. Porcine models have also been widely utilized for studies of the aortic valve, since the heart and cardiovascular system of the pig are really close in size to the human equivalents [68-70]. Furthermore, hypercholesteremia can be induced in rabbits by feeding them a high cholesterol (0.25%) diet for prolonged periods of time (12-16 weeks); this diet induces the development of atherosclerosis and aortic valve calcification [72-74]. Another interesting

in vivo model uses high cholesterol diets supplemented with Vitamin D2 in New Zealand Rabbits to increase transvalvular velocity and induce the presence of calcific nodules in the AV [191]. In each of the cases listed above, the cost of maintaining, breeding, and genetically modifying such large animals is often prohibitive. Thus, the mouse has been explored as a tool for further valve studies by our group and many others.

The mouse has been widely used to study aortic valve disease progression [192]. As wild-type (WT) mouse strains do not develop aortic valve calcification spontaneously, dietary and/or genetic modifications are necessary to induce AV disease. Commonly, mice deficient in the low-density lipoprotein (LDL) receptor (*Ldlr*^{-/-}) are used. *Ldlr*^{-/-} mice with only apolipoprotein B (ApoB)-100 (*Ldlr*^{-/-};only) spontaneously develop mild hypercholesterolemia and reductions in valve orifice diameter (>50%); this leads to increased transvalvular systolic pressure gradients, and left ventricular hypertrophy at the age of ~1.5 years when fed with regular diet [193].

Typically, the Harlan Teklad TD.88137, or “Western” diet, is used in models with a dietary induction component [194]. Towler and colleagues first reported extreme hyperlipidemia (~1040 mg/dL), hyperinsulinemia/hyperglycemia, and mineral deposition in *Ldlr*^{-/-} mice fed Western diet for 16 weeks [195]. *Ldlr*^{-/-} mice fed a similar high-cholesterol diet (0.15%) develop increased valve thickness, macrophage accumulation, superoxide production, activated myofibroblasts and osteoblasts, and mineralization[196]. When mice are regularly exercised while being fed a high-cholesterol diet, these pathological symptoms are significantly reversed [196]. Another recent study by Scatena et al [197] in *LDL*^{-/-}*ApoB*^{100/100} showed that use of diabetogenic and pro-calcific diet induced endothelial dysfunction, inflamed and calcified thickened aortic valve cusps mimicking CAVD features found in patients with type II diabetes mellitus.

Most interestingly, other diets, such as the high-fat, low-cholesterol diet are able to induce early markers of CAVD even in WT mice; thickened leaflets, black particulates which may be von-Kossa-positive phosphate staining, decreased aortic valve opening area,

and increased transvalvular blood velocities are reported, along with CD68-positive macrophage and T-lymphocyte infiltration into the valvular interstitium [198].

In addition to the *Ldlr*^{-/-} model, a second common genetically manipulated model is the endogenously hyperlipidemic [199] ApoE-deficient (*ApoE*^{-/-}) mouse [200, 201]. ApoE allows receptor-mediated removal of very-low density lipoprotein (VLDL) from circulation. ApoE also regulates T-cell proliferation and macrophage function, and it modulates lipid antigen presentation as well as general levels of inflammation and oxidation [202]. *ApoE*^{-/-} mice fed with regular diet develop hypercholesterolemia (~490 mg/dL) [203], and when aged (~2.5 years) they present increased transvalvular velocity, mild aortic regurgitation, SMA and osteocalcin (OCN) expression, macrophage and T-cell infiltration, and nodular calcification [204]. Administration of the “Western diet” to *ApoE*^{-/-} mice for four to five months induces accelerated early disease, with a substantial increase in serum cholesterol (up to ~588 mg/dL), thickened leaflets, activated endothelial cells, and subendothelial lesions rich in macrophages (colocalized with MMP-2/9, cathepsin B, SMA, ALP, Runx2, and OCN expression) [205, 206]. Importantly, there is no evidence of calcification at this early time point, though a bisphosphonate-conjugated imaging particle shows signs of early microcalcification that colocalizes with cathepsin K [205, 206].

Along with these two commonly used hyperlipidemic models, other interesting genetic models that mimic some aspects of CAVD exist. Knockout of the mineral-binding ECM protein matrix GLA protein (*Mgp*^{-/-}) produces spontaneous ectopic apatite formation in the arterial collagen fibrils and von-Kossa-positive calcification in the aortic valve [207]. In addition, an insufficiency of elastin (*Eln*^{+/-}) produces proliferation of VICs and aortic regurgitation [208]. Hypomorphic expression of fibulin-4, an ECM stabilizing protein, results in thickened leaflets and significant functional impairments, as well as positive pSmad2, pSmad1/5/8, and von Kossa staining [209]. Mice deficient in the anti-inflammatory cytokine interleukin-1 receptor antagonist (*Il1rn*^{-/-}) are particularly

important in studying the onset of CAVD. These animals develop thickened aortic valves infiltrated by macrophages and differentiated myofibroblasts when aged, *Il1rn*^{-/-} mice develop calcified lesions with functional impacts on transvalvular blood velocity [158]. Endothelial nitric oxide synthase 3 (eNOS) knockout mice supplemented with a cholesterol-enriched diet with Vitamin D2 (25,000 IU, daily) have been shown to present microcalcifications in the aortic valve sinus in just three months[210]. Furthermore, we have been working on a novel transgenic GATA5 knockout mouse; 15% of this mouse strain has been shown to present bicuspid aortic valve phenotype [211]. As previously stated, BAV patients present AV calcification at an earlier age [28]. We want to capitalize on this phenomenon by combining it with hypercholesterolemia to develop an accelerated model of AV calcification.

Various techniques may be used to measure murine aortic valve function, including ultrasound, magnetic resonance imaging (MRI), catheterization, and *ex vivo* tissue staining. Overall, MRI is the best technique in assessing the degree of aortic stenosis because it causes no injury to the animal and gives information about valve morphology, severity of stenosis and anatomy and function of the heart. Unfortunately, MRI is expensive and requires a high level of sedation. Additionally, catheterization is a powerful technique, but it requires the mice to be fully sedated and may cause internal injuries [75]. To confirm the extent of leaflet calcification, post-mortem sectioning of the aortic valve and staining with dyes such as Alizarin red [76, 77] or von Kossa stain [71, 78] is required. However, to harvest the heart and vasculature, the animal must be sacrificed, and disease progression cannot be monitored. Due to these limitation, ultrasound echocardiographic imaging is most widely used. This method conveys the same information as MRI with less precision. However, the advantages of echocardiography are low levels of sedation required (which decreases the likelihood that the method may interfere with the biological study) and the relatively low cost of the imaging.

Our group and others have proven the utility of echocardiography in assessing the status of aortic stenosis in mice. Two images obtained with echo are shown below. The left panel of Figure 1.7 shows the peak aortic valve velocity for a young (2 months of age) ApoE^{-/-} mice; a peak velocity of 900 mm/s can be observed. The right panel shows the peak aortic valve velocity for aged ApoE^{-/-} (15 months) mice with three months of high-fat diet; the peak velocity is much higher (in the range of 2200 mm/s) indicating that the aortic valve is stenosed. Post-mortem calcification staining on these leaflets showed that valves with severe stenosis have calcification nodules on the leaflets and the aortic valve root. Mice with no stenosis present non-calcified valves and non-calcified root.

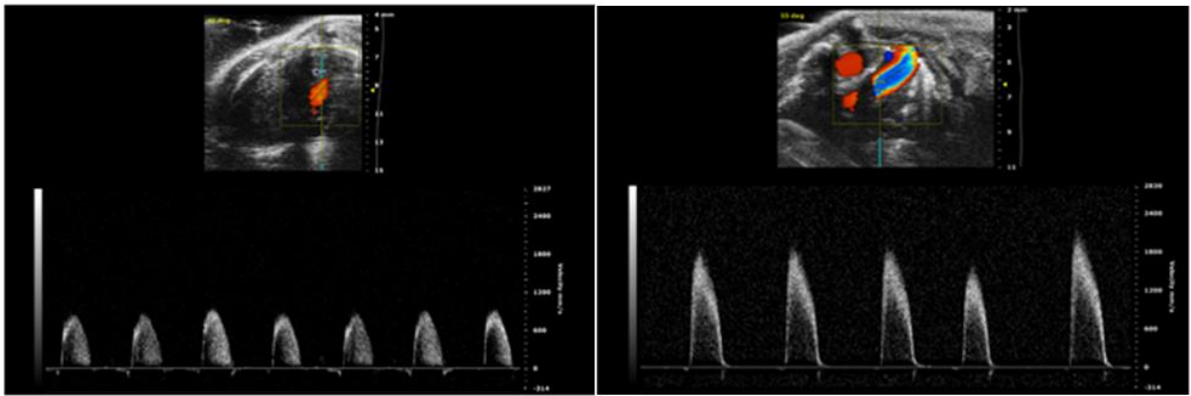


Figure 1.7 Echocardiogram of healthy and diseased mouse aortic valve. The left panel shows the aortic valve velocity of a young, healthy mouse (900mm/s) while the right panel shows the aortic valve velocity of old, hypercholesterolemic mice (2.200 mm/s).

1.6.3 Computational Models of CAVD

Alternative models including several powerful computer imaging techniques are being increasingly used to visualize the dynamics of valve function and dysfunction. A recent study by Weinberg et al [79, 80] proposes a computational model for the aging aortic valve that varies the leaflet thickness and extensibility from data obtained experimentally. Progression of CAVD is modeled by adding calcified zones to the valve. The sites of calcification initiation are the regions of high flexure; these regions show preferential

calcification formation in explanted aortic valves. This model can predict how the peak velocity in the aortic valve and the aortic valve area evolve over time. A comparison between the model by Weinberg et al and experimental data [81] showed a good correlation between the two, proving the utility of computational models for the study of the disease progression. This study can be used clinically to predict degradation of valve function and to determine the best tissue parameters to target in order to diminish the rate of calcification. The data from this paper could also be used to create *in vitro* and *in vivo* models that mimic specific phases of CAVD. These models could be used to better study the different pathologies experienced in the valve can be better studied. Engineered and computer models of valve function and dysfunction have been expansive and comprehensive, giving us new insights into the hemodynamics of CAVD and offering novel tools for future research.

1.7 MicroRNAs and CAVD

1.7.1 Biogenesis of miRNAs

microRNAs (miRNAs) are a large class of evolutionarily conserved, noncoding RNAs typically 18 to 22 nucleotides in length. miRNAs primarily function as post-transcriptional regulators by interacting with the 3' untranslated region (3' UTR) of specific target mRNAs in a sequence-specific manner[212, 213]. A single miRNA can target hundreds of mRNAs. Pri-miRNAs are transcribed by RNA polymerase II and can be derived from individual miRNA genes, from introns of protein coding genes, or from polycistronic transcripts that often encode multiple closely-related miRNAs. Pri-miRNAs are then processed in the nucleus into pre-miRNAs by the RNase Drosha, pre-miRNAs are 70–100 nucleotides hairpin-shaped precursors. Following transport to the cytoplasm, the pre-miRNA is further processed by the RNA endonuclease Dicer to produce a double-stranded miRNA. The fully processed miRNA duplex is then incorporated into a multicomponent protein complex known as an RNA-induced silencing complex (RISC). During this process, one strand of the miRNA duplex is selected as a mature miRNA while

the other strand, known as miRNA*, is rapidly removed and degraded[214-217]. As part of the RISC, miRNAs negatively regulate gene expression through translational repression or mRNA cleavage, depending on the degree of complementarity.

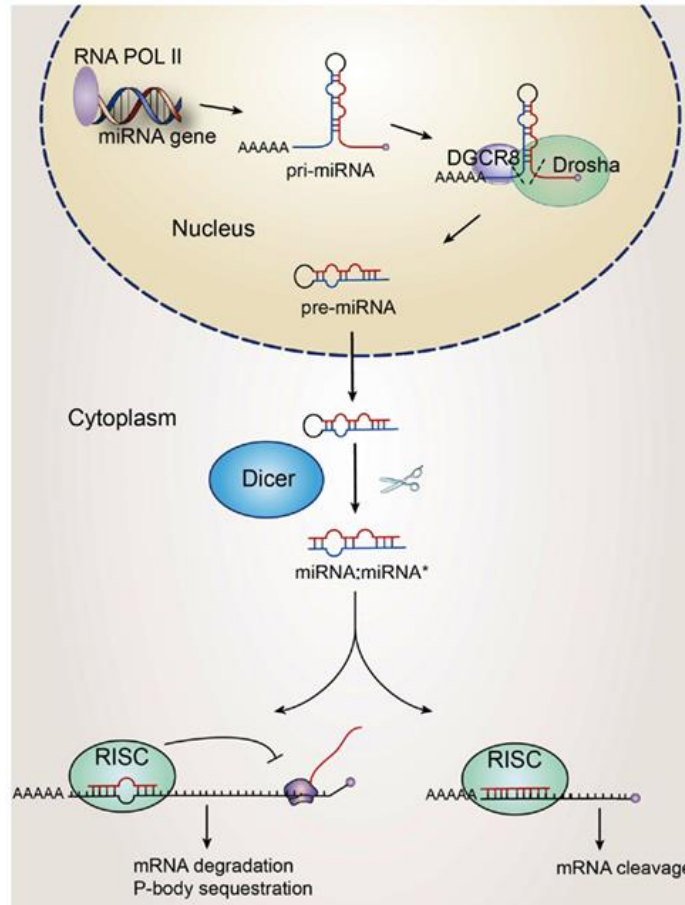


Figure 1.8 Biogenesis of miRNAs

Adapted from Barca-Mayo (2012) [4]

1.7.2 Role of miRNAs in CAVD

While the role of mechanosensitive miRNAs in atherosclerosis is well-established [218], their role in AV biology and disease is only beginning to emerge [5, 219]. To identify mechanosensitive miRNAs in the AV endothelium, we conducted a miRNA array study in human AVECs (HAVECs) exposed to steady flow conditions (LS, unidirectional laminar shear) and d-flow conditions (OS, oscillatory shear). Additionally, we categorized the well-known miRNAs according to their cellular function (Fig. 1.9A) [14]. We also carried out

an *ex vivo* array study using endothelial-enriched RNAs obtained from the fibrosa and ventricularis of healthy porcine aortic valves (PAVs) to identify side-specific miRNAs (Fig. 1.9C) [220]. These studies revealed ~30 shear-sensitive and ~24 side-specific miRNAs [14, 220], and using systems biology analyses we prioritized the list based on potential importance in CAVD (Fig. 1.9B). For coding genes (mRNAs), identifying the differentially expressed genes (>1,000) in various disease conditions such as atherosclerosis and cancer has become routine through gene array or RNA-Seq.

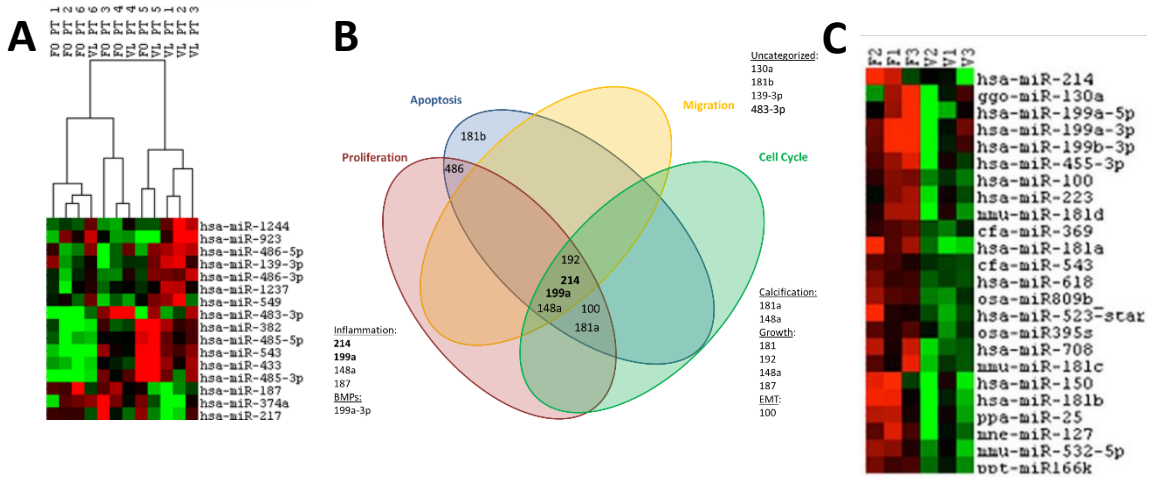


Figure 1.9 Shear-sensitive miRNAs in HAVECs and side-specific miRNAs in Porcine AVs

A) Top shear-sensitive miRNAs in HAVECs comparing fibrosa exposed to OS (FO) with ventricularis exposed to LS (VL). **B)** Categorization of the well-known shear-sensitive genes from our array according to potential cell function. **C)** Top side-specific miRNAs comparing fibrosa and ventricularis from porcine AVs.

The real challenge continues to be identifying those genes that play critical roles in the disease. While systems biology analyses and large-scale functional studies (such as the one we recently developed using a drosophila model [221]) have been incredible helpful, selected genes must still be studied in detail individually. The miRNA (~2,000 in humans) field faces an identical challenge. Recently, we published about the role of miR-214 in

shear-dependent AV calcification, and began to work on two of the most exciting miRNAs so far: miR-181b and miR-483-3p (referred as miR-483). MiR-214 expression is upregulated in the fibrosa endothelium (compared to the ventricularis) and in response to OS conditions (compared to LS). miR-214 also regulates TGF- β 1 in porcine AVs [220]. Interestingly, M1 macrophages can promote AV calcification by delivering miR-214 via micro-vesicles [222]. miR-125b is also upregulated in stenotic AVs compared to controls, and it regulates chemokines in diseased valve macrophages[223]. In contrast, Nigam et al identified miRNAs differentially expressed in aortic stenosis versus aortic insufficiency (miR-26a, -30b and -195) *in vivo* using whole human BAV tissue samples. They also linked these miRNAs to calcification-related genes in VICs, such as SMAD1/3, Runx2, and BMP2 [224]. Similarly, Wang et al [225] conducted miRNA arrays in healthy and diseased valves; these arrays provide a huge variety of novel miRNAs that can be potential therapeutic targets for CAVD. In another study, miR-141 was shown to be significantly decreased in BAVs and to regulate BMP2 [226]. Also, MALAT1, a long non-coding RNA implicated in other cardiovascular diseases, was shown to silence miR-204, leading to increased osteoblastic differentiation in human aortic VICs (HAVICs) via upregulation of SMAD4 and Runx2 [227, 228]. Another study showed that miR-486 and miR-204 are the top up- and down-regulated miRNAs respectively in diseased valves compared to controls. These two miRNAs play also a role in osteogenic differentiation of VICs [229]. Several new miRNAs have been recently shown to mediate AVIC calcification. miR-29b induces AVIC calcification via SMAD3 signaling [230], miR-204-5p promotes osteoblast differentiation via Runx2 upregulation [231], and miR-449c-5p [232] inhibits VIC osteogenic differentiation by silencing SMAD4. Recently, other studies have also

examined the role of miRs in CAVD: miR-616 regulates PON1 expression in CAVD tissues [233], miR-29b promotes calcification by activating the WNT/ β -catenin pathway in VICs [234], miR-92a is upregulated in calcified bicuspid valves and serves as a novel biomarker [235], and miR-195 promotes interstitial calcification in bicuspid valves via SMAD7 targeting [236].

These results demonstrate that several mechanosensitive and side-dependent miRNAs are associated with CAVD; however, miRNAs have yet to show a significant therapeutic potential to prevent or inhibit CAVD. The miRNA field in AV biology and CAVD is still in its infancy, and more studies by numerous groups are needed. For instance, because numerous investigators worldwide study cardiovascular disease (CVD) and cancer, many miR mimics (gain of function) and miR inhibitors such as anti-miRs (loss of function) are now being tested in clinical trials for cancer and CVD.

1.7.3 *miRNAs in the Clinic*

Given the increasing number of *in vivo* studies using miRNAs, some miRNA studies have moved into clinical trials. These miRNAs include anti-miR-122 (both LNA modified and galactose conjugated), anti-miR-103/107 (galactose modified), anti-miR-155 (LNA), miR-29 mimic, miR-16 mimic, and miR-34 mimic [237].

Anti-miR therapies

The first anti-miR therapy was the LNA-modified anti-miR-122, a 15-nucleotide antisense RNA oligo complementary to the 5' end of miR-122. This anti-miR is known as Miravirasen and is intended for the treatment of Hepatitis C Virus (HCV). Preclinical studies in rodents and in non-human primates indicate that Miravirasen passively accumulates in the liver, decreases cholesterol accumulation, and reduces titers of HCV [238-240]. A Phase I clinical trial was initiated in 2009 and no adverse reactions were reported; thus a Phase II trial was launched. In the first Phase II Trial, nine patients were

enrolled in four groups. Each patient received a dose of three, five, or seven mg/kg Miravirsen or placebo once a week for five weeks. Patients who received Miravirsen experienced a significant dose-dependent reduction in HCV load and serum cholesterol levels. [241]. However, a more recent follow-up study showed mutations near the end of the 5' UTR of HCV viral RNA in both *in vitro* samples and in clinical samples [242].

Furthermore, RG-101 (Regulus Therapeutics), is a N-acetyl-D-galactosamine (GalNAc)-conjugated anti-miR against miR-122. RG-101 has also undergone Phase I trials in HCV-infected patients at a single dose of two–four mg per kg. Furthermore, Phase II trials have combined RG-101 with direct-acting antivirals such as Harvoni (a combination of ledipasvir and sofosbuvir, see Regulus Therapeutics, press release dated 7 June 2016). However, this Phase II trials were put on hold by the US FDA after a second case of jaundice was reported (see Regulus Therapeutics, press release dated 1st Nov 2016).

Additionally, RG-125, a GalNAc-conjugated antimiR against miR-103/107, recently entered clinical trials for the treatment of non-alcoholic fatty liver disease. Furthermore, miR-103/107 expression is increased in the liver of obese mice, and it promotes diabetes progression by targeting caveolin 1, a protein involved in insulin signaling. Therefore, miR-103/107 is also being investigated at the pre-clinical stage in mice [243]. Finally, LNA-based anti-miR-155 (MRG-106; miRagen Therapeutics) has recently entered clinical trials to treat patients with cutaneous T cell lymphoma.

miR-mimic therapies

In addition to anti-miRs, miRNA mimics have also entered clinical trials. One of the most advanced miRNA mimics is MRX34, a miR-34 mimic by Mirna Therapeutics. It is encapsulated in a lipid carrier called NOV40. Preclinical studies of mice treated with MRX34 nanoparticles showed an accumulation of miR-34 in tumors, with significant tumor regression [244-247]. MRX34 entered a multicenter-phase I trial in 2013 in patients with primary liver cancer, small cell lung cancer, lymphoma, melanoma, multiple myeloma, or renal cell carcinoma. The trial included a dosage via intravenous infusion

either twice per week or five times per day. At the end of the trial, analysis of white blood cell samples showed significant reduction in miR-34 target mRNAs FOXP1 and BCL2. However, the trial was terminated due to patient deaths (see *Mirna Therapeutics Halts Phase 1 Clinical Study of MRX34*) [248].

In addition, miR-16 mimics have entered Phase I Trials for patients with malignant pleural mesothelioma in a collaboration between EnGeneIC and the Asbestos Diseases Research Institute of Australia. miR-16 was delivered in a nanoparticle with EGFR antibody surface conjugation to facilitate targeting to the tumor site. Preliminary data reported manageable safety in response to infusion of five billion nanocells loaded with 1.5µg of miR-15/16 mimics as a first dose level in the five enrolled patients [249]. Finally, two Phase I clinical trials of the miR-29 miRNA mimic MRG-201 (miRagen Therapeutics) have been started in patients with scleroderma.

Although a considerable number of studies involving miRNA therapeutics have been conducted over the years, only a small number of miRNA therapeutics have moved into clinical development. The biggest challenges in developing miRNA-based therapeutics is maximizing stability and minimizing off-target effects.

1.8 MiR-181b in CAVD

miR-181 family members contain four highly conserved mature miRNAs: miR-181a, -181b, -181c, and -181d. These miRNAs are independently-derived from six precursors located on three different chromosomes: miR-181a-1 and -181b-1 are located on chromosome 1; miR-181a-2 and -181b-2 are located on chromosome 9; miR-181c and -181d are located on chromosome 19. miR-181b-1 and -181b-2 are identical in their mature sequences but are located on different chromosomes [250].

The role of miR-181b is not yet clear. It has been previously studied in the endothelium by Sun et al [251], who showed that miR-181b was a protective miRNA that prevented inflammation by inhibiting NF-κβ activation via silencing of importin-α3.

Another study by Feinberg et al [252] showed that delivery of miR-181b mimic in obese mice lead to decreased endothelial dysfunction and increased expression of eNOS in adipose tissue ECs. Our group recently showed that miR-181b is one of the top shear-sensitive miRNAs in valvular endothelium and is upregulated in OS conditions compared to LS conditions [14]. Due to its high shear-sensitivity and unclear role in valvular endothelium, we have decided to further study the role of miR-181b in the valvular endothelium, and will this be the focus of the aim one of this dissertation.

1.9 ECM degradation and TIMP3 in CAVD

The organization of the extracellular matrix (ECM) in the AV is crucial in ensuring the proper opening and closing of the valve throughout a cardiac cycle. ECM remodeling is one of the hallmarks of CAVD because it is linked to fibrosis, an intermediate step in CAVD[253]. The major proteinases involved in ECM degradation are matrix metalloproteinases (MMPs), include collagenases, gelatinases, stromelysins, matrilysins, membrane-type MMPs, and others [254], and ADAMTS (a disintegrin and metalloproteinase with thrombospondin domains) metalloproteinases [255]. The membrane-anchored ADAM metalloproteinases affect cellular behavior by proteolytically releasing the extracellular domains of cell surface molecules, such as membrane-bound growth factors, cytokines, and cell adhesion molecules. Interestingly, MMPs are upregulated at calcification areas in diseased AVs [256]. However, MMP regulation in CAVD conditions is unknown, and while MMPs have been previously studied in atherosclerosis and several cancers, their role in CAVD has not been defined yet [257, 258]. MMPs are known to degrade extracellular matrix (ECM) in tumor metastasis, allowing for cell migration, infiltration, and growth. ECM remodeling has been previously studied in the context of aortic valve stenosis and calcification [259-262] but the specific role of MMPs and their regulation are yet to be discerned.

Tissue inhibitor of metalloproteinases (TIMPs) are inhibitors of matrix metalloproteinases (MMPs) and of disintegrin-metalloproteinases such as ADAMS or ADAMTSs. The mechanosensitive TIMP3 is especially interesting to our group because we have recently shown that it can be regulated by miR-712 in mouse endothelium. Additionally, treatment of mice with anti-miR-712 leads to decreased matrix remodeling and atherosclerosis by increasing TIMP3 levels [263]. Another study showed that TIMP3 blocks the binding of VEGF to VEGF receptor-2 and inhibits downstream signaling and angiogenesis in the endothelium [264]. However, our group is the first to demonstrate that TIMP3 is shear-sensitive in valvular endothelium and side-specific in human AVs and that it plays a role in shear-sensitive valvular ECM remodeling [265].

1.10 MicroRNA miR-483 in CAVD

miR-483 is an intronic miRNA located in insulin-like growth factor 2 (IGF2). IGF2 is a fetal growth factor that is involved in development and fetal growth [266]. miR-483-3p has been previously studied in the cancer field. It was found to be upregulated in the plasma levels of patients with pancreatic cancer [267], to suppress apoptosis in squamous cell carcinomas [268] and hepatocellular carcinomas [269], and to increase proliferation and migration in esophageal squamous cell carcinoma [270]. miR-483 has also been studied in smooth muscle cells, where it was found to be downregulated by treatment with angiotensin 2 and to regulate four targets of the renin-angiotensin system: AGT, ACE-1, ACE-2, and AGTR2 [271]. Additionally, miR-483 circulating levels were significantly upregulated in heart failure patients after treatment with a left ventricular assist device to improve flow in the heart [272].

In the endothelium, the role miR-483-3p is still unclear. It has been shown to be a protective miRNA suppressing Endothelial-to-Mesenchymal (EndMT) transition in Kawasaki disease patients via silencing of the pro-EndMT gene CTGF [273]; on the other hand, miR-483 has also been shown to induce endothelial progenitor cell dysfunction, and

in vivo its silencing leads to faster thrombus resolution in venous thrombosis [274]. We hypothesize that miR-483-3p is a shear-sensitive and side-specific miRNA in valvular endothelium that inhibits endothelial dysfunction and calcification in the aortic valve by modulating the UBE2C/pVHL/HIF1 α pathway.

1.11 Role of UBE2C and HIF1 α in CAVD

The ubiquitin proteasome pathway is a critical degradation mechanism for most short-lived proteins in eukaryotic cells. Ubiquitination is controlled by a series of ubiquitin ligase enzymes, which are composed of E1 (ub activator), E2 (ub conjugator), and E3 (ub ligase)[275].

UBE2C (also known as UBCH10) is one of ~30 E2 family members. It binds to the anaphase-promoting complex (APC/C), inducing lysine-11 (K11) monoubiquitination on substrates. These monoubiquitinated protein will be recognized by the APC/C complex, and aided with another E2 ligase (Ube2s). The monoubiquitinated proteins will be polyubiquitinated and sent for proteosomal degradation [276, 277]. The APC/C complex mainly regulates progression through the mitotic phase of the cell cycle and to control entry into the S phase [278]; however, recently APC/C has been shown to also play a role in other cell functions such as hypoxia [279], apoptosis [280], senescence [281], autophagy [282], or metabolism [283]. Of special interest to us is the role of APC/C in hypoxia because APC/C targets Von Hippel-Landau protein (pVHL), which is a E3 ubiquitin ligase known to target hypoxia-inducible factor 1 α (HIF1 α) for proteasomal degradation [279, 284]. HIF1 α is a transcription factor induced in hypoxia [285], cancer [286], and disturbed flow conditions [287]; it upregulates expression of genes (Fig. 1.10) such as TWIST11 (EndMT regulator), VEGF (angiogenesis regulator), RUNX2 (osteoblastic differentiation), or MCT4 (energy metabolism) [288].

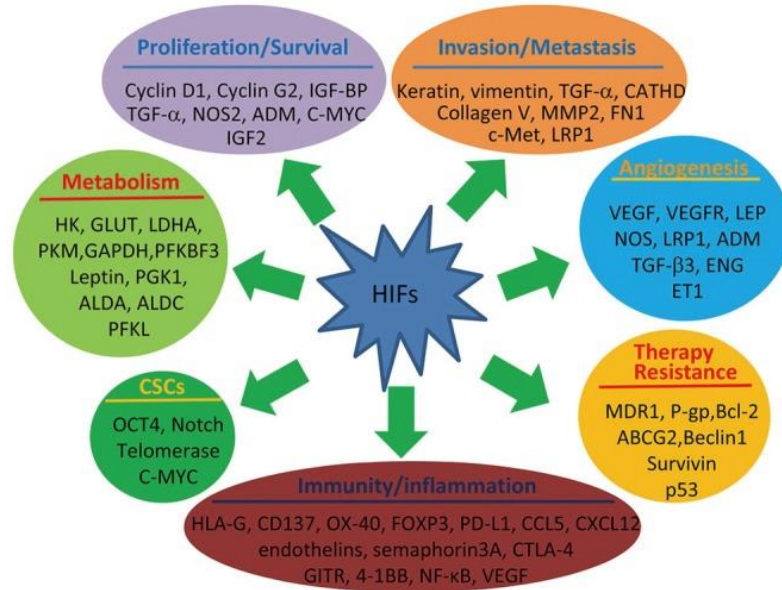


Figure 1.10 Target genes of HIF1 α

Adapted from Yu et al (2017) [2]

HIF1 α is regulated in a two-step process: prolyl hydroxylases (PHDs) modify HIF1 α with hydroxyl groups [289], which are then recognized by pVHL and sent for proteasomal degradation (Fig. 1.11).

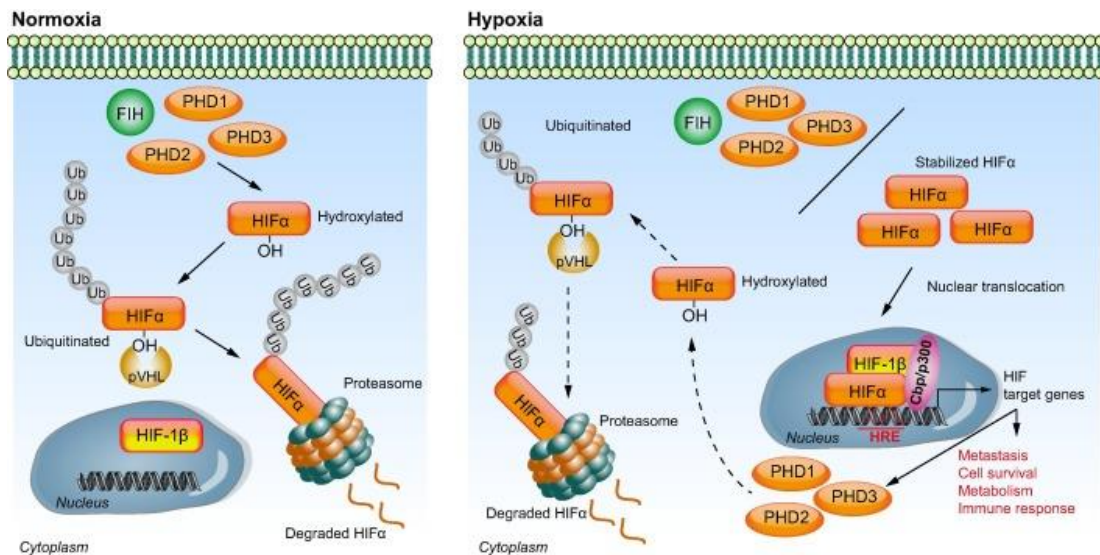


Figure 1.11 Regulatory mechanism of HIF1 α

Adapted from Wilson et al (2014) [3]

Previous literature has shown that UBE2C and HIF1 α are activated in numerous cancers including breast [290, 291], bladder [292, 293], and colon cancer [294, 295]. Therefore, we hypothesize that UBE2C plays a role in HIF1 α upregulation via degradation of pVHL. Importantly, HIF1 α has been linked to CAVD [296], and many of the gene targets of HIF1 α are known to mediate key CAVD pathogenic pathways: inflammation (TNF α , IL6) [297], EndMT (snail) [298], fibrosis (TGF- β 1), and osteogenesis (Runx2 and VEGF) (See Fig. 1.10).

Due to the important role of HIF1 α in cancer development, several therapeutic agents have been developed and are currently in clinical trials for various cancers. EZN-2968 is an antisense nucleotide inhibitor that has been studied in patients with refractory solid tumors and it was found that administration of this drug via IV infusion for 6-weeks lead to decreased levels of HIF1 α mRNA and protein as well as some of its target genes however, due to non-research related complications, the trial ended before any changes on tumor size could be assessed [299]. Of special interest to us is PX478, a water-soluble chemical inhibitor of HIF1 α , that modulates mRNA and protein levels of HIF1 α independent of oxygen levels of pVHL levels and that has been tested in a phase I clinical trial in advanced lymphoma tumor patients [300, 301]. Since there exist numerous FDA approved or emerging cancer drugs that target the HIF1 α pathway and UBE2C, some could be repurposed as anti-CAVD drugs.

A substantial portion of this chapter was published in:

1. Fernandez Esmerats J, Heath JM, Jo H: Shear-sensitive genes in aortic valve endothelium. *Antioxid Redox Signal* 2015.
2. Fernandez Esmerats J, Heath JM, Rezvan A, Jo H: Hemodynamics and Mechanobiology of Aortic Valve Calcification, *Biomedical Engineering: Frontier Research and Converging Technologies Volume 9*, pages 237-261, 2016

2 SPECIFIC AIMS AND HYPOTHESES

2.1 Significance and Impact

Because of an increasing aging population in the US and other developed countries, CAVD has become a major cause of cardiovascular deaths [10, 302]. The main treatment alternatives for CAVD patients are AV repair or replacement by surgical or transcatheter methods [9, 10]; presently, no pharmacological treatment options are available. This is in large part due to a lack of mechanistic understanding of the disease; therefore, there is an urgent need for 1) a better understanding of the molecular mechanisms of CAVD, and 2) the development of therapeutics to prevent, slow down, and/or reverse the disease by targeting key molecular players.

MicroRNAs have emerged as key regulators of cell phenotypes and diseases. Multiple studies have been conducted to specifically study the role of mechanosensitive miRNAs in CAVD (**Ch. 1.7.2**). However, prior to this project, there were no studies on miR-181b or miR-483 in valvular endothelium, or investigations into these miRNAs as potential therapeutic targets for CAVD. Studying the specific role of miR-181b and miR-483 may lead to new therapies to help prevent and treat CAVD.

Additionally, accelerated animal models to test therapies developed *in vitro* and *ex vivo* are needed. To this end, we have developed an accelerated animal model by combining GATA5 knockout mice, known to develop bicuspid AV, with our new hypercholesterolemic animal model via PCSK9-AAV injection. Bicuspid AV is one of the major risk factor for CAVD and is known to accelerate the development in CAVD in human patients [43]. When we combine bicuspid AVs with hypercholesterolemia in mice, we can induce AV sclerosis and calcification in just four months. This model will provide a faster and more clinically translatable tool for researchers across the world to test new therapeutics in CAVD.

2.2 Rationale

We have identified miR-181b and miR-483 as two novel, shear-sensitive miRNAs in the valvular endothelium conserved in mammalian species. miR-181b has been previously studied in cardiovascular diseases such as atherosclerosis [303] or aneurisms [304], as well as in cancer in mice and humans [250, 305]; however, the role of miR-181b in the valvular endothelium was unknown. Furthermore, Aim 1 established that miR-181b controls valvular ECM degradation, a key precipitating event in CAVD, by controlling MMP activity via silencing of TIMP3.

Although miR-483 has been previously studied in the cancer field as well as in Kawasaki disease patients [273], its role and shear-sensitivity in the valvular endothelium were unknown. The focus of Aim 2 is to demonstrate its shear-sensitivity and its role in endothelial biology and AV calcification. miR-483 shear-sensitivity was shown to be controlled by the well-known shear-sensitive transcription factor KLF2[5, 66]. We also established that miR-483 controls inflammation and EndMT in the valvular endothelium via regulation of the E2 ligase UBE2C. In addition, we found that UBE2C ubiquitinated pVHL, which lead to activation of HIF1 α and the transcription of its target genes. Furthermore, we conducted *ex vivo* therapeutic studies with miR-483 mimic and a FDA approved chemical inhibitor of HIF1 α (PX478) and found that these two treatments lead to a significant decrease in AV calcification.

Last, we are interested in developing an accelerated animal model of CAVD because this field is lacking a fast and reliable animal model for mechanistic and therapeutic studies. To this end, we will be working with GATA5 knockout mice known to develop bicuspid AV phenotype in ~15% of mice. Combining BAV, a known risk factor for CAVD in humans, with hypercholesterolemia, via AAV-PCSK9 injection and high-fat diet, we were able to develop an accelerated animal model for CAVD.

2.3 Innovation

The finding that miRNAs are induced by disturbed blood flow is relatively recent and is supported by both *in vitro* studies in ECs and limited *in vivo* studies in mice [66, 306]. However, the mechanisms by which miRNAs can lead to CAVD are still not fully understood. Although some miRNAs have already been implicated in CAVD[14, 15, 231, 233], there have been no previous studies of miR-181b or miR-483 in valvular endothelium and CAVD. Our innovative study linking miR-181b to ECM degradation via TIMP3 degradation introduces a novel mechanistic pathway for shear-induced matrix remodeling in AV endothelium.

Due to the lack of extensive research surrounding miR-483 in ECs, investigation of its potential target genes and functional changes with anti-miR-483 or miR-483 mimics will be crucial to understanding its role in the endothelium. Modulation of miR-483 *in vitro* has given important insight into the role miR-483 plays in EC inflammation and EndMT. Results from these studies indicated that miR-483 regulates inflammation and EndMT by silencing the E2 ligase UBE2C. We also identified a novel mechanistic pathway in which UBE2C upregulates HIF1 α and its target genes by ubiquitinating and degrading pVHL, a E3 ligase that is responsible for HIF1 α degradation. Our *ex vivo* calcification studies showed that induction of miR-483 using a mimic or inhibition of HIF1 α using a chemical inhibitor (PX478), significantly decreases AV calcification in porcine tissues.

Furthermore, we have developed an accelerated animal model of CAVD by using GATA5 knockout mice and inducing hypercholesterolemia via AAV-PCSK9 injection[307]. These mice present bicuspid AV phenotype at a rate of ~15% and combined with hypercholesterolemia, AV fibrosis and calcification can be induced in four months.

2.4 Project Objective

We know that laminar, unidirectional flow upregulates protective genes and downregulates “pro-CAVD” genes while disturbed flow results in the opposite

phenomenon; however, the mechanism by which flow controls EC gene expression is not yet fully understood. The goal of this project was both to determine how miR-181b and miR-483 respond to flow, cause altered gene expression, and regulate CAVD development as well as to develop an accelerated *in vivo* model of CAVD.

2.5 Overall Hypothesis

Our overall hypothesis is that disturbed flow conditions, such as the one endogenously observed in the fibrosa, controls expression of genes and miRNAs that play a role in endothelial dysfunction, a critical early stage of CAVD. Specifically, we are interested in studying the role of two novel shear-sensitive miRNAs: miR-181b and miR-483. MiR-181b is a pro-CAVD miRNA upregulated in OS conditions that targets TIMP3. Silencing of TIMP3 upregulates MMP activity and leads to increased ECM degradation. MiR-483 is a protective miRNA upregulated in LS conditions that inhibits inflammation and EndMT by silencing the E2 ubiquitin ligase UBE2C and the HIF1 α pathway.

Current animal models for CAVD are unable to accurately recreate the CAVD pathology found in human patients (sclerosis and leaflet calcification). Furthermore, in order to allow researchers to better understand CAVD and to provide a fast and accurate system to test new therapeutics, there is a need for an accelerated animal model. Our approach takes advantage of a congenital valve disease known as bicuspid AV, a well-known risk factor for CAVD that induces AV calcification at much earlier ages than patients with tricuspid AVs [30, 308]. To this end, we will be using GATA5 knockout mice which have been shown to develop bicuspid AV (~15% of the mice) [211] and inducing hypercholesterolemia via injection of an AAV gain-of-function PCSK9 complemented with high-fat diet. Our preliminary data showed that mice with bicuspid AVs present increased AV velocity, sclerosis, and calcification in just four months.

2.6 Specific Aim I: Demonstrate the mechanosensitivity of miR-181b in HAVECs and its role in ECM remodeling

We discovered miR-181b in our previous microRNA array comparing endothelial-enriched RNA from each side of healthy porcine AVs [220]. miR-181b was found to be upregulated in the fibrosa compared to the ventricularis. In this aim, we validated that miR-181b is upregulated by OS in HAVECs. We then proceeded to identify shear-sensitive targets of miR-181b by conducting an *in silico* analysis comparing shear-sensitive targets in our HAVEC array to computationally predicted targets of miR-181b. We identified GATA6, SIRT1, and TIMP3 from our initial validation studies and decided to focus on TIMP3 because it is a gene known to inhibit MMP activity and ECM degradation, a key step in AV sclerosis. Our functional studies showed the OS-induced MMP activity in valvular endothelial cells is miR-181b-dependent via silencing of TIMP3. Furthermore, silencing miR-181b in OS conditions leads to significant decrease in MMP activity in AV endothelium.

2.7 Specific Aim II: Determine the shear-sensitivity of miR-483, its targets and their function in endothelial dysfunction and AV calcification

We discovered miR-483 from our HAVEC array [14], where miR-483 was significantly upregulated in LS conditions compared to OS conditions. Furthermore, we harvested endothelial-enriched RNAs from each side of healthy porcine AVs and found that miR-483 is upregulated in the ventricularis layer (endogenously exposed to LS) compared to the fibrosa (endogenously exposed to OS). Our functional studies showed that miR-483 regulates inflammation, EndMT, and proliferation in HAVECs. To discover the target genes responsible for miR-483 endothelial function, we conducted an *in silico* analysis and found two shear-sensitive target genes of miR-483: ASH2L and UBE2C. Interestingly, knockdown of UBE2C alone dramatically prevented OS-induced endothelial

inflammation, demonstrating its dominant role. Although both UBE2C and ASH2L are likely to play major roles in CAVD, they are involved in potentially two very complex and different pathways (UBE2C on ubiquitin-dependent pathways and ASH2L on epigenetic regulation through histone modifications), and studying both simultaneously would interfere with focused studies; therefore, we decided to concentrate on UBE2C.

We discovered that UBE2C binds to pVHL, a E3 ligase that ubiquitinates and degrades HIF1 α , leading to its degradation which in turn stabilizes HIF1 α and allows transcription of its targets. This silencing of pVHL regulates inflammation and EndMT. To test whether miR-483 or HIF1 α could be potential therapeutics for CAVD, we conducted *ex vivo* studies in porcine AVs in osteogenic media and treated the tissues with a miR-483 mimic or a HIF1 α inhibitor (PX478). We found that both treatments significantly decreased calcification.

2.8 Specific Aim III: Develop an accelerated *in vivo* animal model for CAVD

As discussed in the introduction (**chapter 1.6.2**), several models of CAVD currently exist [13, 192, 200, 309-311]. However, these models have been unable to present significant degrees of sclerosis and calcification in the leaflet area of AVs [200, 312]. This lack of a fast and reliable animal model for AV calcification in the leaflets and not just in the root is slowing down mechanistic and therapeutic studies of CAVD. To address this issue, we decided to look into the main risk factors of CAVD and found that bicuspid AV is known to accelerate development of CAVD [44, 308]. Therefore, we decided to create a novel mouse model of CAVD using GATA5^{-/-} mice (provided by Dr. Mona Nemer [211]) that have been shown to develop BAVs in 15 % of the cohort versus littermate-control mice with tricuspid AVs. In order to accelerate the development of CAVD, we injected these mice with AAV-PCSK9 (which degrades hepatic LDL receptor) to induce hypercholesterolemia [307]. Our preliminary results showed that the BAV mice can develop AV sclerosis (histomorphometry), stenosis (transaortic velocity by

echocardiography), and calcification (Osteosense 680). These studies showed promising results but require further studies to demonstrate how well does this model mimic human AV lesions.

3 METHODS

3.1 Cell Culture and Shear Experiments

3.1.1 *HAVECs*

Side-specific Human Aortic Valve Endothelial Cells (HAVECs) [from the fibrosa endothelium (fHAVECs) and ventricularis endothelium (vHAVECs)] were isolated from noncalcified AVs obtained from heart transplant surgeries ($n = 6$) (according to an Institutional Review Board-approved protocol at Emory University and Georgia Institute of Technology) using a brief collagenase digestion and gentle scraping method [14]. Confluent cells were sorted for endothelial purity in the following manner: fHAVECs and vHAVECs were incubated in 5 μ l of DiI-acetylated LDL (acLDL; BTI) per 1 ml of complete media for 4 h before cell sorting using FACS Aria I (BD Biosciences). Human Aortic Endothelial Cells (HAECs) and human umbilical vein ECs (HUVECs) purchased from Lonza were used as positive controls. Human aortic SMCs (HASMCs) were used as a negative control.

Cells were cultured in 100 mm dishes (Falcon 353003) coated with 0.1% gelatin (Sigma Aldrich G9391) for 1 hr at 37°C. Cells were used at Passages 5-7 for experiments. The media composition is MCDB131 (MediaTech) supplemented with 0.002 μ g/ml FGF, 0.010 μ g/ml EGF, 0.001 μ g/ml VEGF, 0.002 μ g/ml IGF, 50 μ g/ml ascorbic acid, 0.001mg/ml hydrocortisone, 1% ECGS, 10%FBS, 1% L- glutamine, and 1% penicillin-streptomycin.

3.1.2 *Human embryonic kidney cells 293 (HEK)*

HEK cells were purchased from ATCC and cultured in gelatin coated plates with media composed of DMEM (4.5g/L glucose), 10% FBS, 1% L- glutamine, and 1% penicillin-streptomycin.

3.2 Shear Stress experiments

3.2.1 Cone and Plate Viscometer

Briefly, cells were cultured to 100% confluency and then subjected to shear stress in our cone-and-plate viscometer for 24 Hr. Cells subjected to LS experienced a unidirectional shear stress of 15 dyn/cm², whereas cells subjected to OS experienced an oscillating shear stress of 5 dyn/cm² at 1Hz. Alignment of ECs under LS was visually confirmed by microscopy. Cells were scraped in 600 µL HBSS (Corning 45000-462) and pelleted by centrifugation at 5000 rpm for 1 minute. One third was resuspended with Qiazol (Qiagen 79306) and the rest was resuspended in phosphate-buffered RIPA with glycerol (Boston Bioproducts BP-421) and protease inhibitor (Sigma Aldrich 11697498001).

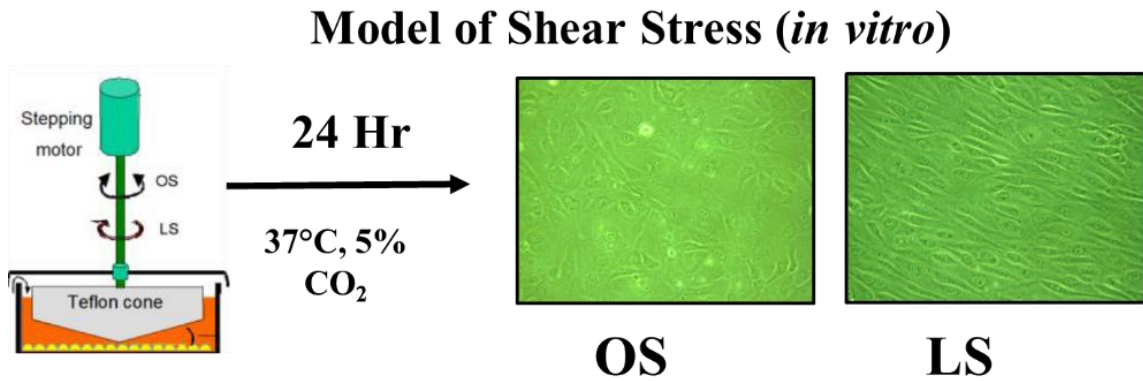


Figure 3.1 LS aligns endothelial cells

3.2.2 *Ibidi* shear stress experiments

Shear stress was applied to confluent HAVECs using an *Ibidi* pump system (*Ibidi*, Munich, Germany). Cells (3.3×10^5) were loaded onto μ -slides I^{0.4} (*Ibidi*) and placed in an incubator at 37°C with 5.0% CO₂. Slide surfaces were treated with 0.1% gelatin prior to cell loading to improve cell adhesion. These μ -slides hold a volume of 100 µL, with a channel height of 400 µm and a cell culture surface area of 2.5 cm² (5 mm width × 50 mm

length). We loaded HAVECS onto μ -slides overnight before induction of shear to ensure optimal adhesion and prevent cells from lifting off.

The Ibidi pump system was set up per the company's instructions and proprietary software was used to control the level of shear applied to cells by controlling total media flow rate through the channels of known dimensions. We used the red type perfusion tubing set that connects to the μ -slide and can induce shear stress of 4-40 dyn/cm². Sterile filters (Syringe Filter PES .22um Sterile 50, 0.22- μ m pore size, EMD millipore) were used to filter the air entering the tubing system, via an air pressure pump, which applied the force required to maintain the flow rate of the media through the tubing and across the μ -slide. The air pressure pump responds to the company's proprietary software and provides air to the perfusion sets at the designated pressure with a range of -100 mbar to +100 mbar. The air pumped into the system came from the incubator itself and thus contained 5% CO₂. Our initial studies show that after 3 days cells show alignment to LS conditions (Figure 3.2B) and the cobble-like cell shape characteristic of OS conditions (Figure 3.2C).

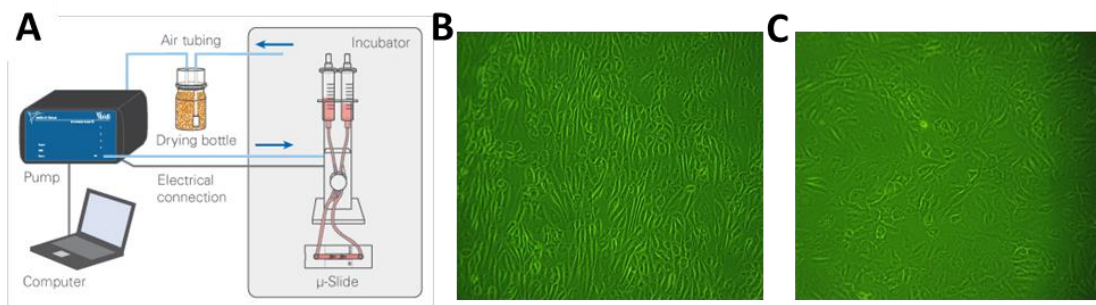


Figure 3.2 Ibidi shear system aligns HAVEC in LS conditions

3.3 Quantitative real-time PCR (qPCR) for validation of miRNAs

Total RNA was purified by the Qiagen miRNeasy Kit (217004), and reverse-transcribed into cDNA using the Qiagen miScript II Reverse Transcriptase Kit (218161). The resulting cDNA was subjected to qPCR using the Qiagen mature hsa-miR-181b-5p (MIMAT0000257: 5'AACAUCAUUGCUGUCGGUGGGU-3' MS00006699), mature has-miR-483-3p (MIMAT0002173: 5'UCACUCCUCUCCUCCCGUCUU-3

MS00009751) or RNU6b (218193) as the forward primer and Universal Primer (218193) as the reverse primer, SYBR Master Mix (ThermoFisher 4472903), and the ABI StepOne Plus qPCR machine. The PCR conditions were 95°C, 15 min, followed by 45 cycles of 94°C, 15 s; 55°C, 30 s, and 70°C, 30 s. RNU6B was used as a housekeeping control. Fold changes between samples were determined for all targets using the $\Delta\Delta C_t$ method [313].

3.4 Quantitative real-time PCR (qPCR) for validation of mRNAs

Total RNA was purified using the Qiagen miREasy kit and reverse transcribed for use in a two-step qRT-PCR using the High Capacity cDNA Reverse Transcription Kit (Applied Biosystems 4368814). The resulting cDNA was subjected to qPCR using the primers in **Table 3.1** (human) and **Table 3.2** (pig), SYBR Master Mix (ThermoFisher 4472903), and the ABI StepOne Plus qPCR machine. The PCR conditions were 10 min at 95°C, followed by 40 cycles of 95°C for 5 s and 60°C for 30 s. 18S was used as a housekeeping control. Fold changes between samples were determined for all targets using the $\Delta\Delta C_t$ method.

Table 3.1 Primer sequences for qPCR for human samples

	Forward	Reverse
18S(human/pig)	AGGAATTGACGGAAGGGCACCA	GTGCAGCCCCGGACATCTAAG
VCAM1 (human)	CATTGACTTGCAGCACCACA	AGATGTGGTCCCCTCATTCTG
ICAM1 (human)	CACAAGCCACGCCTCCCTGAACCTA	TGTGGGCCTTTGTGTTTTGATGCTA
MCP-1 (human)	GCAGAAGTGGGTTCAGGATT	TGGGTTGTGGAGTGAGTGTT
IL-1β (human)	CCACAGACCTTCCAGGAGAATG	GTGCAGTTCAGTGATCGTACAGG
IL-6 (human)	AGACAGCCACTCACCTCTTCAG	TTCTGCCAGTGCCTCTTTGCTG
UBE2C (human)	CTGGCGATAAAGGGATTTCTGCC	GCGAGAGCTTATACCTCAGGTC
ASH2L (human)	TTCCTGGAGACCTCTACAGAGC	CCTTCTCTCAACCACAGTCAG
PSAT1 (human)	ACTTCCTGTCCAAGCCAGTGGA	CTGCACCTTGTATTCCAGGACC
pVHL (human)	GACACACGATGGGCTTCTGGTT	ACAACCTGGAGGCATCGCTCTT
HIF1α (human)	TATGAGCCAGAAGAACTTTTAGGC	CACCTCTTTTGGCAAGCATCCTG
Twist1 (human)	CGGACAAGCTGAGCAAGAT	CTGGAGGACCTGGTAGAGGA
Snail (human)	TGCAGGACTCTAATGGAGAGTT	GACAGAGTCCCAGATGAGCA
Slug (human)	CTGGCCAAACACAAGCAG	ACCCAGGCTCACATATTCTT
Transgelin (human)	CTGAGGACTATGGGGTCATC	TAGTGCCCATCATTCTTGGT

Table 3.2 Primer sequences for qPCR for pig samples

	Forward	Reverse
18S(human/pig)	AGGAATTGACGGAAGGGCACCA	GTGCAGCCCCGGACATCTAAG
UBE2C (pig)	ACAGTGAAGTTCCTCACGCC	ATGTTGGGTTCTCCGAGCAG
ASH2L (pig)	CTTTCCGGCCATCTCACTGT	GCCTCCCATCCACTTCTGTC
KLF2(pig)	GACCACGATCCTCCTTGACG	GCATCAAGCCTCGATCCTCT
VCAM1(pig)	ACCAGCTCCACAGATTCCTG	TCCCTGGGAGCAACTTGAAC
Runx2(pig)	GCCTTCAAGCCATCACCTCAA	GAGAACGCTGGCGATACCC

3.5 RNA Extraction from organs and qPCR

Mice were sacrificed using CO₂ and the liver, lung, kidney, and spleen was collected from each animal. The organs were snap-frozen in liquid nitrogen and crushed by mortar and pestle in liquid nitrogen. After crushing, an aliquot of the tissue was placed in Qiazol and disrupted by metal beads in a tissue lyser (BioSpec 11079132SS). Total RNA was purified and reverse-transcribed as previously described. The resulting cDNA was subjected to qPCR as previously described.

3.6 Transfection of Nucleic Acids

For miRNA modulation studies we plated HAVECs for 24 hours prior to transfection with either anti-miR-483 (Exiqon LNA Power Inhibitor 4100225-001) or anti-miR-181b (Life technologies 4464084) for inhibition or miR-483 mimic (Exiqon 472350-001) or miR-181b mimic (Life Technologies 4464066) for overexpression respectively. 1 part of oligonucleotide/Oligofectamine (Invitrogen 12252011) mixture in Opti-MEM media (Gibco 31985070) were added to 4 parts of OPTIMEM in the plate for final dosages of 100 nM for anti-miR or 5-10 nM miR-mimic. Four hours after transfection, the media was replaced with standard HAVEC media. A non-target “scrambled” miRIDIAN microRNA Mimic Negative Control (Dharmacon CN-001000-01-05) was used as a control

in mimic experiments and a nontarget LNA oligonucleotide (Custom-made from Exiqon) was used as a control in anti-miR experiments.

We used the same protocol to transfect siRNAs to silence the expression of target genes. We used siRNAs to silence UBE2C (SMARTpool, Dharmacon L-004693-00-0005), ASH2L (SMARTpool, Dharmacon L-019831-00-0005), KLF2 (Thermo Scientific AM16708), pVHL (ON-TARGETplus, Dharmacon L-003936-00-0005) and HIF1 α (EZN-2968, Exiqon). The concentration of each siRNA was determined with a dose curve study in HAVECs where cells were treated with different concentrations of siRNA for 48 hours and expression of the target gene was measured via qPCR.

Plasmids were transfected using Lipofectamine 3000 (ThermoFisher Scientific L3000008) using Opti-MEM media (Gibco 31985070). GFP or RFP plasmid was used in order to determine transfection efficiency. Briefly, the plasmids were mixed in serum-free medium with Lipofectamine 3000 and P3000 and added to the cells. After four hours, media was changed to regular medium. The plasmids were: pSELECT-GFP-hLC3 (Invitrogen psetz-gfplc3), pCMV6-UBE2C Myc-DDK-tagged (Origene technologies, RC208741), RpCMV-DsRed-Express2 (RFP, SnapGene pIRES2 DsRed-Express 2), pRc-CMV-HA-pVHL-WT, HA-pVHL-RRR, HA-pVHL-KRR, HA-pVHL-RKR or HA-pVHL-RRK [314, 315].

3.7 **PX478 treatment**

PX478 is an FDA-approved chemical inhibitor of HIF1 α by inhibiting transcription, translation and stability of HIF1 α [300, 301]. PX478 was purchased from MedKoo Scientific (MedKoo 202350-1g) and diluted in sterile saline at a concentration of 20mM. Cells or tissues were treated with a concentration of 20 μ M of PX478.

3.8 **Gelatinase assay**

In order to determine the activity of MMPs in HAVECs, we used the EnzChek Gelatinase/Collagenase Assay kit (Thermo Fisher). The kit utilizes a gelatin substrate from

porcine skin, labeled with fluorescein, which can be degraded by gelatinases and collagenases such as MMPs. The level of substrate degradation is reflected by fluorescent signal, absorption 495 nm/emission 515 nm, read via Biotek plate reader. We incubated 100 μ l HAVEC lysate suspended in kit buffer with 20 μ g DQ gelatin substrate for 2 hours, and then recorded fluorescent signal for each sample. Values were adjusted by subtracting fluorescent signal of blank wells, and normalizing to total sample protein content.

3.9 In vitro MMP inhibition

We analyzed the specific contribution of MMPs to the gelatinase fluorescence using MMP chemical inhibitor GM6001 (Millipore), which efficiently inhibits many MMPs, including MMP-1, 2, 3, 8, and 9. The cell lysate was collected, and gelatinase assay was performed as described above.

3.10 Monocyte Adhesion Assay

Following shear, cells were washed and incubated with fluorescently labeled THP-1 human peripheral blood mononuclear leukocytes (ATCC TIB-202) in serum-free media at 37°C for 30 minutes. THP-1 cells were labeled with 5 μ L of BCECF-AM (1mg/ml, Molecular Probes B1150) at 37°C for 30 minutes. 500,000 THP-1 cells were added per dish in a volume of 5 mL. Non-adherent THP-1 cells were washed away with and bound cells were fixed with 4% paraformaldehyde (Sigma Aldrich) and visualized by fluorescent microscopy at 5X magnification (Olympus) and quantified using ImageJ.

3.11 Protein assay and Western Blotting for Inflammatory Markers

Cell lysate was centrifuged at 12,000g for 10 minutes at 4°C to remove cell debris. The protein-containing supernatant was collected in a separate tube and 2.5 μ L was added to a 96 well plate. Bicinchoninic acid (BCA) was diluted 1:50 in Reagent A (Pierce 23225) and 97.5 μ L of the reagent was added to each protein-containing well. Protein standards were prepared by diluting bovine serum albumin (2mg/mL, Pierce 23209). After a 30-

minute incubation at 37°C, the absorbance was read by a microplate reader at 562 nm and a linear calibration curve was established.

Each protein sample was diluted in 1X RIPA and 6X reducing loading dye (Boston Bioproducts) to achieve a total protein amount of 15-25 µg, then subsequently boiled at 95°C for 5 minutes. Proteins were electrophoresed in 1X running buffer (Tris-Glycine pH 8.8) using a 8-12% polyacrylamide gel. Following electrophoresis, the proteins were transferred to a polyvinylidene fluoride (PVDF) membrane (BioRad) and blocked in 5% (w/v) nonfat milk in Tris-Buffered Saline with 0.1% Tween (TBST) for 1 hour at room temperature. Membranes were incubated with the primary antibody solution overnight at 4°C. Following primary antibody exposure, the membrane was washed and incubated with secondary antibody (1:3000) (goat anti-rabbit, goat anti-mouse or goat anti-rat HRP, Santa Cruz SC-2004, SC-2005 or Thermo Fisher Scientific 31470) for 1 hour at room temperature. After washing, the membrane was developed using Immobilon Western Chemiluminescent HRP (EMD Millipore, WBKLS0500) and Blue Lite Autorad Film (VWR, 490001-950).

Table 3.3 List of Antibodies used for Western blotting and Immunostaining

Antibody	Species	Cat. No.	Company
UBE2C (Ubch10)	Rabbit	Ab12290	Abcam
ASH2L	Rabbit	A300-108A	Bethyl Laboratories
pVHL	Rabbit	SAB4200434	Sigma Aldrich
HIF1 α	Rabbit	A300-286A	Bethyl Laboratories
GAPDH	Rabbit	sc-25778	Santa Cruz Technologies
B-Actin	Mouse	A5316	Sigma Aldrich
Myc-tag	Mouse	2276S	Cell Signaling Technologies
HA-tag	Rat	11867423001	Sigma Aldrich
KI-67	Rabbit	Ab15580	Abcam

3.12 pVHL and HIF1 α staining in shear stress conditions

Cells were seeded in IBIDI slides (Corning) coated in 0.1% gelatin at a density of 50,000 cells per slide. 24 hours later, cells were transfected with siUBE2C or left untreated. 24 hours after transfection, cells were sheared for 72 hours either in LS or OS conditions. After shear, cells were rapidly fixed in 4% paraformaldehyde and permeabilized in 0.1% Triton X-100 (Sigma Aldrich) in PBS for 10 minutes, followed by blocking in 20% goat serum (Jackson ImmunoResearch, 005-000-121) in PBS for 1 hour. After blocking, cells were incubated with pVHL or HIF1 α (1:100) antibodies (see **Table 3.3**) overnight at 4°C followed by incubation with secondary antibody (1:250) (Alexa Fluor 568 conjugated goat anti-rabbit, Life Technologies) and imaged using a fluorescent microscope.

3.13 *In silico* analysis

We conducted an *in silico* analysis to determine potential shear-sensitive targets of our miRNAs. We used our previously published HAVEC array [14] to discover shear-sensitive genes in HAVECs, we used genes with at least a 50% difference in expression ($p < 0.05$) between LS and OS conditions. We compared these genes with predicted target genes of either miR-181b or miR-483 using online miRNA-gene interactions from miRtarbase (<http://mirtarbase.mbc.nctu.edu.tw/php/index.php>) and miRwalk (<http://zmf.umm.uni-heidelberg.de/apps/zmf/mirwalk/>).

3.14 3'UTR Luciferase assay

First, we transfected HAVECs with a 3'UTR luciferase plasmid containing the 3'UTR of human TIMP3 with the binding site for miR-181b containing firefly and renilla luciferase. 24 hours after plasmid transfection, we transfected miR-181b mimic and 24 hours later measured changes in expression of luciferase. We used a non-targeting miRNA mimic control as an experimental control. We collected the cells and measured expression of firefly and renilla luciferase and normalized to protein content.

3.15 Scratch migration assay

Cell monolayers were scratched with a 200- μ L pipette tip. The monolayer was washed once and the medium was replaced with Optimem reduced-serum (2%FBS) media. After 6 hours, the number of cells migrated into the scratch area were quantified microscopically using NIH ImageJ.

3.16 TUNEL assay for apoptosis quantification

Detection of cell apoptosis was performed by using the In Situ Cell Death Detection Kit; Fluorescein TUNEL kit (Roche Diagnostics, Mannheim, Germany). Cells were fixed with 4% paraformaldehyde in DPBS (pH 7.4) for 20 min, washed with HBSS for 30 min, permeabilized with 0.1% Triton X-100 and 0.1% sodium citrate in HBSS (2 min on ice), and rinsed twice with HBSS. Staining was performed by incubating tissue sections for 1 h at 37°C in a humidified chamber in the dark in 50 μ l of TUNEL reaction mixture. DAPI counterstaining was used to improve image contrast. Positive apoptotic cells could be identified by using the green fluorescence on the microscope. Negative controls were prepared by incubating fixed and permeabilized tissue sections in 50 μ l of TUNEL label solution (without terminal transferase). Positive controls were prepared by incubating fixed and permeabilized tissue sections with DNase for 10 min prior to labeling.

3.17 Immunofluorescence Staining

Frozen sections were permeabilized in 0.1% Triton-X in PBS for 10 minutes, followed by blocking in either 20% donkey serum or goat serum (Jackson ImmunoResearch, 005-000-121 or 017-000-121) in PBS for 1 hour. Slides were incubated in the primary antibody detailed in **Table 3.3** overnight at 4°C followed by incubation with secondary antibody (1:250 v/v) (Alexa Fluor 568 conjugated goat anti-rabbit, goat anti-rat, or donkey anti-goat, Life Technologies). Slides were then mounted using DAPI-mounting media (Sigma Aldrich F6057) and imaged using a fluorescent microscope.

3.18 Mouse De-paraffinization and Immunostaining

Briefly, sections were deparaffinized using the following protocol:

1. Xylene: two 3-minute dips.
2. 1:1 Xylene:100% ethanol: 3-minute dip.
3. 100% ethanol: 3-minute dip.
4. 95% ethanol: 3-minute dip.
5. 70% ethanol: 3-minute dip.
6. 50% ethanol: 3-minute dip.
7. Water: keep in water until staining.

Following de-paraffinization, slides were stained with hematoxylin and eosin or Alizarin red, or immunostained as described below.

3.19 Hematoxylin and Eosin Staining

Frozen sections or paraffin-embedded sections were stained using the American MasterTech H&E kit. The protocol is the following:

1. Rinse in running tap water for two minutes
2. Incubation in Harris hematoxylin for five minutes
3. Rinse in running tap water for two minutes
4. Incubation in differentiating solution for one minute
5. Rinse in running tap water for two minutes
6. Incubation in Bluing solution for thirty seconds
7. Rinse in 70% ethanol for one minute
8. Incubation in Eosin for one minute
9. Dehydration via three changes of 100% ethanol
10. Incubation in 100% xylene for one minute
11. Mount in Permount
12. Image using Hamamatsu Nanozoomer

3.20 Alizarin red staining

Frozen sections or paraffin-embedded sections were stained using 2% Alizarin Red Stain (Lifeline Cell Technology CM-0058). Briefly, sections were fixed with 4% paraformaldehyde for 15 minutes followed by two washes with PBS. Slides were stained in the alizarin red solution for 90 seconds followed by two washes with DI water.

3.21 Statistical Analysis

Statistical analyses were carried out with Graph-Pad Prism v6 (GraphPad Software). All error bars reported are standard error of the mean unless otherwise indicated. Pairwise comparisons were performed using one-way Student's t-tests. Multiple comparisons of means were performed using one-way analysis of variance followed by Tukey's multiple comparison tests. Differences between groups were considered significant at P-values below 0.05.

4 Role of miR-181b in extracellular matrix remodeling in CAVD

4.1 Introduction

The sclerosis and calcification of the aortic valve is a side-specific phenomenon, correlated with the differential shear stresses observed during the cardiac cycle. Each side of the valve experiences a distinct shear profile sensed by the overlying endothelium. The ventricularis layer faces the ventricle and experiences a high-magnitude and pulsatile, unidirectional, laminar shear stress (LS) and rarely calcifies. The fibrosa layer facing the aorta experiences low magnitude and oscillatory shear stress (OS). This endothelial layer exhibits a highly inflammatory phenotype, expressing abundant adhesion molecules and other inflammatory markers, and downregulating anti-inflammatory signals such as Klf2. The fibrosa preferentially exhibits sclerosis and calcification, with large nodules and macrophage infiltration mimicking atherosclerosis observed in the spongiosa and interstitium near this valve face. In vitro, LS conditions applied to aortic valve endothelial cells upregulate CAVD-protective genes such as KLF2, KLF4 and eNOS, whereas OS conditions upregulate pro-CAVD genes and paracrine mediators such as BMP4, Cathepsin-K, and matrix metalloproteinases MMP-2 and MMP-9 [14, 316].

Notably, the matrix metalloproteinases (MMPs) have been correlated with valve disease in various studies of human and porcine valves. MMP levels are known to be higher at sites of calcification in both the endothelium and the interstitial cells. However, the mechanism by which MMPs are upregulated in CAVD conditions has not yet been discerned, and while their causative role in cancers and atherosclerosis has been shown, their contribution to CAVD remains undefined [257, 258, 317]. MMPs are known to degrade extracellular matrix (ECM) to allow for cellular growth, migration, or infiltration as observed in tumor metastasis. The remodeling of the ECM has been previously studied in the context of aortic valve stenosis and calcification [259-262], but the activity of MMPs in that phenomenon are still unknown. In addition, the potentially important mechanism by

which low and oscillatory shear-stress may mediate MMP activity and extracellular matrix degradation in CAVD have not been previously characterized.

In order to find novel pathways regulating CAVD in the aortic valve, our group has recently performed a microarray exploring side- and shear-dependent RNA expression in aortic valve endothelium [318]. We isolated endothelial enriched RNA from fresh porcine valves to determine which RNA is uniquely expressed on each side of the valve. In addition, we subjected human aortic valve endothelial cells (HAVECs) to LS or OS for 24 hours to determine mechanosensitive RNA expression. Our array revealed many side- and shear-dependent microRNAs (miRNAs). miRNAs are short (18-22) nucleotide sequences which bind to the 3'-untranslated regions (3'UTR) of mRNA thereby regulating protein expression by degradation of mRNA targets or by suppression of translation [319]. Despite their characterization in other cardiovascular systems, miRNAs have not been thoroughly explored in the AV endothelium. In the interstitium, these mediators have proven to be critical for regulation of osteogenic transformation: miRNA-30b was shown to prevent interstitial cells transforming into calcifying cells [320], and miRNA-141 targets TGF- β and BMP-2 signaling, which are critical for valvular interstitial osteoblastic differentiation leading to tissue calcification[226]. From our array analyses, we discovered one microRNA, miR-181b, that is abundant in HAVECs and consistently upregulated in OS *in vitro*. This microRNA was also predicted to regulate the previously undefined TIMP3/MMP pathway, and thus was chosen as a potential novel therapeutic candidate for further study.

MiRNA-181b has been shown to be shear-sensitive in aortic valve endothelial cells [14] as well as side-specific in porcine aortic valves [220] however, its potential role in CAVD has yet to be discovered. In order to determine the mechanistic role of miR-181b in HAVECs, we conducted an *in silico* analysis to determine its predicted and partially validated target genes. From this analysis we found that miRNA-181b targets TIMP3, a known inhibitor of MMPs that has been previously shown to be shear-sensitive and critical

in preventing matrix remodeling in atherosclerosis [263]. Via overexpression and inhibition of miR-181b along with TIMP3 3'UTR luciferase reporter studies, we found that TIMP3 is a direct target of miR-181b. Through a series of gelatinase assays showing HAVEC MMP activity, we found that miR-181b suppresses TIMP3 in OS conditions leading to increased ECM degradation and remodeling (Fig. 4.1). These findings provide a novel therapeutic target for CAVD by targeting miR-181b or TIMP3 to prevent ECM remodeling and degradation characteristic of CAVD pathology.

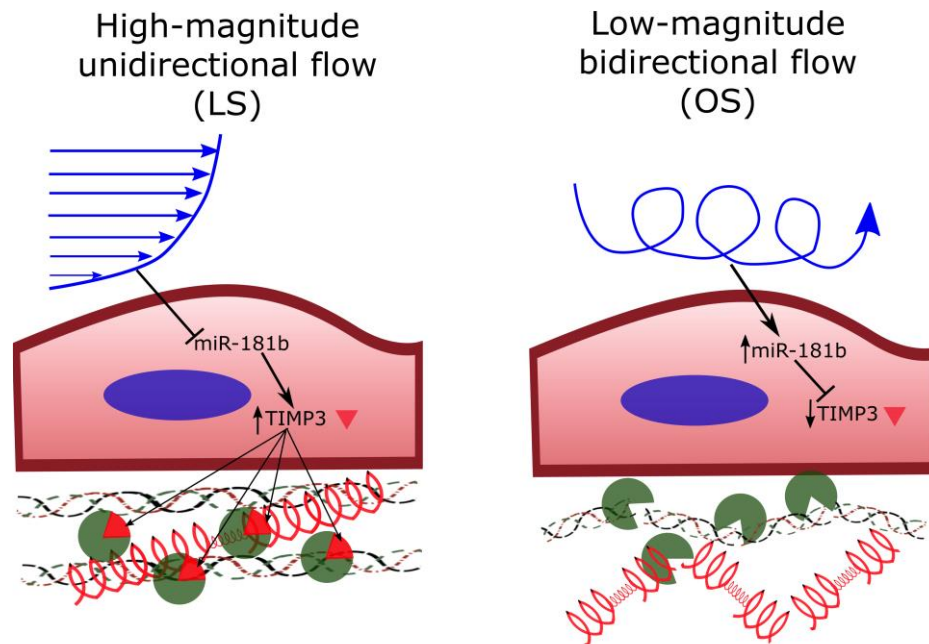


Figure 4.1 miR-181b induces endothelial ECM degradation by targeting TIMP3

High-magnitude laminar shear stress at the ventricularis suppresses endothelial expression of miR-181b, leading to an increase in TIMP3 expression. TIMP3 inhibits MMP activation and extracellular matrix degradation, protecting the ventricularis from further events leading to valve calcification. Low-magnitude oscillatory shear stress at the fibrosa stimulates endothelial expression of miR-181b, which downregulates TIMP3, leading to increased MMP activity and extracellular matrix degradation. This remodeling of the ECM may lead to aortic valve sclerosis and calcification through multiple mechanisms.

4.2 Results

4.2.1 miR-181b is side-specific and shear-sensitive in valvular endothelium

miR-181b was found to be side-specific in our microarray where it was upregulated by two-fold in the fibrosa (exposed to OS) compared to the ventricularis (exposed to LS) in porcine valvular endothelium (Fig. 4.2A). Interestingly, miR-181b was also shear-sensitive in our HAVEC microRNA array where we observed a significant 15% increase in miR-181b expression in OS compared to LS conditions (Fig. 4.2B). To validate the shear-sensitivity of this miRNA we exposed HAVECs to LS or OS conditions for 24 hours and measured miRNA expression of three miRNAs in the miR-181 family (miR-181a, -181b, and -181c) as well as miR-15a, a control miRNA known not to be shear-sensitive (Fig. 4.2C). Our results showed that only miR-181b was shear-sensitive being upregulated by more than six-fold in OS compared to LS conditions in HAVECs.

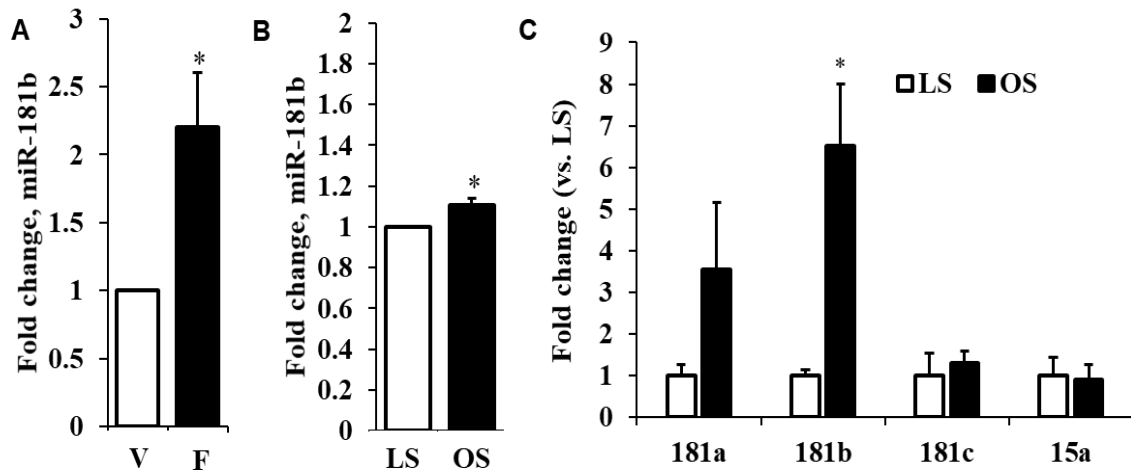


Figure 4.2 miR-181b is side-specific and shear-sensitive in valvular endothelium

A) Expression of miR-181b in the ventricularis (V) and fibrosa (F) layer of porcine valvular endothelium from our microarray. **B)** Expression of miR-181b in HAVECs exposed to LS or OS conditions for 24 hours from our microarray. **C)** HAVECs were exposed to LS or OS conditions for 24 hours and expression of miR-181a, -181b,-181c, and -15a was quantified via qPCR normalized to U6. n=4-8, *p<0.05.

4.2.2 TIMP3 is a potential shear-sensitive target of miR-181b

To identify potential shear-sensitive targets of miR-181 we conducted an *in silico* analysis using predicted targets of miR-181b from miRTarBase

(<http://mirtarbase.mbc.nctu.edu.tw/>) and miRwalk (<http://zmf.umm.uni-heidelberg.de/apps/zmf/mirwalk2/>) comparing to genes that are downregulated in OS conditions from our previously published HAVEC array [14]. From this study we identified six target genes: NLK, GATA6, CDX2, TIMP3, VSNL1, BCL2 and SIRT1. We probed for these genes in sheared HAVECs in LS or OS conditions for 24h, and we found that GATA6, TIMP3 and SIRT1 were highly shear-sensitive, showing a significant decrease in OS compared to LS conditions (Fig. 4.3A). Because of its known role in matrix degradation and our group's previous work in studying TIMP3 in atherosclerosis [263], we focused on TIMP3 for further study. To further validate its shear-sensitivity we harvested endothelial-enriched RNAs from each layer of healthy porcine AVs and measure mRNA expression of TIMP3 via qPCR and found that there was a ~35% decrease of TIMP3 expression in the fibrosa compared to the ventricularis (Fig. 4.3B)

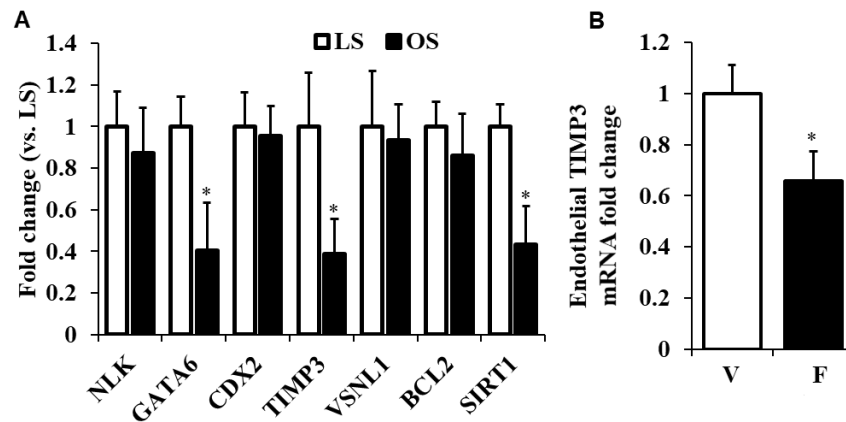


Figure 4.3 TIMP3 is shear-sensitive in HAVECs

A) HAVECs were exposed to LS or OS conditions for 24 hours and mRNA expression of the potential predicted targets of miR-181b was assessed via qPCR. **B)** Endothelial-enriched RNAs were harvested from each side of porcine AVs and expression of TIMP3 was assessed via qPCR. n=4-6, *p<0.05.

TIMP3 is an inhibitor of extracellular matrix degradation through MMP inhibition that potentially links previous studies describing increased ECM degradation in stenotic or calcific valves compared to healthy valves [258, 317]. As a functional readout of matrix remodeling in HAVECs, we conducted a gelatinase assay using DQ gelatin [321], which

has been shown to correlate with MMP activity and matrix degradation [318] . Correlating with the loss of TIMP3 in OS, we observed a 2.5-fold increase in gelatinase activity in HAVECs sheared in OS compared to LS conditions (Fig. 4.4). Our hypothesis is that the miR-181b/TIMP3 pathway is a critical mediator of the OS-induced MMP activity observed in HAVECs.

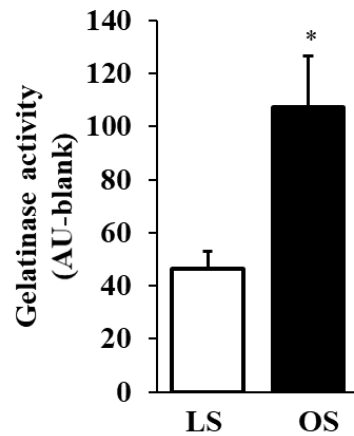


Figure 4.4 OS induces MMP activity in HAVECs

HAVECs were exposed to LS or OS conditions and MMP activity was assessed via DQ gelatin assay.

4.2.3 miR-181b regulates TIMP3 expression

Next, we want to determine whether miR-181b regulates expression of TIMP3. First of all, we conducted a dose curve to find the optimal miR-181b dose by treating HAVECs with miR-181b mimic or mimic-control for 48 hours and measured expression of miR-181b via qPCR (Fig. 4.5A). We found that there was a dose-dependent increase in miR-181b expression when treating HAVECs with a miR-181b mimic and from our results we decided to use 5nM as it increased miR-181b expression by ~1000 fold compared to the control mimic. We then treated HAVECs with miR-181b or mimic control at 5nM for 48 hours and measured mRNA expression of all the target genes identified in our *in silico* analysis via qPCR (Fig. 4.5B). GATA6, TIMP3 and SIRT1 expression was consistently downregulated when miR-181b was overexpressed.

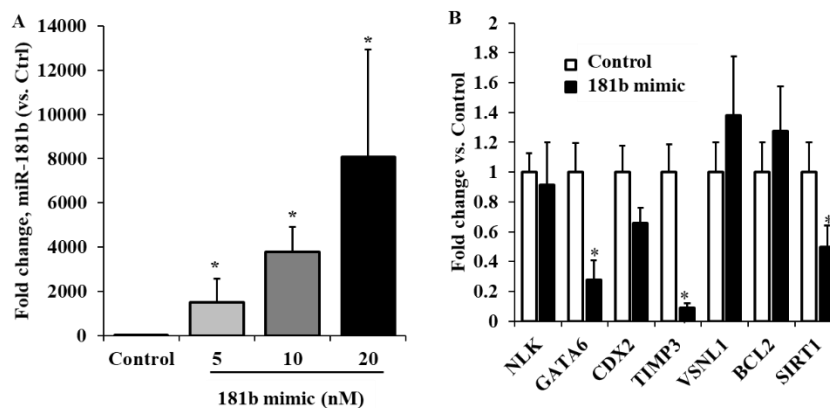


Figure 4.5 miR-181b upregulation decreases GATA6, TIMP3 and SIRT1 expression

A) HAVECs were transfected with different doses of miR-181b mimic for 48 hours and expression of miR-181b was quantified via qPCR. B) HAVECs were transfected with miR-181b mimic or control at 5nM for 48 hours and expression of potential target genes of miR-181b was quantified via qPCR. n=4, *p<0.05.

Next, we conducted a similar experiment but instead of overexpressing miR-181b we silenced its expression by using a miR-181b inhibitor (anti-181b). We treated HAVECs with anti-181b or anti-miR control at a dose of 100nM and measured expression of miR-181b (Fig. 4.6A) or its potential target genes (Fig. 4.6B) via qPCR. We observed that GATA6, TIMP3 and SIRT1 were upregulated when miR-181b was silenced. Even though we observed consistent results with these three genes we will be focusing on TIMP3 due to our previous experience with TIMP3 and its role in ECM degradation, critical step in CAVD pathogenesis [263].

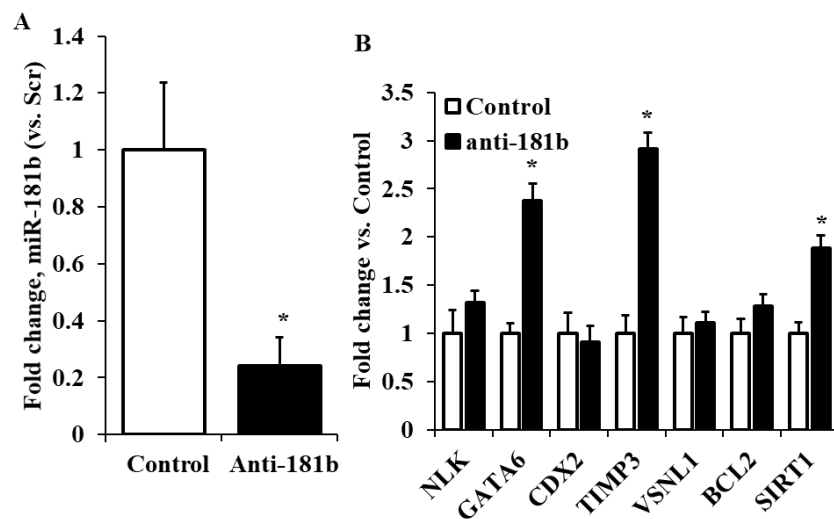


Figure 4.6 MiR-181b inhibition upregulates GATA6, TIMP3 and SIRT1

A,B) HAVECs were transfected with anti-Control (Control) or anti-miR-181b for 48 hours and expression of miR-181b (**A**) or potential target genes of miR-181b (**B**) was quantified via qPCR. n=4, *p<0.05.

Last, to further validate that miR-181b directly binds to the 3'UTR of TIMP3 we designed a plasmid with the 3'UTR sequence of TIMP3 where miR-181b potentially binds to TIMP3 tagged to a firefly luciferase protein. We treated transfected HAVECs with this plasmid and 24 hours later we conducted a second transfection with miR-181b mimic. After 24 hours we measured firefly luciferase signal and normalized to protein content in each sample (Fig. 4.7). Our results showed that there was a dose-dependent decrease in

luciferase signal which demonstrated that miR-181b directly binds to the 3'UTR of TIMP3 regulating its expression.

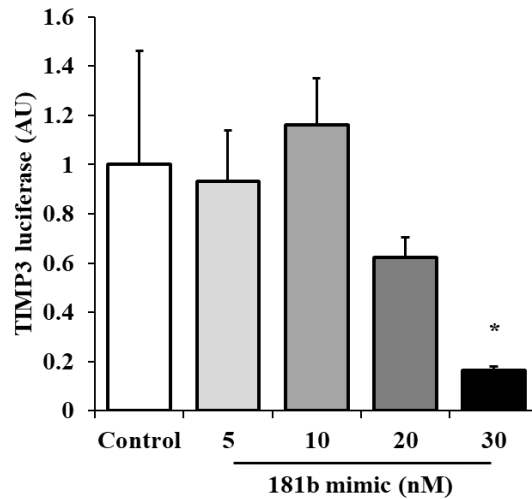


Figure 4.7 MiR-181b directly binds to the 3'UTR of TIMP3

HAVECs were co-transfected with a luciferase plasmid containing the 3'UTR TIMP3 sequence where miR-181b binds and miR-181b mimic or control. After 48 hours luciferase expression was quantified and normalized to protein content. n=4, *p<0.05

4.2.4 miR-181b regulates ECM degradation via silencing of TIMP3

We found that miR-181b regulates TIMP3, an inhibitor of tissue metalloproteinases, therefore, we hypothesize that miR-181b regulates ECM degradation via silencing of TIMP3. To this end, we studied whether miR-181b regulates ECM degradation in HAVECs by upregulating miR-181b (via miR-181b mimic) or silencing miR-181b (via anti-miR-181b) in HAVECs for 48 hours and measuring MMP activity (Fig. 4.8) via DQ gelatin assay. We found that upregulation of miR-181b lead to increased gelatinase activity while the opposite was observed when miR-181b was downregulated.

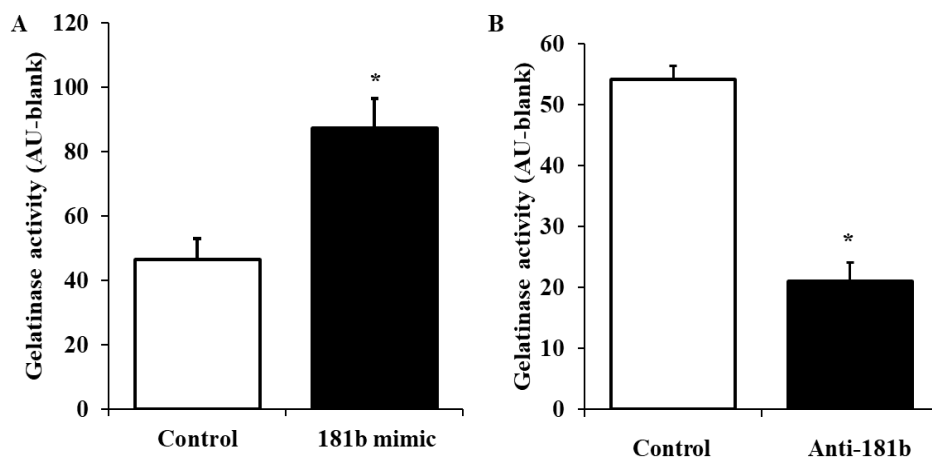


Figure 4.8 MiR-181b regulates ECM degradation in HAVECs

A,B) HAVECs were transfected miR-181b mimic (**A**), anti-miR-181b (**B**), or its respective controls for 48 hours and MMP activity was assayed via DQ gelatin assay. n=4, *p<0.05

We then proceeded to determine if the effect of miR-181b in MMP activity was TIMP3-dependent. First, we treated HAVECs with anti-miR-181b and siRNA targeting TIMP3 (siTIMP3) for 48 hours and measured MMP activity via DQ gelatin assay (Fig. 4.9A). Our results showed that **1)** silencing of TIMP3 increases gelatinase activity and **2)** the decrease of gelatinase activity that we observed when silencing miR-181b can be prevented by silencing TIMP3. Second, we treated HAVECs with miR-181b mimic and GM6001 (MMP inhibitor) at 30nM for 48 hours and measured MMP activity via DQ gelatin assay (Fig. 4.9B). From this study we found that **1)** use of MMP inhibitor decreased gelatinase activity in HAVECs and **2)** the increase in gelatinase activity that occurred when miR-181b was upregulated can be reverted by using an MMP inhibitor such as GM6001. These results showed that miR-181b regulates ECM degradation by silencing TIMP3 which increases MMP activity.

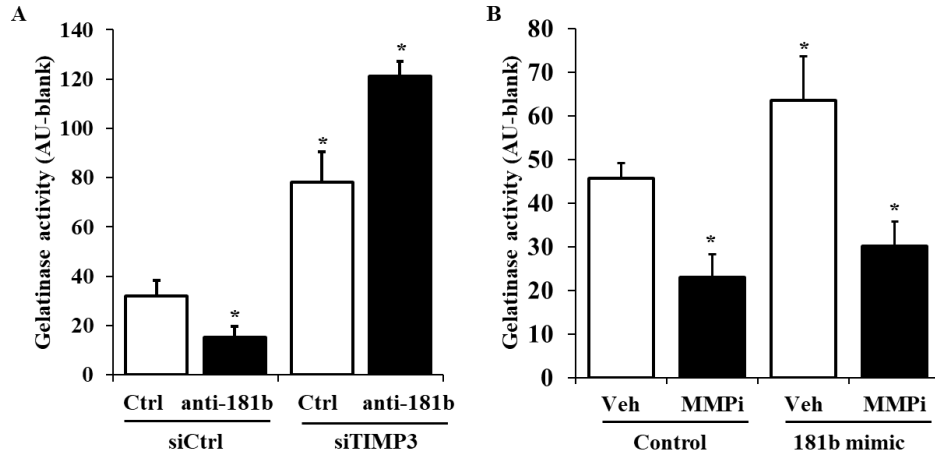


Figure 4.9 miR-181b regulates ECM degradation by silencing TIMP3

A) HAVECs were co-transfected with anti-miR-181b, siTIMP3, or its respective controls for 48 hours and gelatinase activity was assayed via DQ gelatin assay. **B)** HAVECs were transfected with miR-181b mimic and treated with GM6001 (MMP inhibitor) at 30nM for 48 hours and gelatinase activity was measured via DQ gelatin assay. n=4, *p<0.05.

4.2.5 miR-181b regulates shear-regulated ECM degradation in HAVECs

To test whether OS-induced MMP activity is controlled by mechanosensitive miR-181b, we subjected HAVECs treated with miR-181b mimic to either LS or OS conditions for 24h. First, we quantified the levels of miR-181b after shear was applied and we found that miR-181b levels were increased dramatically in both LS and OS after miR-181b treatment (Fig. 4.10A), and this increase in miR-181b expression correlated with increased gelatinase/MMP activity in both shear stress conditions (Fig. 4.10B). Notably, the usually low levels of gelatinase activity observed in LS were increased 4-fold after treatment with miR-181b mimic. We performed the same studies using HAVECs treated with anti-miR-181b under LS and OS. Anti-miR-181b treatment decreased miR-181b by 80% (Fig. 4.10C), and the normally high levels of MMP activity observed in OS were abrogated upon anti-miR-181b treatment (Fig. 4.10D). These data suggest that the shear-dependent change in matrix degradation we observed in HAVECs is dependent on miR-181b, which may be a master miRNA regulator of shear-dependent matrix changes in the aortic valve endothelium.

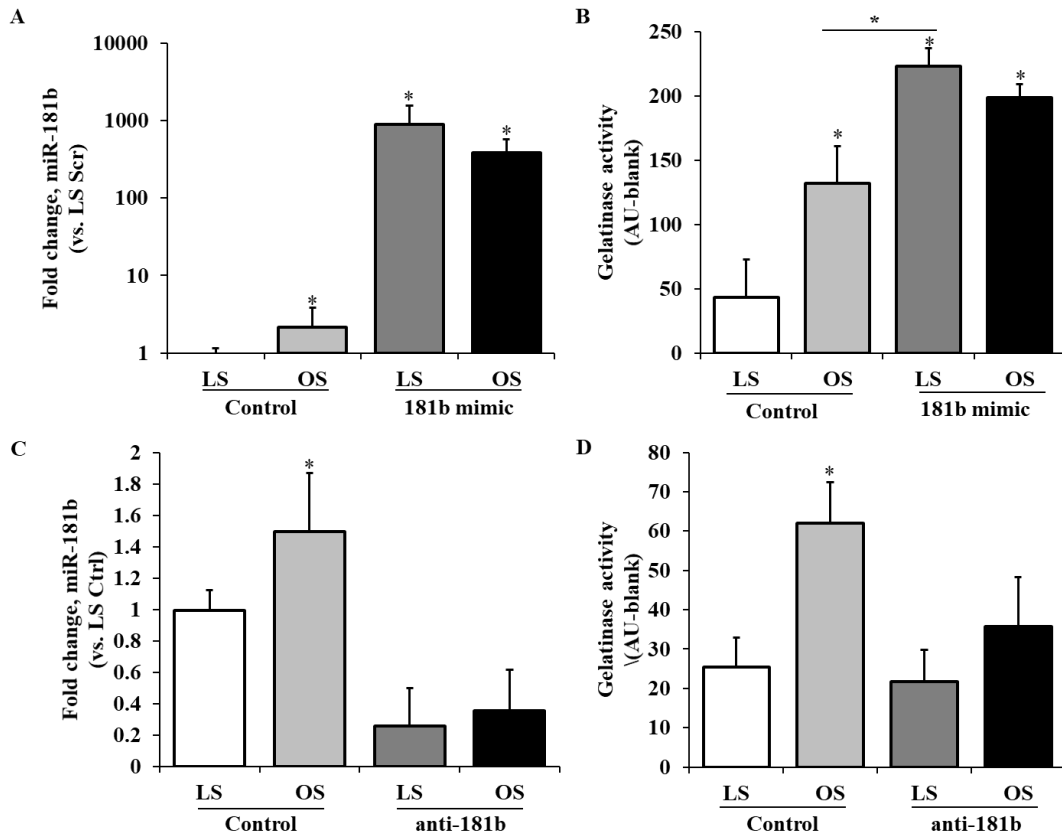


Figure 4.10 miR-181b is responsible for shear-dependent ECM degradation

A-B) HAVECs were transfected with miR-181 mimic (181b mimic) or mimic control at 5nM for 24h before application of 24h shear-stress conditions either LS or OS. Expression of mir-181b was quantified via qPCR (**A**), and MMP activity was measured via gelatinase activity assay (**B**). **C-D)** HAVECs were transfected with anti-miR-181b (anti-181b) or anti-miR control at 100nM for 24h previous to application of either LS or OS. Expression of mir-181b was quantified via qPCR (**C**) and MMP activity was measured via gelatinase activity assay (**D**). n=4, *p<0.05.

4.3 Discussion and future directions

These studies are the first to show a direct effect of mechanosensitive miRNAs on matrix degradation in the aortic valve endothelium. While the levels and activity of MMPs have been suggested in previous studies to play a role in the degradation of the valvular extracellular matrix contributing to calcification [261, 322, 323], this work suggests a causative endothelial mechanosensitive pathway responsible for this phenomenon. MMPs

are critical for the progression of cardiovascular disease, including atherosclerosis [324-326] and ischemia reperfusion injury [327, 328]. However, MMP activity has not been shown to participate directly in valve calcification, and MMP-mediated ECM degradation may participate in the progression of inflammatory cell infiltration [260, 329]. Here, we have highlighted a novel pathway, showing TIMP3 inhibition of MMP activity is vital for maintenance of valve endothelial cell homeostasis, and disturbed flow leads to downregulation of TIMP3 via mechanosensitive microRNA-181b. This increases MMP activity and leads to increased matrix degradation, known to lead to worsened valve sclerosis and calcification [21, 330].

While TIMP3 has previously been identified as a major regulator of matrix remodeling [331], our current work is the first to identify its role in the valve endothelium. In separate studies, our group has shown that TIMP3 is downregulated by disturbed flow in atherosclerosis via miR-712, which leads to exacerbated MMP activity and lesion formation [318]. The study highlighted here shows a similar role for TIMP3 in the valvular endothelium, although under the control of a different mechanosensitive microRNA, miR-181b. We have performed a microarray to determine microRNAs that are mechanosensitive in HAVECs and porcine valves [220], which proved a powerful tool in determining microRNAs which may be regulated by differential flow in the valve. The array revealed miR-181b to be significantly upregulated in disturbed flow and the porcine fibrosa, which was confirmed by qPCR shown in these studies..

The targeting of TIMP3 by microRNA-181b has been described in the context of cancers, including gastric cancer [305] and hepatocellular carcinoma [332]. In these diseases, miR-181b suppresses TIMP3 and increases MMP activity, allowing for tumor growth and infiltration into the surrounding tissue environment. These studies correlate with our observations that miR-181b downregulates TIMP3 in the valve endothelium, which increases matrix remodeling, critical for valve sclerosis and calcification. The analysis of this pathway in previous studies may also point toward a regulatory pathway

upstream: Wang et al. found that miR-181b can be induced by alteration of transforming growth factor-beta and its Smad targets [332]. This pathway and its relevance to the aortic valve warrant further study in the valve endothelium and is a focus of our future work.

Our current studies demonstrate the pathological role of microRNA-181b induced by disturbed flow in valve endothelium. Our work clearly shows that mechanosensitive microRNA-181b targets and downregulates TIMP3 via binding to the TIMP3 3'UTR, leading to increased MMP-mediated degradation of extracellular matrix. This microRNA in particular has been studied at length in various endothelial cells and diseases [303, 304, 333, 334]. It seems to play a conflicting role in disease progression or protection depending on tissue and disease context. In elegant and thorough studies, microRNA-181b was shown to protect against atherosclerosis by inhibiting endothelial inflammation [303]. Circulating miR-181b was found to be reduced in the blood of patients with coronary artery disease and ApoE^{-/-} mice fed with high-fat diet also presented lower levels of miR-181b in the aortic intima layer. Systemic delivery of miR-181b in ApoE^{-/-} fed with high-fat diet inhibited atherosclerotic lesion formation, proinflammatory gene expression and the influx of lesional macrophages and CD4⁺ T cells in the vessel wall. While our current work shows an opposing role for this microRNA in the valve, this incongruity may indicate a complex system of regulation of microRNA-181b that is context-dependent. In certain cancers, miR-181b is tumorigenic [335], while it may regulate glucose levels in adipose tissue [334]. Thus, our work combined with the previously defined pathways of miR-181b regulation indicate a tissue-specific role for this microRNA. While more work is required to determine the reasons for the differences observed between our studies and others, we have clearly observed a pathological role for miR-181b in the valve endothelium.

We have also shown here that microRNA-181b targets other genes in HAVECs, including SIRT1 and GATA6. These studies are the first to demonstrate the mechanosensitivity of both of these genes, and their targeting by microRNA181b. In fact, the role of SIRT1 and GATA6 in the valve has not yet been described. Thus, these represent

novel targets for future studies. Both of these genes are known to play a protective role in atherosclerosis: in an angiotensin-induced model of atherosclerosis, SIRT1 induces endothelial relaxation and may inhibit the formation of foam cells in the vasculature [336]. GATA6 protects against intimal hyperplasia by controlling smooth muscle cell differentiation as well as inhibiting VCAM-1 expression in treated endothelial cells [337]. Both of these targets present novel avenues of study in the aortic valve, and prove to be as important as TIMP3 in maintaining valvular homeostasis and tissue integrity. When taken together, the wide array of functions controlled by target genes of miR-181b suggest that this miRNA may be a master regulator of aortic valve endothelial cells under disturbed flow, orchestrating a complex a multi-faceted change in the phenotype of the cells and the structure of the whole valve. The pathway we have highlighted in this Aim may be just one of many important for this change, and thus further analysis is necessary to obtain a better overall picture of miR-181b network regulation.

A substantial portion of this chapter was published in:

Fernandez Esmerats J.*, Heath JM*, Khambounenheuang L., Kumar S. Jo H., “Mechanosensitive microRNA-181b Regulates Aortic Valve Endothelial Matrix Degradation by Targeting TIMP3”, *Cardiovascular Engineering and Technology*, 2017

5 Role of miR-483 in HAVEC biology and AV calcification

5.1 Introduction

In this Aim, we focus on studying the role the novel shear-sensitive miRNA from our HAVEC array, miR-483. Recently, miR-483 has been shown to target the connective tissue growth factor (CTGF), which mediates EndMT in human umbilical vein ECs [273]. In another study using vascular smooth muscle cells and heart cells, treatment with angiotensin II reduced expression of miR-483, which was shown to target four members of the renin-angiotensin system: AGT, ACE-1, ACE-2 and AGTR2 [271]; however, the role of miR-483 in HAVEC biology and CAVD is still unknown. Our initial studies validated our array results showing that miR-483 is shear-sensitive *in vitro* in sheared HAVECs as well as in porcine AVs where we found that miR-483 is expressed in a side-dependent manner in the valvular endothelium.

Here, we found that UBE2C is a major target of miR-483 [338]. UBE2C, also known as UBCH10, is an E2 ubiquitin conjugating enzyme. While overexpression of UBE2C is well documented in various cancer tissues and cells [277, 290, 292, 294, 339], its role in endothelial function and cardiovascular disease is yet to be determined. Ubiquitination is upregulated in calcified valves [340], but its underlying mechanisms and whether it plays any role in AV calcification or endothelial function is unknown. Interestingly, Hypoxia-Inducible Factor 1- α (HIF1 α) expression, which is controlled by Von Hippel Lindau protein (pVHL) [284, 285, 341, 342], is upregulated by d-flow conditions in vascular ECs and atherosclerotic conditions [343]. UBE2C is a member of the Anaphase Promoting Complex/Cyclosome (APC/C), which is also known to bind to pVHL [279]. Therefore, we hypothesize that UBE2C regulates the HIF1 α pathway by post-transcriptionally regulating pVHL via ubiquitination.

In this Aim, we show the novel mechanism by which the miR-483 target, UBE2C, regulates the pVHL and HIF1 α pathway, leading to endothelial inflammation, EndMT, and subsequent AV calcification. We also show evidence suggesting that miR-483 mimic and HIF1 α inhibitors may serve as potential therapeutics to prevent and treat CAVD.

5.2 Results

5.2.1 *miR-483 is side-specific and shear-sensitive in valvular endothelium*

miR-483 was found to be shear-sensitive in our microRNA array where we found that LS upregulated its expression compared to OS conditions [14]. Here, we validated the shear-sensitivity of miR-483 by exposing HAVECs to LS or OS conditions for 24 hours and measuring expression of miR-483 via qPCR (Fig. 5.1A). We found that there was a ~70% decrease of miR-483 expression in OS compared to LS conditions. Next, we wanted to study whether miR-483 was expressed in a side-specific manner in aortic valves. We harvested healthy porcine aortic valve leaflets and isolated endothelial-enriched total RNAs from each side of the valve and measured expression of miR-483 via qPCR (Fig. 5.2B) where we found that there was a ~two-fold increase in miR-483 expression in the ventricularis (endogenously exposed to LS) compared to the fibrosa (endogenously exposed to OS). These studies validated our previous array data and showed that miR-483 is also a side-specific miRNA in the aortic valve which further reinforces our hypothesis that miR-483 is a protective miRNA that protects the ventricularis from disease.

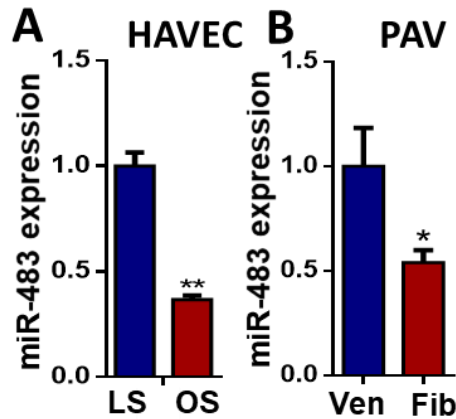


Figure 5.1 Regulation of miR-483 in HAVECs

HAVECs were treated with 10nM of miR-483 mimic or 100nM of anti-miR-483 (or controls) for 24 h and expression of miR-483 was assessed via qPCR. n=4, *p<0.05

5.2.2 *miR-483 regulates inflammation, EndMT, proliferation and apoptosis in HAVECs*

Once we validated the shear- and side-sensitivity of miR-483 we proceeded to determine the functional role of miR-483 in valvular endothelium. To this end we have studied the following functions: inflammation, EndMT, proliferation, apoptosis and migration. To study the role of miR-483 we treated cells with a miR-483 mimic at a dose of 10nM (to overexpress miR-483), an anti-miR-483 at a dose of 100nM (to inhibit expression of miR-483) or its respective controls. After treating HAVECs with miR-483 mimic or anti-miR-483 for 48 hours, we collected the cells and measured expression of miR-483 via qPCR and found that treatment with the miR-483 mimic increased expression of miR-483 by ~280-fold while treatment with anti-miR-483 silenced miR-483 by ~75% compared to their respective controls in HAVECs (Fig. 5.2).

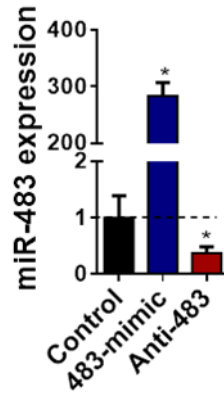


Figure 5.2 Regulation of miR-483 in HAVECs

HAVECs were treated with 10nM of miR-483 mimic or 100nM of anti-miR-483 (or controls) for 24 h and expression of miR-483 was assessed via qPCR. n=4, *p<0.05

The first endothelial function that we studied was inflammation. We have assessed inflammation by conducting a monocyte adhesion assay, and by measuring inflammation markers. HAVECs were treated with miR-483 mimic or anti-miR-483 in static conditions for 48 hours and monocyte adhesion assay (Fig. 5.3A) or measurement of inflammation markers via qPCR (Fig. 5.3B) was performed. Our results showed that increased levels of

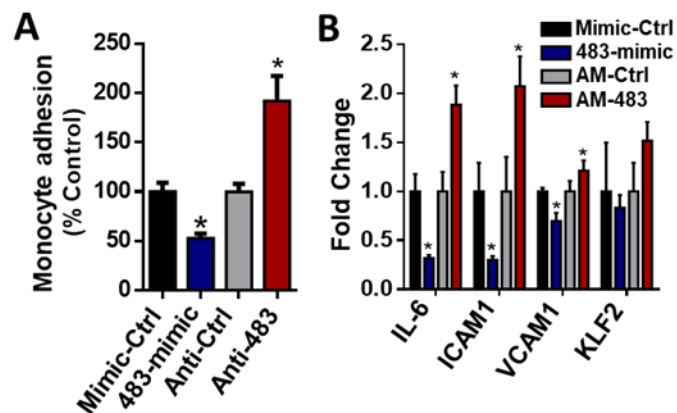


Figure 5.3 miR-483 regulates inflammation in static HAVECs

A,B) Inflammation studies were conducted in HAVECs by treating with a miR-483 mimic (483-mimic) or control (Mimic-Ctrl) or a miR-483 inhibitor (Anti-483) or control (Anti-Ctrl). Monocyte adhesion assay was conducted (**A**) as well as quantifying the inflammation markers IL-6, ICAM-1, VCAM-1 or KLF2 (**B**). n=6-10, *p<0.05.

miR-483 lead to a decrease in monocyte adhesion and a decrease in pro-inflammatory markers such as IL-6, VCAM1 and ICAM1 while silencing of miR-483 induced endothelial inflammation.

To determine the functional role of miR-483 in shear-induced endothelial inflammation we treated HAVECs with miR-483 mimic or anti-miR-483 for 24 hours and exposed the cells to OS or LS conditions respectively for 24 hours. Monocyte adhesion (Fig. 5.4A) and inflammation marker quantification (Fig. 5.4B and 5.4C) was conducted. We found similar results as in static conditions, increased levels of miR-483 decreased OS-induced inflammation while silencing of miR-483 lead to increased inflammation in LS-

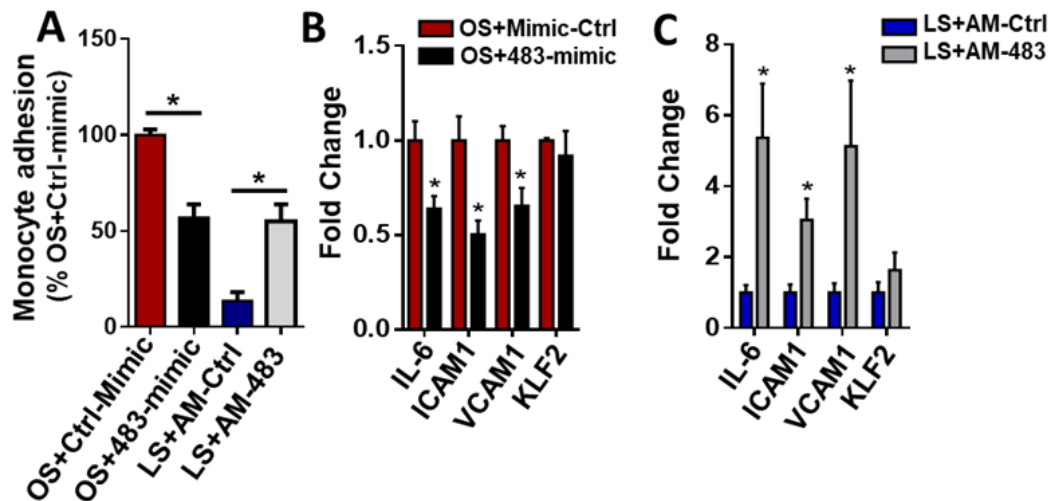


Figure 5.4 miR-483 regulates shear-induced inflammation in HAVECs

A-C) Inflammation studies were conducted in HAVECs by treating with a miR-483 mimic (483-mimic) or control (Mimic-Ctrl) and applying OS shear stress conditions or a miR-483 inhibitor (Anti-483) or control (Anti-Ctrl) and applying LS shear stress conditions. Monocyte adhesion assay was conducted (**A**) as well as quantification of the inflammatory markers IL-6, ICAM-1, VCAM-1 or KLF2 (**B**, **C**). n=6-10, *p<0.05.

conditions. These results showed that miR-483 plays a role in static as well as shear-induced inflammation in HAVECs.

Next, we studied the role of miR-483 in EndMT as it is a cellular process well-known to be involved in the pathogenesis of CAVD [344]. To this end, we treated HAVECs with miR-483 mimic in static conditions for 48 hours and measured expression of EndMT markers via qPCR (Fig. 5.5A). From this study we observed that miR-483 did not affect EndMT in static conditions. Knowing that EndMT is highly regulated by shear stress we decided to treat HAVECs with miR-483 mimic or anti-mir-483 for 24 hours and then expose the cells to OS or LS conditions for 24 hours respectively. We then quantified expression of EndMT markers in shear conditions (Fig. 5.5B and 5.5C) via qPCR. These studies showed that treatment with miR-483 mimic in OS conditions leads to a significant decrease in Twist1, Snail and Transgelin while treatment with anti-miR-483 in LS conditions leads to increased levels of Twist1, Snail, Transgelin and Slug. These results

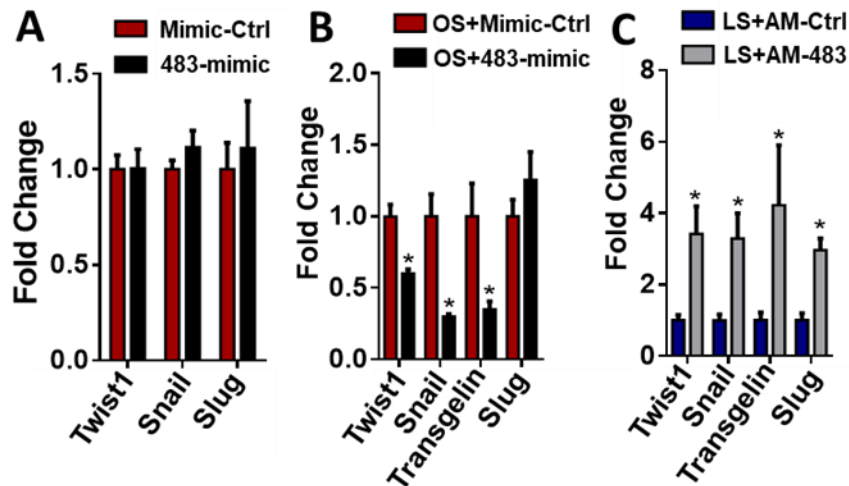


Figure 5.5 miR-483 regulates shear-induced EndMT

A) HAVCs were treated with miR-483 mimic for 48 hours and expression of EndMT markers was quantified via qPCR. B,C) HAVECs were transfected with miR-483 mimic or anti-miR-483 for 24 hours and exposed to OS or LS shear conditions for 24 hours respectively. Expression of EndMT markers was quantified via qPCR. n=4, *p<0.05.

showed that miR-483 controls shear-induced EndMT in HAVECs and that treatment with miR-483 mimic leads to decreased EndMT in disturbed flow conditions

We have also studied proliferation, apoptosis and cell migration by treating HAVECs with miR-483 mimic or anti-miR-483 for 48 hours and then conducting functional studies for each of the different cellular functions. To measure proliferation, we fixed the treated HAVECs and stained with KI-67, a well-known marker of proliferation[345], and quantified percentage of cells that were positive for this marker (Fig. 5.6A). We found that treatment with miR-483 mimic leads to decreased proliferation while silencing of miR-483 via anti-miR-483 treatment leads to increased proliferation. Next, we studied apoptosis by conducting a TUNEL assay and quantifying percentage of apoptotic cells (Fig. 5.6B). We observed that anti-miR-483 leads to increased apoptosis while treatment with miR-483 mimic had no effect on apoptosis. Last, we measured cell

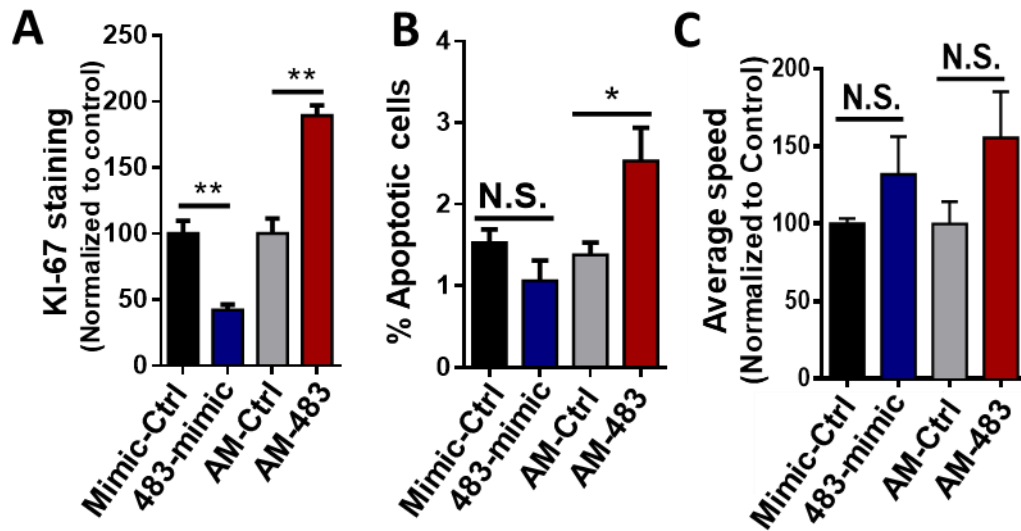


Figure 5.6 miR-483 regulates proliferation and apoptosis but has no effect in cell migration.

A) Proliferation (via KI-67 staining), B) apoptosis (via TUNEL staining), and C) migration (via scratch assay) were assessed in HAVECs treated with miR-483 mimic or anti-miR-483. n=3-6, *p<0.05

migration by conducting a scratch assay and measuring the average speed of the scratch closure (Fig. 5.6C) and found that miR-483 had no effect on HAVEC migration.

Overall, our data suggests that miR-483 plays a role in HAVEC inflammation, EndMT, proliferation and apoptosis. These functions are known to be involved in CAVD and therefore it reinforces our hypothesis that miR-483 plays a protective role in the ventricularis side. However, we will focus on studying inflammation and EndMT as there are the most critical functions relevant to CAVD.

5.2.3 *KLF2 regulates expression of IGF2 and miR-483*

miR-483 is located in the intronic region of the Insulin-like growth factor 2 (IGF2) between exons 7 and 8 (Fig. 5.7A). Interestingly, KLF2, a well-known shear-sensitive gene in the endothelium [5, 306], was found to upregulate expression of IGF2 in a study conducted by Dekker et al [346]. Therefore, we hypothesize that KLF2 will drive the expression of IGF2 and miR-483 (Fig. 5.7A). We first measured the expression of KLF2, IGF2 and miR-483 by qPCR in HAVECs exposed to LS or OS for 24 hours (Fig. 5.7B) and found that these three genes were significantly upregulated in LS compared to OS

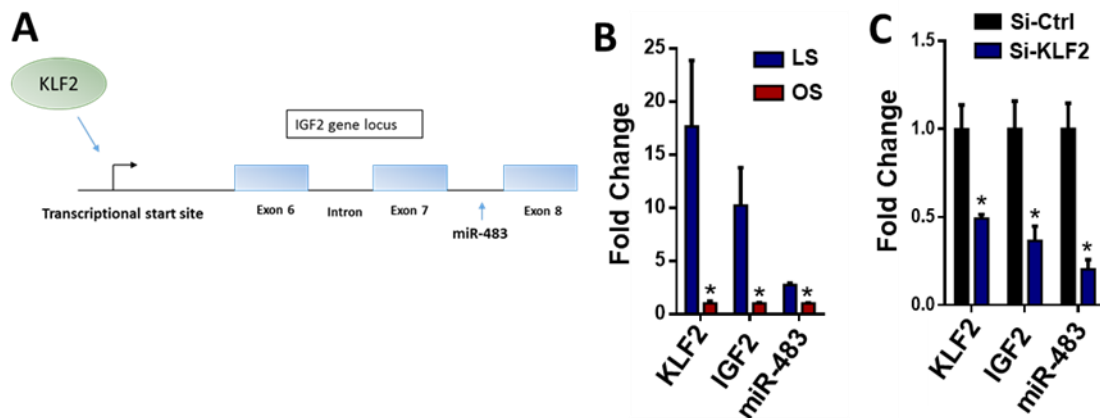


Figure 5.7 miR-483 is an intronic miRNA in IGF2 regulated by KLF2

A) Genomic location of miR-483 in the IGF2 gene. **B)** HAVECs were exposed to LS or OS shear stress conditions for 24 hours and expression of KLF2, IGF2 and miR-483 was quantified via qPCR. **C)** HAVECs were treated with siKLF2 for 24 hours and expression of KLF2, IGF2 and miR-483 was quantified via qPCR. n=4, *p<0.05.

conditions. We then treated HAVECs with siKLF2 at 50nM for 48 hours and quantified the expression of KLF2, IGF2 and miR-483 by qPCR (Fig. 5.7C) and found that decrease of KLF2 leads to decreased levels of IGF2 and miR-483 thus suggesting that KLF2 regulates IGF2 and miR-483 expression in HAVECs. It has been previously shown that KLF4 regulates expression of miR-483 in the endothelium [273] but this is the first time it has been shown that the shear-sensitive KLF2 regulates miR-483 expression.

5.2.4 miR-483 regulates shear-dependent expression of UBE2C and ASH2L

To determine the mechanisms by which miR-483 exerts its function in valvular endothelium we identified shear-sensitive targets regulated by miR-483. To this end, we conducted an *in silico* analysis comparing predicted targets of miR-483 (950 predicted genes by the miRWalk and miRTarBase databases) with OS-induced genes (239 genes) from our previous HAVEC transcriptome array study (Fig. 5.8A) [14]. This *in silico*

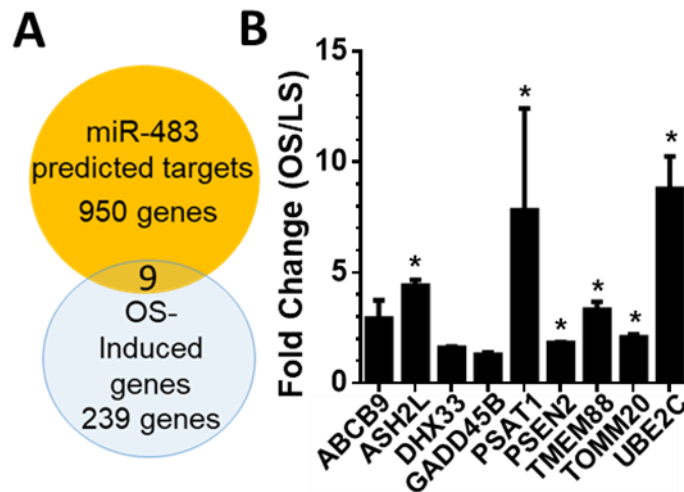


Figure 5.8 In silico analysis to identify potential shear-sensitive targets of miR-483

A,B) An *in silico* analysis was conducted by comparing predicted targets of miR-483 (from miRwalk and mirtarbase databases) with OS-induced genes in HAVECs from our previously published array ⁹, resulting in 9 potential shear-sensitive target genes (**A**). The shear-sensitivity of these 9 genes was validated by qPCR in HAVECs exposed to LS or OS conditions for 24h (**B**). n=4, *p<0.05

analysis revealed nine genes that were predicted gene targets of miR-483 and shear-sensitive genes in our HAVEC transcriptome microarray: ABCB9, ASH2L, DHX33, GADD45B, PSAT1, PSEN2, TMEM88, TOMM20, and UBE2C (Fig. 5.8B). To validate their shear-sensitivity, HAVECs were exposed to LS or OS conditions for 24 hours and the expression of these nine genes was measured by qPCR. This study indicated that just six of these nine genes were increased by OS compared to LS conditions in HAVECs (Fig. 5.9B).

We next determined which of these six shear-sensitive genes were regulated by miR-483 using the miR-483-mimic or anti-miR-483. The results showed that ASH2L, UBE2C and PSAT1 were consistently downregulated when HAVECs were treated with a miR-483 mimic (Fig. 5.9A) and they were upregulated when HAVECs were treated with anti-miR-483 (Fig. 5.9B) while the other three genes did not respond to changes to miR-483 expression in HAVECs.

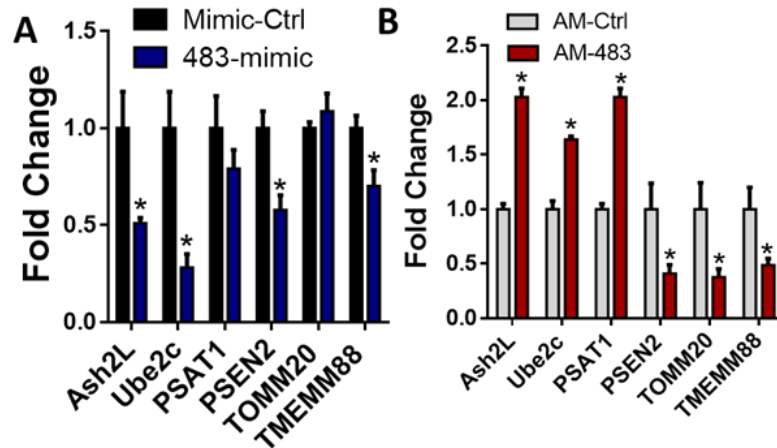


Figure 5.9 ASH2L, UBE2C and PSAT1 are regulated by miR-483 in static HAVECs

A,B) HAVECs were treated with miR-483-mimic or anti-miR-483 for 48 hours. Expression of predicted targets of miR-483 was assessed in cells treated with miR-483 mimic (**A**) or anti-miR-483 (**B**) by qPCR. n=4, *p<0.05.

We further validated if the shear-sensitive expression of ASH2L, UBE2C and PSAT1 were mediated by miR-483 by treating HAVECs with miR-483 mimic or anti-miR-

483 for 24 hours followed by OS or LS for 24 hours. Cell lysate was collected and expression of ASH2L, UBE2C and PSAT1 was measured by qPCR. Our results showed that shear-dependent expression of ASH2L and UBE2C was controlled by miR-483 in HAVECs while PSAT1 was not (Fig. 5.10A and 5.10B). We then determined if UBE2C and ASH2L were also shear-sensitive as the protein level by exposing HAVECs to LS or OS conditions and measuring protein expression of UBE2C and ASH2L by western blot. At the protein level, OS exposure significantly increased ASH2L and UBE2C expression compared to the LS condition in HAVECs (Fig. 5.10C and 5.10D).

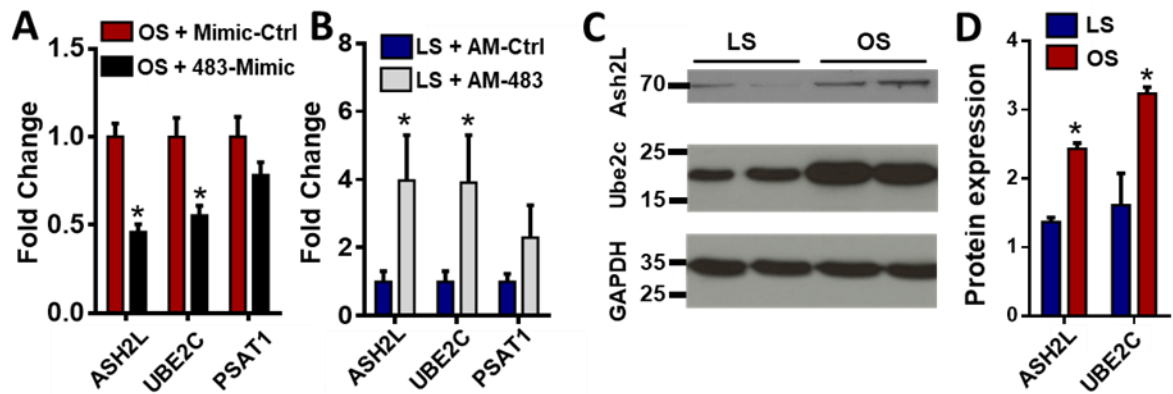


Figure 5.10 UBE2C and ASH2L are shear-sensitive targets of miR-483 in HAVECs

A,B) The three top predicted shear-sensitive targets of miR-483 (Ash2L, UBE2C and PSAT1) were validated by treating HAVECs with either a 483-mimic or an anti-miR-483 in OS conditions (**A**) or LS conditions (**B**) respectively. **C,D)** Shear-sensitivity of Ash2L and UBE2C at the protein level was quantified in HAVECs exposed to LS or OS shear stress conditions. GAPDH protein levels were quantified as loading control. **D)** Quantification of western blot bands using ImageJ. n=3-4, *p<0.05

ASH2L is a histone methyltransferase responsible for the trimethylation of histone 3 lysine 4 (H3K4me3). This epigenetic modification induces chromatin opening allowing for gene transcription [347]. H3K4me3 has been shown to be upregulated in lymphatic endothelial cells [348] as well as in aortic valve stenosis where it was shown to be upregulated in the promoter region of pro-osteogenic genes in a Notch1^{+/-} mouse model of AV stenosis [349]. UBE2C is an E2 ligase in the ubiquitin pathway that interacts with the

Anaphase promoting complex (APC/C) [350]. Interestingly, ubiquitination has been shown to be upregulated in calcified human AVs [340] thus making UBE2C a more interesting target for further study and the main focus of this thesis Aim. UBE2C has been previously shown to be regulated by miR-483 via 3'UTR luciferase assay [338] and to further validate that miR-483 regulates its expression in HAVECs we treated HAVECs with miR-483 for 24 hours followed by 24 hours of OS. Cells were collected, and western blotting was conducted to measure protein levels of UBE2C (Fig. 5.11A). We found that miR-483 decreased OS-induced levels of UBE2C. Last, we stained sclerotic human valves and stained for UBE2C (Fig. 5.11C) and found that UBE2C was significantly upregulated in the fibrosa layer compared to ventricularis (Fig 5.11D). These results demonstrated that UBE2C is regulated *in vivo* by the endogenous shear stress conditions and that it may play a role in the development of side-specific CAVD.

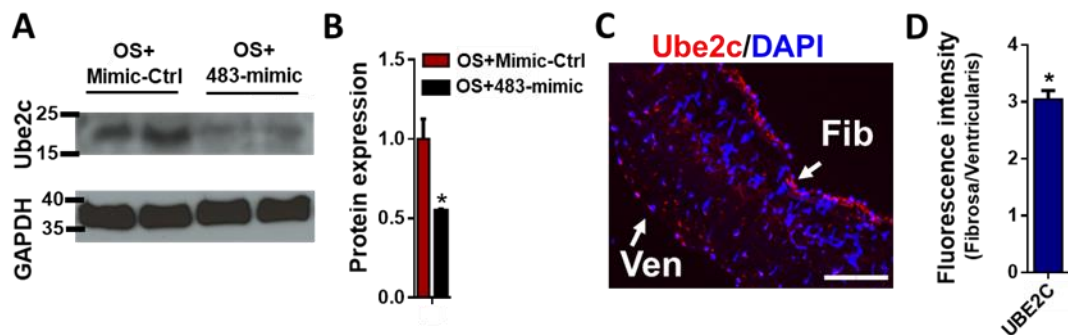


Figure 5.11 UBE2C is side-specific and is regulated by miR-483 in OS conditions

A,B) HAVECs were treated with miR-483 mimic for 24 hours followed by OS for 24 hours. Protein expression of UBE2C was measured by western blotting (**A**) and quantified via ImageJ (**B**). **C,D)** Non-calcified human AVs were stained with UBE2C antibodies and with DAPI (**C**). Quantification was conducted via ImageJ (**D**). n=3-5, *p<0.05.

5.2.5 miR-483 exerts its anti-inflammatory role via silencing of UBE2C

As we have previously shown, miR-483 reduced valvular endothelial inflammation (Fig. 5.3 and 5.4). To determine whether UBE2C played a role in the anti-inflammatory role of miR-483 we transfected HAVECs with anti-miR-483 or siUBE2C alone or co-transfected with anti-miR-483 and siUBE2C and measured inflammation via monocyte

adhesion (Fig. 5.12A) and quantified the pro-inflammatory markers VCAM1 and ICAM1 (Fig. 5.12B). We found that silencing of UBE2C decreased inflammation while silencing of anti-miR-483 increased inflammation. Interestingly, when we silence both UBE2C and miR-483 we observed inflammation levels similar to our control conditions showing that the pro-inflammatory effect of anti-miR-483 can be prevented by silencing UBE2C. To further validate the pro-inflammatory role of UBE2C, HAVECs were transfected with a UBE2C overexpression plasmid (1 μ g and 2.5 μ g), and we conducted a monocyte adhesion assay (Fig. 5.12C). This study showed a UBE2C-dose-dependent increase in monocyte adhesion.

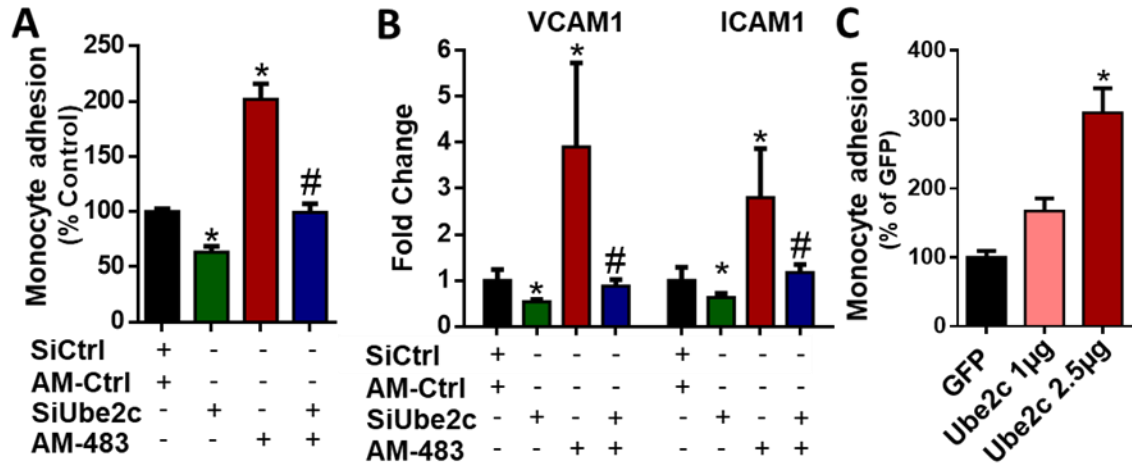


Figure 5.12 UBE2C regulates miR-483 dependent anti-inflammatory effect in HAVECs

A,B) HAVECs were co- transfected with siUBE2C or siCtrl and anti-miR-483 (AM-483) or anti-miR-control (AM-Ctrl), followed by monocyte adhesion (**A**) and qPCR analysis for inflammatory markers (**B**). **C)** HAVECs transfected with UBE2C overexpression plasmid or GFP plasmid were used for monocyte adhesion assay. n=6-10, *p<0.05.

5.2.6 UBE2C mediates OS-induced endothelial inflammation and EndMT

Next, we tested if OS-induced pro-inflammatory and pro-EndMT endothelial responses could be reverted by knockdown of UBE2C in HAVECs by treatment with siUbe2c. UBE2C knockdown prevented OS-induced monocyte adhesion and induction of the pro-inflammatory markers (VCAM1 and ICAM1) without affecting KLF2 or ASH2L

expression in HAVECs (Fig. 5.13A and B). Moreover, siUBE2C treatment significantly reduced several markers of EndMT (TWIST1, TAGLN and SLUG) (Fig. 5.13C). Together, these results showed that UBE2C is indeed a key miR-483 target gene, which plays a dominant role in OS-induced pro-inflammatory and pro-EndMT responses in HAVECs.

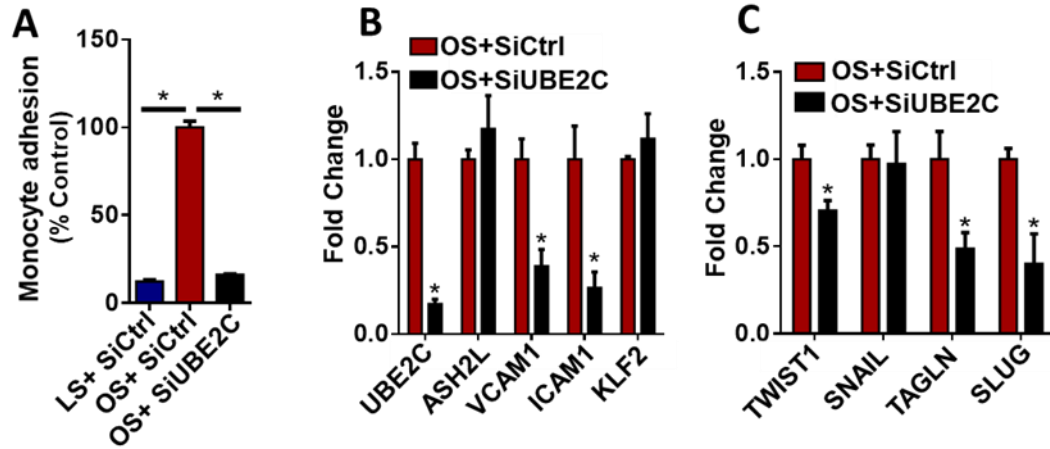


Figure 5.13 UBE2C regulates OS-induced endothelial inflammation and EndMT

A-C) HAVECs treated with siUBE2C or siRNA control (SiCtrl) for 24 hours, followed by OS or LS conditions for another 24 hours. Then, monocyte adhesion (**A**) and qPCR analyses for markers of inflammation (**B**) and EndMT (**C**) were carried out normalized to 18S. n=6-10, *p<0.05.

5.2.7 *pVHL* and *HIF1 α* are shear-sensitive in HAVECs and are regulated by *UBE2C*

We hypothesized that the increase in UBE2C (due to the loss of miR-483 under the OS condition) leads to ubiquitination and degradation of pVHL, which in turn increases HIF1 α levels, leading to increased expression of its target genes, endothelial inflammation and EndMT (Fig. 5.14A). First, we found that the expressions of pVHL and HIF1 α were highly shear-sensitive, but inversely regulated in HAVECs. Under LS exposure for 72 hours in the Ibidi® shear system, expression of pVHL was high, while HIF1 α expression was undetectable. In contrast, under OS, pVHL was low while HIF1 α was high at the protein and mRNA levels (Fig. 5.14B-D).

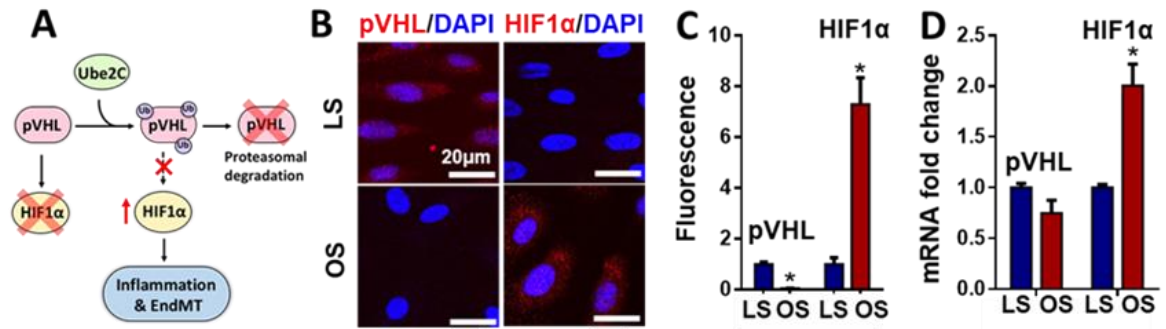


Figure 5.14 pVHL and HIF1 α are shear-sensitive in HAVECs

A) Depicts a hypothesis that overexpression of UBE2C ubiquitinates pVHL, leading to increased HIF1 α level, endothelial inflammation and EndMT. **B-D)** HAVECs sheared for 72 hours by LS or OS were immunostained with antibodies for pVHL or HIF1 α (**B**) and quantification of the image was done using ImageJ (**C**), or by qPCR (**D**) normalized to 18S. n=4, *p<0.05

Next, we studied whether the shear-sensitivity observed in pVHL and HIF1 α was regulated in a UBE2C-dependent manner. To this end, we treated HAVECs with siUBE2C and applied LS or OS conditions and measured protein levels of pVHL and HIF1 α . We found that UBE2C silencing significantly increased pVHL expression while preventing HIF1 α induction under the OS condition (Fig. 5.15 A-D), demonstrating that UBE2C regulates shear-dependent expression of pVHL and HIF1 α .

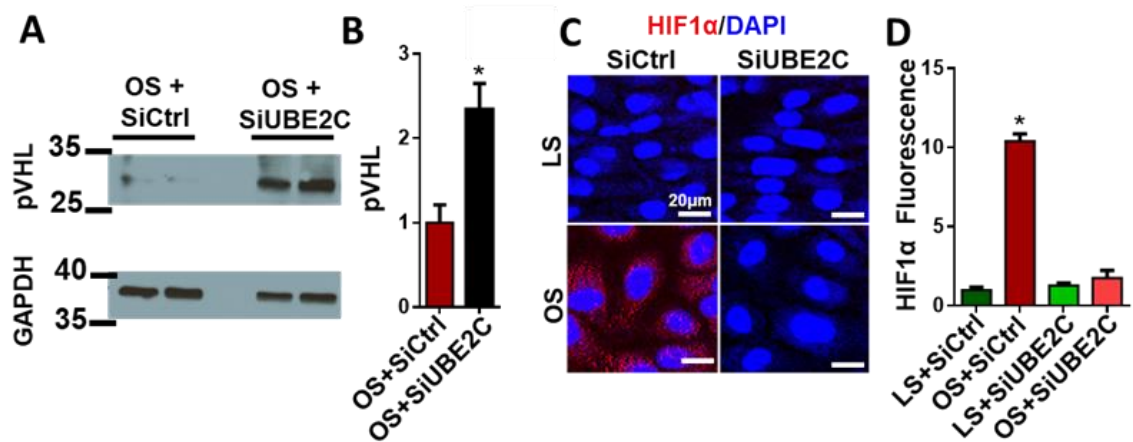


Figure 5.15 UBE2C mediates shear-dependent expression of pVHL and HIF1 α

A) HAVECs treated with siCtrl or siUBE2C for 24 hours, followed by exposure to OS for 24 hours were analyzed by Western blot (A) and ImageJ quantification (B) for pVHL. For HIF1 α study, HAVECs exposed to OS for 72 hour were immunostained with the HIF1 α (C) and Image J quantified (D). n=4-6. *p<0.05

Next, we tested whether the shear-dependent expression of UBE2C, pVHL, and HIF1 α observed in HAVECs *in vitro* was consistent *in vivo* using immunohistochemical staining on human AVs. UBE2C and HIF1 α expression was significantly higher in the fibrosa-side of the human AV leaflets, whereas pVHL expression was higher in the ventricularis-side (Fig. 5.16A and B). Furthermore, markers of inflammation (VCAM1), EndMT (TWIST1), and calcification (RUNX2) (Fig. 5.16A and B) were highly expressed in the fibrosa side demonstrating side-dependent expression of pro-CAVD markers. These staining results clearly corroborate the side-dependent expression of UBE2C, pVHL, and HIF1 α , with markers of inflammation, EndMT, and calcification in the fibrosa side of human AVs.

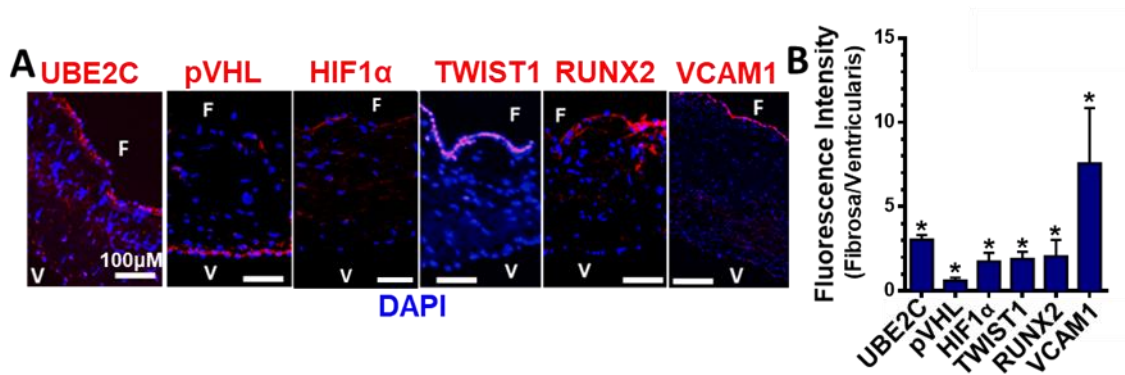


Figure 5.16 UBE2C, pVHL and HIF1 α are expressed in a side-dependent manner in human AV leaflet

A) Human AVs with sclerosis were stained with antibodies to UBE2C, pVHL, HIF1 α , Twist1 and Runx2 with DAPI nuclear staining, and B) shows quantification of the fluorescent intensities of each staining in endothelial layer on each side using Image J. Mean \pm sem n=5, *p<0.05. F: fibrosa, V: ventricularis.

5.2.8 UBE2C binds and ubiquitinates pVHL, leading to its degradation.

We next examined how UBE2C (a E2 ubiquitin ligase) regulates pVHL expression. Although UBE2C is a member of APC/C, which is known to bind and ubiquitinate pVHL for proteasomal degradation [279], it was unknown whether UBE2C can mediate pVHL ubiquitination. Therefore, we tested whether UBE2C mediates pVHL expression in a ubiquitination-dependent manner. To this end, HAVECs were transfected with siUBE2C, and ubiquitinated proteins were immunoprecipitated and western blotted using a pVHL antibody. We found that knockdown of UBE2C decreased ubiquitinated pVHL levels in the immunoprecipitates (Fig. 5.17A). This result was independently validated by immunoprecipitating pVHL first, followed by ubiquitin western blotting, demonstrating that ubiquitination of pVHL was reduced when UBE2C was knocked down in HAVECs (Fig. 5.17B). As expected, levels of pVHL in these cell lysates were increased when

UBE2c was silenced as quantified by ImageJ and normalized to β -ACTIN (Fig. 5.17C and D).

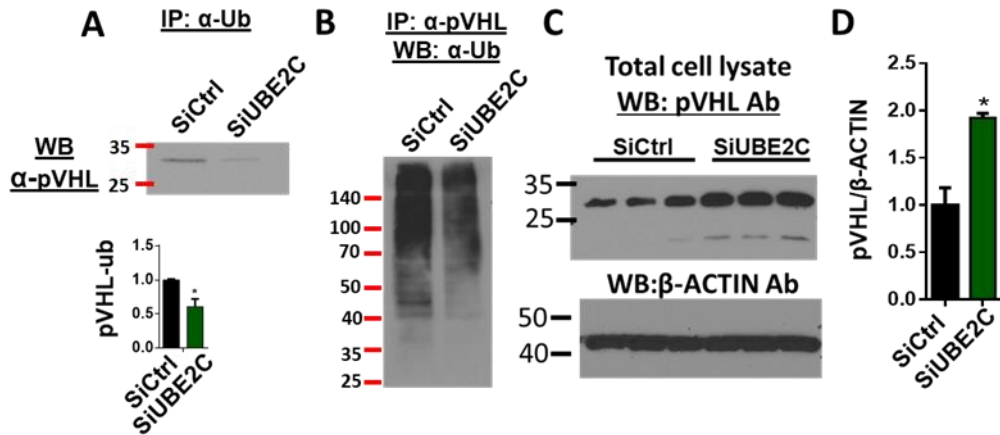


Figure 5.17 UBE2C regulates pVHL ubiquitination in HAVECs

A-B) HAVECs transfected with siUBE2C or siCtrl were immunoprecipitated with an antibody for ubiquitin (Ub) (**A**) or pVHL (**B**) and Western blotted with the pVHL (**A**) or Ub (**B**) antibody. **C-D)** Cell lysate control was western blotted for pVHL and β -ACTIN (**C**) and quantified by ImageJ. n=3 *p<0.05

Since UBE2C has never been shown to bind and ubiquitinate pVHL, we tested whether they associate with each other by co-transfecting HEK cells with plasmids overexpressing UBE2C or RFP as a control and HA-pVHL-WT or HA-pVHL-RRR mutant. The HA-pVHL-RRR mutant has its three Lys ubiquitination sites (K159, K171 and K196) modified to Arg so that they cannot be ubiquitinated [314, 315]. We used HA-tag antibody to immunoprecipitate HA-pVHL-WT and HA-pVHL-RRR. UBE2C co-immunoprecipitated with either HA-pVHL-WT or HA-pVHL-RRR (Fig. 5.18A). Interestingly, the pVHL Western blot of HA-pVHL immunoprecipitates showed bands at ~28, 34, 55, 80 kDa, potentially representing poly-ubiquitinated pVHLs in a manner dependent on UBE2C and pVHL-ubiquitination sites (Fig. 5.18A). Furthermore, the Western blot using the ubiquitin antibody for the HA-pVHL immunoprecipitates showed

ubiquitinated proteins at ~35, 40, 85, 100 kDa in a manner dependent on UBE2C and pVHL-ubiquitination sites (Fig. 5.18B).

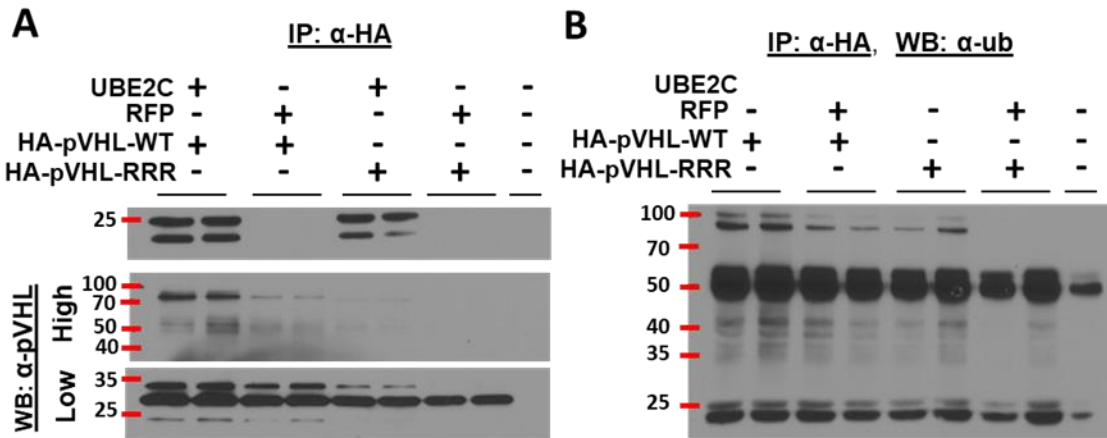


Figure 5.18 UBE2C binds and ubiquitinates pVHL

A,B) HEK cells co-transfected with myc-UBE2C or RFP plasmid (1 μ g) and HA-pVHL-WT or HA-pVHL-RRR mutant plasmids (0.5 μ g) for 48 hours were immunoprecipitated using the antibody to HA-tag and Western blotted with antibodies to UBE2C or pVHL (**A**) (exposed using High intensity ECL and Low intensity ECL) or to Ubiquitin (**B**). Untreated (Unt) HEK cells were used as a control.

Next, we tested whether UBE2C regulates pVHL levels in a ubiquitination-dependent manner by co-transfecting HEK cells with plasmids overexpressing UBE2C or RFP control and HA-pVHL WT or mutants. Four different HA-pVHL double or triple mutants on the three Lys ubiquitination sites were used (RRR, KRR, RKR, and RRK) in comparison to WT [314, 315]. Expression of pVHL-WT and the three pVHL double mutants, but not the RRR triple mutant was decreased as UBE2C expression increased in a dose-dependent manner (Fig. 5.19 and 5.20). This result clearly demonstrates that pVHL degradation is UBE2C-dependent and it requires at least one of the three Lys ubiquitination

sites. These results also demonstrate that UBE2C binds to pVHL and mediates its degradation by the ubiquitination-dependent manner.

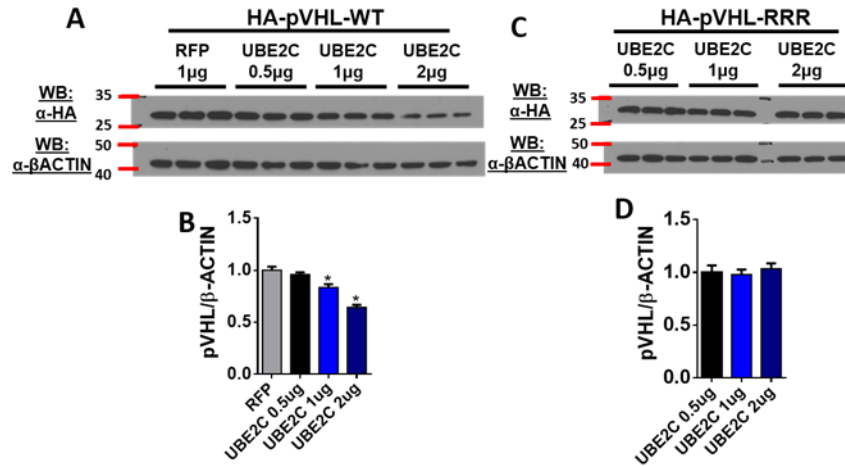


Figure 5.19 Degradation of pVHL by UBE2C requires pVHL ubiquitination sites

A-D) HEK cells co-transfected with HA-pVHL-WT or HA-pVHL-RRR mutant plasmids and increasing dose of UBE2C (0.5-2μg) or RFP plasmids for 48 hours were lysed and Western blotted with antibodies to pVHL and b-actin as an internal control (**A,C**), and ImageJ quantitated (**B,D**). n=3 *p<0.05.

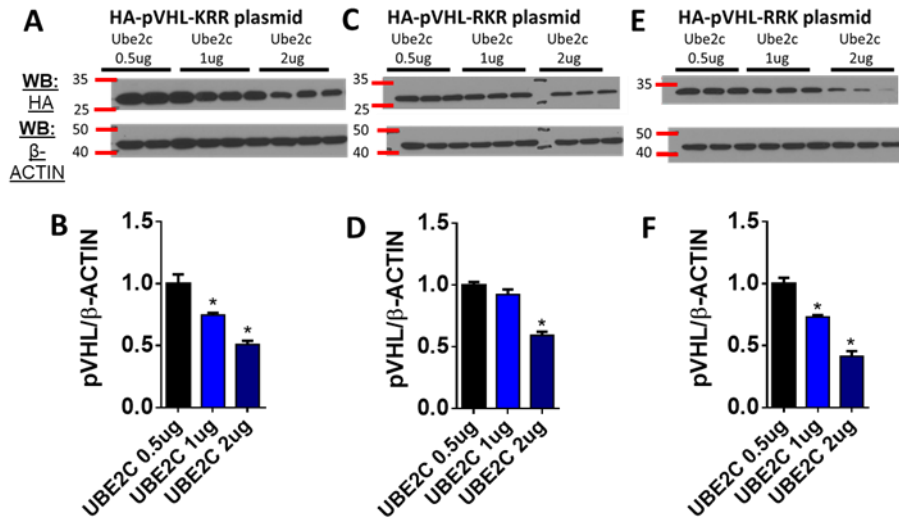


Figure 5.20 UBE2C degrades pVHL in a lysine-dependent manner

A-F) HEK cells were co-transfected with UBE2C (myc-tagged UBE2C) and HA-tagged pVHL plasmids HA-pVHL-KRR (**A, B**), HA-pVHL-RKR (**C, D**) or HA-pVHL-RRK (**E, F**). Western blots for HA-tag and β-ACTIN was conducted (**A, C, E**) and pVHL was quantified using ImageJ. n=3, *p<0.05

5.2.9 *pVHL and HIF1 α mediate UBE2C-dependent inflammation and EndMT in HAVECs.*

Next, we tested whether pVHL and HIF1 α regulate endothelial inflammation and EndMT by using sipVHL or siHIF1 α in HAVECs. Knockdown of pVHL increased monocyte adhesion (Fig. 5.21A) as well as markers of inflammation and EndMT (Fig.5.21B). We also found that knockdown of pVHL did not affect HIF1 α mRNA levels. This was expected (Fig. 5.21B) as pVHL is known to regulate HIF1 α protein levels via ubiquitination and proteasome degradation [284, 351].

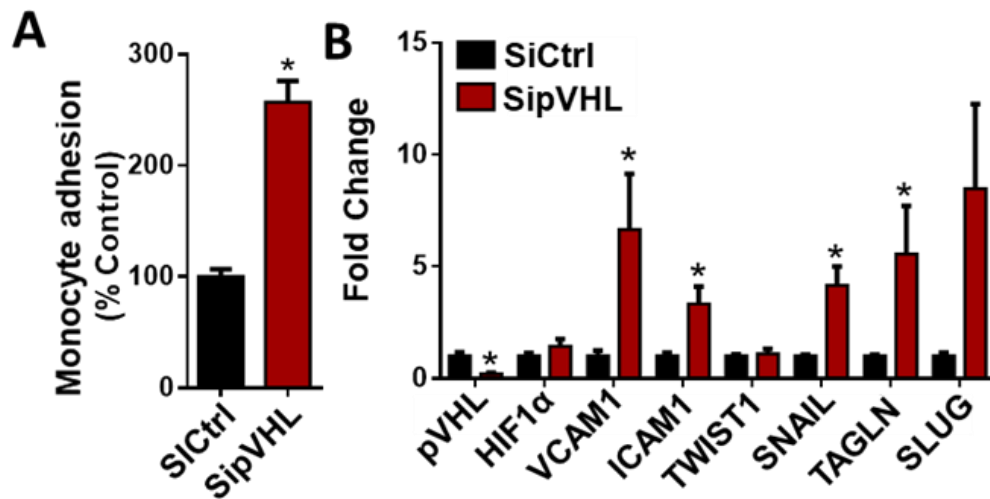


Figure 5.21 Silencing of pVHL leads to increased endothelial inflammation

A, B) HAVECs were transfected with sipVHL for 48 hours. Treated cells were then used for monocyte adhesion assay (**A**) or qPCR analyses for markers of inflammation and EndMT (**B**) normalized to 18S. n=4. *p<0.05.

In contrast, knockdown of HIF1 α via siHIF1 α inhibited monocyte adhesion (Fig. 5.22A) and markers of inflammation and EndMT, while not affecting pVHL levels (Fig. 5.22B). We then tested whether UBE2C-induced endothelial inflammation and EndMT is mediated by either pVHL or HIF1 α , using siUBE2C, sipVHL or siHIF1 α in combination. Knockdown of both, UBE2C and pVHL, induced endothelial inflammation and EndMT (Fig. 5.22C and D). In contrast, silencing of both, UBE2C and HIF1 α , inhibited inflammation and EndMT (Fig. 5.22C and D). These results suggest that endothelial inflammation and EndMT, induced by UBE2C, is mediated by pVHL and HIF1 α in HAVECs.

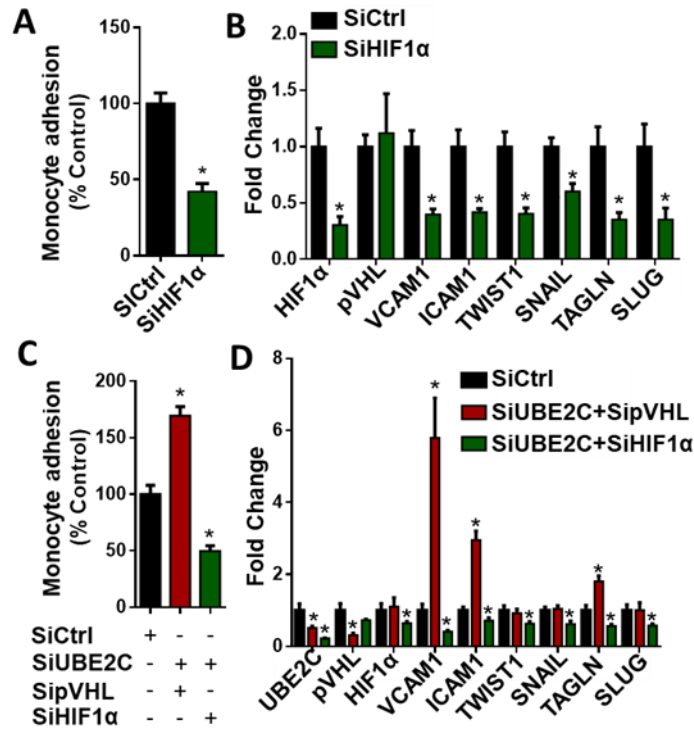


Figure 5.22 pVHL and HIF1 α mediate UBE2C-induced endothelial inflammation and EndMT.

A, B) HAVECs were transfected either individually with siHIF1 α , and SiCtrl (**A, B**) or co-transfected with sipVHL or siUBE2C (**C, D**) for 48 hours. Monocyte adhesion assay (**A, C**) or qPCR analyses for markers of inflammation and EndMT (**B, D**) normalized to 18S were done. n=4. *p<0.05.

5.2.10 *MiR-483 mimic and HIF1 α chemical inhibitor PX478 inhibit calcification in porcine aortic valves*

Next, we tested whether the shear-dependent miR-483, UBE2C, pVHL and HIF1 α pathway plays a significant role in CAVD. To this end, miR-483 mimic and the HIF1 α inhibitor PX478 were selected as treatments. We cultured freshly obtained healthy porcine AV leaflets in osteogenic media [352] for 14 days to induce AV calcification (Fig. 5.23A). Treatment with the miR-483 mimic (20nM every three days) significantly inhibited AV calcification as measured by Alizarin Red staining (Fig. 5.23B and C) and Arsenazo assay

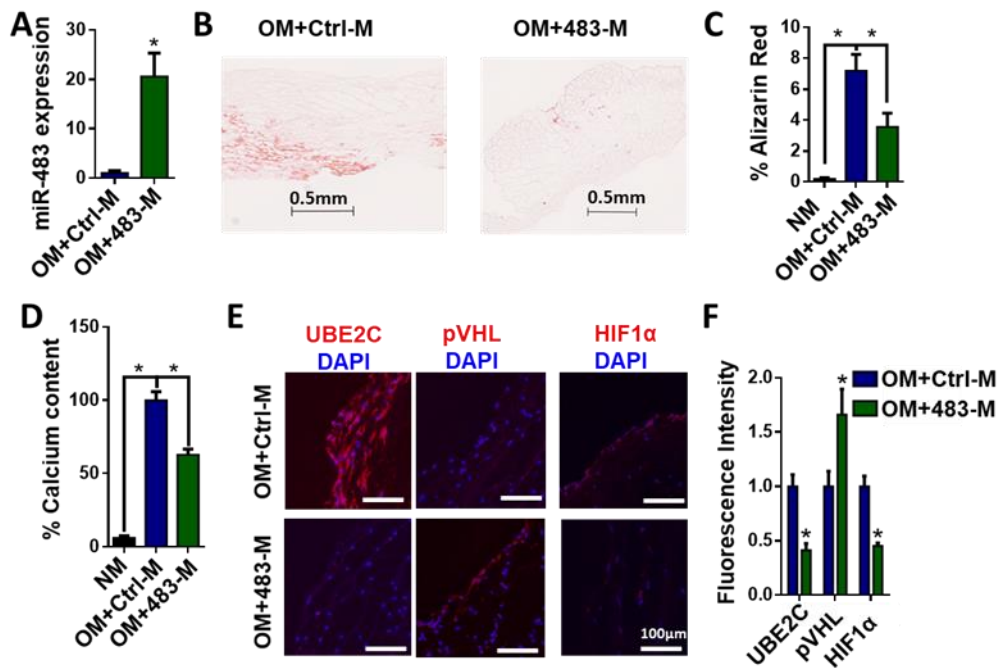


Figure 5.23 The miR-483-mimic reduces AV calcification by silencing of Ube2c

A) Freshly harvested porcine AV leaflets were transfected with miR-483 mimic or Ctrl mimic (20nM) every 3 days for two weeks in osteogenic media (OM). AV leaflets were then divided for total RNA isolation and qPCR assay for miR-483 (A), immunohistochemical assay using Alizarin Red (B, C) and antibodies for UBE2C, pVHL and HIF1 α (E, F) and Arsenazo calcium assay (D). Alizarin images were quantified using Matlab (B, C) while the fluorescence images (E, F) were quantified by ImageJ. n=8, *p<0.05.

(Fig. 5.34D). The anti-calcific effect of miR-483 was mediated by decreasing UBE2C and HIF1 α while upregulating pVHL (Fig. 5.23 E and F).

Additionally, we decided to study the potential therapeutic role of HIF1 α inhibitors currently used in clinical trials for cancer treatment. To this end, we treated porcine AVs with PX478 (20 μ M replenished every three days) which showed a dramatic inhibition of AV calcification (Fig. 5.24 A-C) and significantly decreased HIF1 α expression (Fig. 5.24

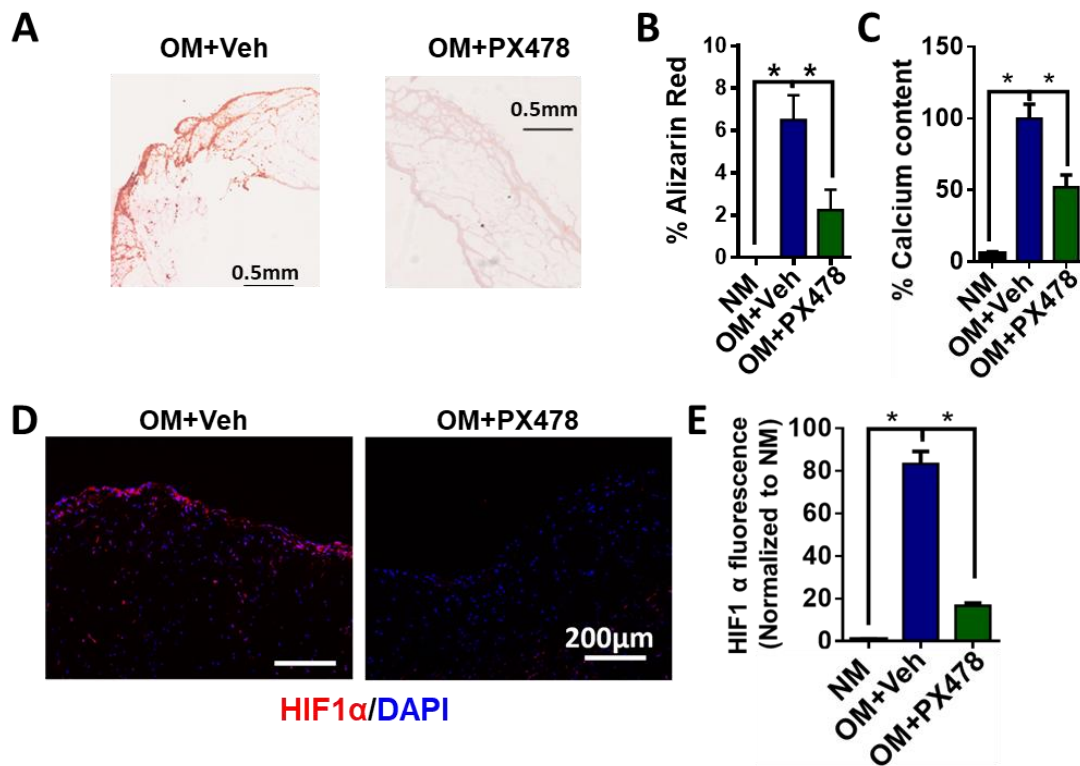


Figure 5.24 HIF1 α inhibitor PX478 reduces AV calcification

A) Freshly harvested porcine AV leaflets were transfected with PX478 (20 μ M) or saline every 3 days for two weeks in osteogenic media (OM). AV leaflets were then divided for immunohistochemical assay using Alizarin Red (A,B) and antibody for HIF1 α (D,E) and Arsenazo calcium assay (C). Alizarin images were quantified using Matlab (A,B) while the fluorescence images (D,E) were quantified by ImageJ. n=8, *p<0.05.

D and E). These results demonstrate the therapeutic potential of targeting miR-483 and the HIF1 α pathway in CAVD.

5.3 Summary and discussion

The main findings of this aim are that miR-483 is a novel shear-sensitive and side-dependent miRNA that regulates endothelial inflammation and EndMT by targeting UBE2C, which in turn regulates pVHL and HIF1 α under normal atmospheric conditions, ultimately leading to AV calcification. We also found that miR-483 mimic as well as the HIF1 α inhibitor PX478 effectively reduced AV calcification of porcine AVs *ex vivo*.

We found that miR-483 expression is increased by LS and in the ventricularis side which is exposed to s-flow, while decreased by OS and in the fibrosa side which is exposed to d-flow. Our results demonstrated that miR-483 potently regulates endothelial function by protecting against inflammation, proliferation, and EndMT. The role of miR-483 was reported mostly in cancer cells where it regulates proliferation [268, 353] and apoptosis [268, 269, 354]; however, the role of miR-483 is still unclear in the cardiovascular system. Recent data showed that miR-483 mediates EndMT by targeting CTGF in human umbilical vein ECs [273]. Angiotensin II was shown to inhibit expression of miR-483 targeting the renin-angiotensin system genes in smooth muscles and heart [271]. These genes including CTGF, however, were not shear sensitive in our gene array study using HAVECs and porcine AVs [14, 220]; therefore, we did not study them. miR-483 is located in the intronic region of insulin-like growth factor 2 (IGF2), and that it was shown to be mediated by KLF4 [273]. Similarly, we found that expression of miR-483 and IGF2 are mediated in a KLF2-dependent manner in HAVECs.

We have identified UBE2C and ASH2L as two shear-sensitive targets of miR-483 through our *in silico* and validation studies. ASH2L is a member of the COMPASS complex responsible for histone 3 lysine 4 tri-methylation, an important epigenetic

modification that induces expression of numerous genes [347]. Although it is likely that ASH2L plays a critical role in epigenetic modification of endothelial function and CAVD, we decided to save this study for the future because investigating this highly complex pathway simultaneously with UBE2C studies would make the scope of this aim too diffuse. In addition, our studies showed that UBE2C alone plays a dominant role in regulation of inflammation and EndMT, further supporting our rationale to focus on UBE2C in this study.

UBE2C is a member of the APC/C and is known to catalyze the initial mono-ubiquitination of protein substrates such as cyclins [355-357]. Once cyclins are mono-ubiquitinated, another E2 ligase, Ube2s, then elongates the ubiquitin chain (poly-ubiquitination) leading to their proteasomal degradation [358, 359]. Interestingly, pVHL is another well-known substrate of both APC/C [279] and Ube2s [360, 361], but it was unknown whether UBE2C regulates pVHL ubiquitination. Additionally, OS was shown to stabilize HIF1 α expression under normal atmospheric conditions in vascular endothelial cells by activating NF- κ B and inducing expression of the deubiquitinating enzyme Cezanne [343]; however, it was unknown whether pVHL, a well-known HIF1 α regulator [284, 285, 341, 342], is regulated by shear stress and regulates HIF1 α expression under flow conditions. We found that pVHL is highly shear-sensitive, losing its expression in OS in HAVECs and in the fibrosa side exposed to d-flow in a UBE2C-dependent manner. Conversely, OS increased HIF1 α expression in a UBE2C-dependent manner in HAVECs and in the fibrosa side. These findings suggest that UBE2C regulates pVHL and HIF1 α expression in HAVECs. Although there is an increase in HIF1 α expression under OS condition, it is interesting to note that siRNA-mediated knockdown of UBE2C is able to

significantly reduce the HIF1 α expression by post-translational pVHL-mediated degradation preventing the downstream HIF1 α signaling cascade.

Mechanistically, we found that UBE2C targets pVHL by binding and mediating its degradation in a ubiquitination-dependent manner. Furthermore, our data using the pVHL ubiquitination site mutants indicates that binding of UBE2C to pVHL is independent of the ubiquitination sites on pVHL; however, the UBE2C-dependent degradation of pVHL requires at least one of its ubiquitination sites. The degradation of pVHL further led to increased stabilization of HIF1 α , which in turn induced endothelial inflammation, EndMT and AV calcification (Fig. 5.25).

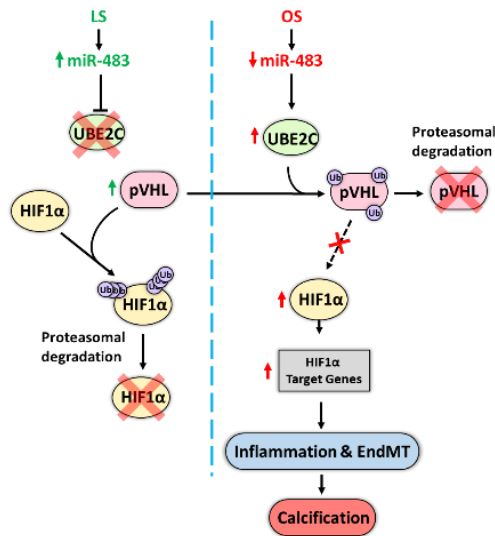


Figure 5.25 Working hypothesis

To our knowledge, this is the first time that UBE2C and pVHL are shown to be shear-sensitive and play a role in endothelial inflammation and EndMT. We also found that HIF1 α is also shear-sensitive and is a potent pro-inflammatory and pro-EndMT protein in HAVECs. Using the combination of UBE2C, pVHL and HIF1 α siRNAs, we found that pVHL and HIF1 α mediate the UBE2C-dependent inflammation and EndMT.

Currently, the only treatment option for CAVD patients is AV replacement or repair and there are no effective medical therapies. Therefore, there is an urgent need for

developing CAVD therapies [210]. Our study demonstrates that miR-483 and HIF1 α - pathway are potential therapeutic targets for CAVD. Treatment with the miR-483 mimic or the HIF1 α inhibitor PX478 significantly reduced AV calcification of porcine AVs demonstrating their potential as novel anti-CAVD therapeutics. Notably, numerous clinical trials are underway using various HIF1 α inhibitors for cancer treatments [2, 362, 363]. Our study with PX478 demonstrates the potential of repurposing some of these FDA-approved HIF1 α drugs to prevent and treat CAVD. Given our findings, it may be interesting to monitor those patients treated with HIF1 α inhibitors for CAVD and atherosclerosis.

While our current *in vitro* studies focus mostly on studying the effect of shear stress on AV endothelial cells, it is important to note that the expression of UBE2C, pVHL, HIF1 α and markers of inflammation, EndMT and AV calcification is regulated in a side-dependent manner *in vivo* as we observed in the human AV tissues. These findings suggest that the miR-483-dependent UBE2C/pVHL/HIF1 α pathway established based on the *in vitro* studies is relevant under *in vivo* conditions as well, where AVs are exposed to multiple mechanical forces such as pressure and stretch in addition to shear stress.

In conclusion, we identified a shear-sensitive and side-dependent miRNA, miR-483, which targets UBE2C in AV endothelial cells. In turn, the aberrant expression of UBE2C leads to degradation of pVHL, which increases HIF1 α level resulting in endothelial inflammation, EndMT and AV calcification. The miR-483 mimic and HIF1 α inhibitor are novel potential CAVD therapeutics.

6 Development of an accelerated animal model of CAVD using GATA5 mice

6.1 Introduction

Several mouse models of CAVD have been developed [13, 192, 200, 309-311]. The majority of these models involve various genetically engineered strains (ApoE^{-/-}, LDLR^{-/-}, Klotho^{-/-}, Notch1^{+/-}, eNOS^{-/-}) with or without additional supplements, surgery, or physical injury to mimic various pro-CAVD conditions [192]. While most of them develop some features of CAVD, AV sclerosis, and stenosis; bona-fide calcification as measured by Alizarin red or micro-CT within the leaflets has rarely been observed [200, 312]. This rarity of mouse models that can easily and reproducibly develop AV leaflet calcification similar to humans within a reasonable time-frame (less than ~4 months), is a well-known roadblock that should be addressed in order to make mechanistic studies of CAVD more feasible. We now have developed a congenital BAV mouse model that develops a robust AV leaflet thickening and calcification within 4 months on a high fat-diet.

BAV is the most common congenital heart valve disease and is well-known to accelerate progression of CAVD, it is thought to have a genetic etiology due to the increased prevalence once one member of a family presents BAV phenotype. To better understand the potential genetic implications for CAVD, several genetic studies have been conducted comparing tricuspid AV patients with BAV patients [364-366]. From these studies, GATA5 was found to be associated with BAV. GATA5 is a member of the GATA family of transcription factors that regulate cell expansion and differentiation. Its absence in mice lead to increased blood pressure, endothelial dysfunction, age-dependent organ damage, hypertension, and BAV. Mechanistically, its loss disrupts proper endothelial signaling and homeostasis [367]. GATA5^{-/-} mice (provided by Dr. Mona Nemer [211]) have been found to develop BAVs in 15 % cohort vs littermate-control tricuspid AV mice

as well as present increased AV velocity and thickened AV leaflets. Therefore, we will use this model combined with a gain-of-function AAV-PCSK9 (which degrades hepatic LDL receptors) to induce hypercholesterolemia [307]. Our preliminary studies have shown that these BAV mice developed robust AV sclerosis (histomorphometry), stenosis (transaortic velocity by echocardiography) and calcification (Osteosense 680). Additionally, we showed a drug delivery method to treat AV leaflets with oligonucleotide as proof-of-concept for future therapeutic studies.

6.2 Results

6.2.1 Injection of PCSK9 induces hypercholesterolemia in GATA5 knockout mice

In order to determine whether GATA5^{-/-} knockout mice have a bicuspid or tricuspid AV, we conducted ultrasound echocardiography at 8 weeks of age and assessed aortic valve velocity using pulse-wave doppler imaging modality (Fig. 6.1). The aortic valve velocity for a healthy mouse is in the range between 700-1400mm/s [310]. Therefore,

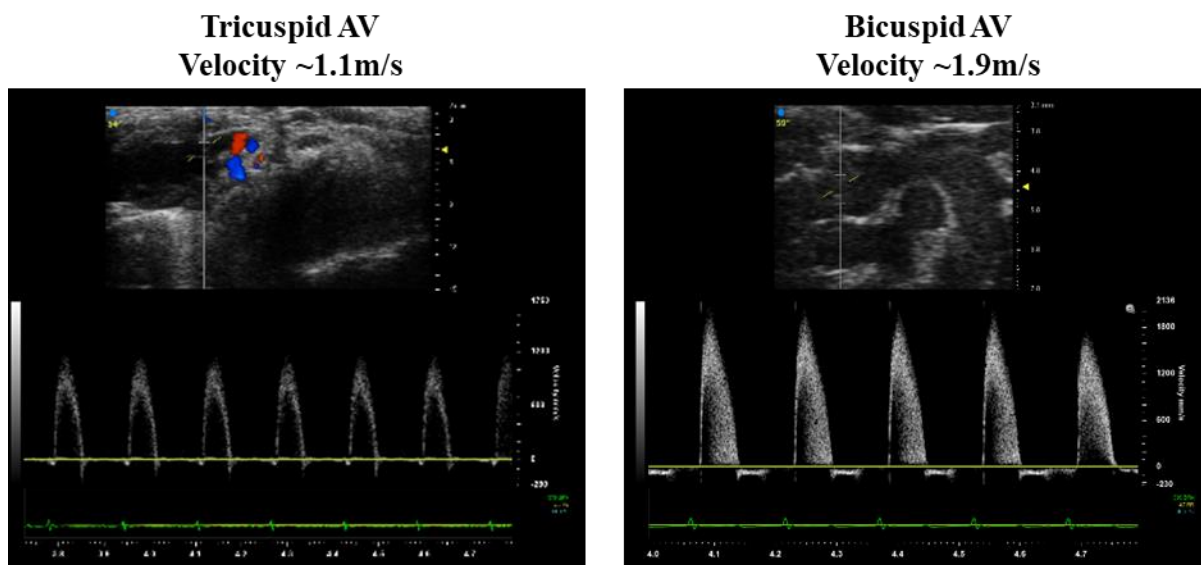


Figure 6.1 GATA5^{-/-} mice with bicuspid AV present higher AV velocity by ultrasound

At 2 months of age, the AV velocity of GATA5 KO mice was assessed by ultrasound in order to determine AV phenotype.

we considered our mice to have bicuspid AV phenotype whenever the AV velocity exceeded 1400mm/s.

After AV velocity was assessed and mice were separated according to AV phenotype, we injected the mice with an AAV-PCSK9 mutant (gain-of-function) to induce hypercholesterolemia supplemented with high-fat diet [307]. After PCSK9-injection mice were kept on high-fat diet for four months and ultrasound echocardiography was conducted monthly to monitor changes in AV velocity (Fig. 6.2A B). As control we had un-injected mice fed with high-fat diet. At the end of the study, the mice were sacrificed; and plasma samples were collected and sent for cholesterol quantification (Fig. 6.2C). Our studies

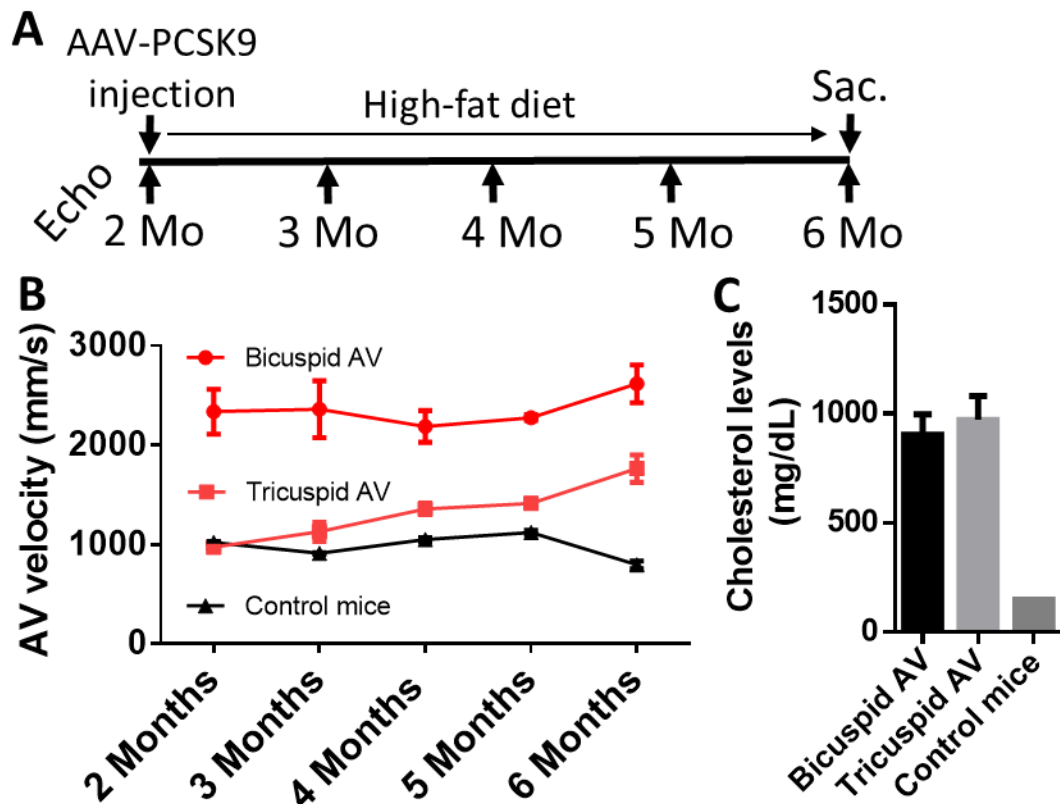


Figure 6.2 $GATA5^{-/-}$ mice develop BAV and AV sclerosis.

$GATA5^{-/-}$ mice with BAV vs tricuspid AV vs wild-type controls were used to measure trans-AV velocity (n=3) (B). All $GATA5^{-/-}$ mice were injected with AAV-PCSK9 and fed high fat diet for 4 months (A), hypercholesterolemia was induced (C).

showed all PCSK9-injected mice presented increased cholesterol levels as well as increase in AV velocity by the end of the study.

6.2.2 *GATA5*^{-/-} bicuspid AV mice develop sclerosis and calcification

Aortic valves from *GATA5*^{-/-} mice were harvested at the end of the study and embedded in paraffin for sectioning. H&E staining was conducted on the sectioned AVs (Fig. 6.3) and they were imaged using Hamamatsu Nanozoomer. From these stainings we found that the BAV mice had developed significant sclerosis (valve thickening) compared to both the tricuspid AV group or the control group. Interestingly, we observed a small increase in valve thickness between PCSK9-injected tricuspid AV mice and un-injected control mice; which would explain the increase in AV velocity observed between these two groups at 4 months of age (Fig. 6.2B). Furthermore, we found that both bicuspid or tricuspid mice had atherosclerotic plaque in the aortic sinus area compared to the control mice.

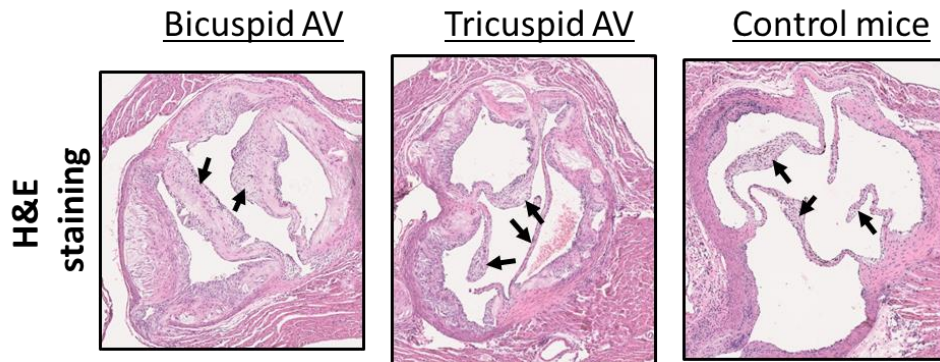


Figure 6.3 . Hypercholesterolemic BAV *GATA5*^{-/-} mice develop AV sclerosis

GATA5^{-/-} were stained with H&E to study sclerosis (arrows). Shown are representative of three mice.

In order to assess presence of calcification, we conducted Osteosense 680 staining on the AV sections from the *GATA5*^{-/-} mice (Fig. 6.4). We found that BAV mice showed

positive staining on the leaflets (arrows) characteristic of microcalcification nodules in the AV leaflets.

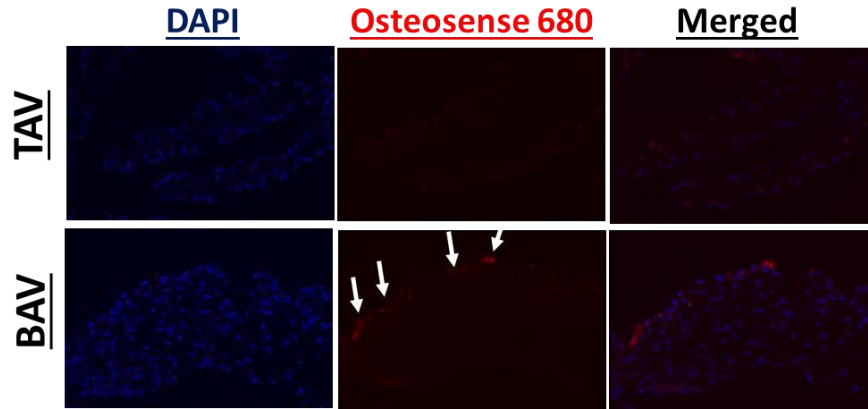


Figure 6.4 Hypercholesterolemic BAV $GATA5^{-/-}$ mice develop AV calcification

$GATA5^{-/-}$ were stained with Osteosense 680 to study calcification (arrows).

6.2.3 *Ube2c* levels are increased in BAVs of $GATA5$ mice

Ube2c has previously been shown to be a critical mediator in AV calcification (Aim 2). Therefore, we tested whether sclerotic and calcified mice AV leaflets presented higher levels of *Ube2c* compared to non-sclerotic AV leaflets. We stained BAVs and TAVs of

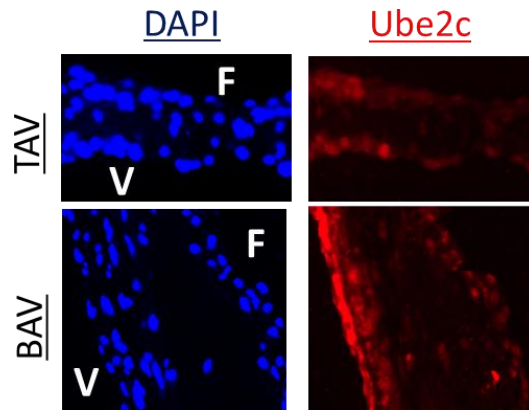


Figure 6.5 BAVs have higher *Ube2c* expression compared to TAV in $GATA5^{-/-}$ mice as shown by

Ube2c staining was conducted on AV leaflets from our $GATA5$ study.

GATA5 mice with an antibody against Ube2c (Fig. 6.5); which showed that BAV leaflets had higher expression of Ube2c compared to non-sclerotic TAV leaflets. This suggests that Ube2c may play a role in the pathogenesis of AV sclerosis and calcification.

6.2.4 SubQ injection of fluorescently labeled siRNA is delivered to the AV.

Having identified miR-483 as a potential therapeutic target for CAVD, we decided to conduct pilot drug-delivery studies with fluorescently labeled siRNA that presents a similar structure to miRNA mimics in mice. This was done to determine if we can deliver oligonucleotides to mice AV leaflets. 10-week-old wild-type mice were injected with 1mg/kg of fluorescently labeled siRNA (Alexa-Fluor 555) or saline control subcutaneously (subQ). Three hours after injection, the hearts were harvested, embedded in OCT, and cryosectioned. We then conducted DAPI staining and imaged in a fluorescent microscope to determine whether our siRNA delivery was successful. We observed that the

fluorescently-labeled siRNA was successfully delivered to the AV (Fig. 6.6) while control mice showed no signal on the AV leaflets.

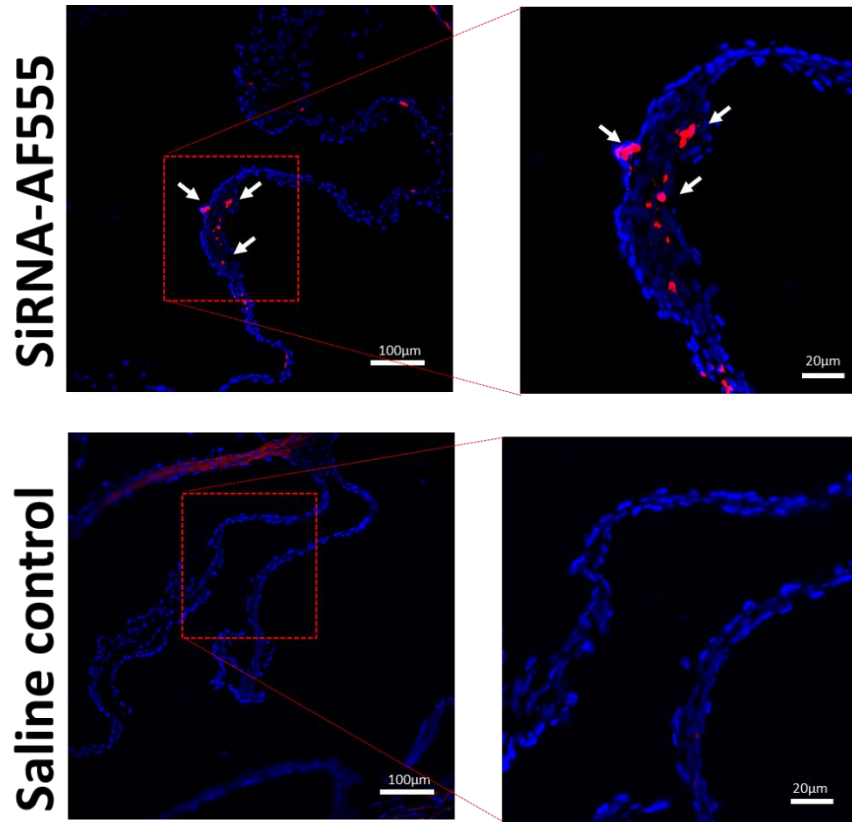


Figure 6.6 SiRNA delivery to the AV by using SubQ injection.

Ten-week-old wild-type mice were injected with siRNA-AF555 (or saline control) at a dose of 1mg/kg for three hours. Hearts were then sectioned and stained with DAPI prior to imaging in a fluorescent microscope.

6.3 Summary and discussion

Our results showed that we have developed an accelerated model of CAVD by combining two CAVD risk factors: bicuspid aortic valve, a well-known CAVD risk factor, and, hypercholesterolemia. Mice as young as eight weeks of age can be treated with AAV-PCSK9 to induce hypercholesterolemia; and after four months of being fed a high-fat diet, a mild increase in aortic valve velocity can be observed. These BAV mice also develop mild sclerosis as well as microcalcifications in the leaflets. We have also demonstrated that

we can target the AV by subQ injection of a fluorescently labeled siRNA giving us a tool to test our miRNA therapeutics *in vivo*.

We are interested in testing the therapeutics developed in Aim 2 of this model in order to determine whether treatment with the miR-483 mimic or the HIF1 α inhibitor PX478 can prevent sclerosis and calcification in HAVECs. Furthermore, this accelerated model could be used not only to determine if our therapeutics can prevent CAVD, but also if they can reverse or stop progression of CAVD. To this end, we could start our *in vivo* studies and two months into the high-fat diet we could start treatment with miR-483 mimic or PX478 and determine if we can reverse sclerosis and calcification on these mice.

Additionally, we will crossbreed the GATA5^{-/-} mice with Ube2c transgenic mice that overexpress Ube2c (kindly provided by Dr. Van Deursen [368]) in order to demonstrate whether overexpression of Ube2c in mice accelerates the pathogenesis of CAVD. We expect that if we treat these mice with PX478, it will prevent CAVD; thus demonstrating that Ube2c exerts its function by upregulation of HIF1 α .

7 DISCUSSION

7.1 Summary

In this dissertation, we have discovered and studied two novel shear-sensitive miRNAs in the aortic valve endothelium: miR-181b and miR-483-3p (miR-483); and studied their functional role in aortic valve endothelial biology and CAVD by examining their respective targets (TIMP3 and UBE2C respectively) and the pathways in which they are involved. These miRNAs were first identified in our HAVEC and porcine AV microRNA array and were validated *in vitro* and *in vivo* in this dissertation. We have also developed a novel accelerated *in vivo* model for CAVD combining two well-known risk factors of CAVD: bicuspid aortic valve (BAV) via GATA5 knockout in mice, and hypercholesterolemia via AAV-PCSK9 injection.

MiR-181b was discovered in our side-specific porcine AV microRNA array, where it was shown to be upregulated in the endothelium of the fibrosa side (prone to AV calcification) compared to the ventricularis side (mostly spared from disease). Furthermore, miR-181b was found to be significantly upregulated in low-magnitude oscillatory shear stress conditions (OS) compared to high-magnitude unidirectional shear stress conditions (LS) in our HAVEC array, and was validated by qPCR in HAVECs. We found that in HAVECs, TIMP3, GATA6, and SIRT1 were shear-sensitive genes regulated in a shear-dependent manner by miR-181b. We focused on TIMP3 due to our previous experience with this target gene in atherosclerosis [263]. We further demonstrated that miR-181b directly binds to TIMP3 via a 3'UTR luciferase assay. TIMP3 is a tissue inhibitor of metalloproteinases that we found to inhibit MMP activity in HAVECs. Additionally, we found that miR-181b increases MMP activity in HAVECs via TIMP3 silencing. Interestingly, we also showed that OS induces MMP activity in a miR-181b

dependent manner, which can be reversed by silencing miR-181b using anti-miR-181b. Thus, miR-181b provides a novel therapeutic target to reduce ECM degradation and AV sclerosis.

We first discovered miR-483 in our HAVEC microRNA array, where it was upregulated in LS conditions compared to OS conditions. We further validated miR-483 *in vitro* in HAVECs and *in vivo* in porcine AVs and found it to be upregulated in LS conditions and in the ventricularis side compared to OS conditions and the fibrosa side respectively. We assessed the functional role of miR-483 in HAVECs via monocyte adhesion and inflammation marker quantification (inflammation), EndMT marker quantification (EndMT), scratch assay (migration), TUNEL assay (apoptosis), and KI67 staining (proliferation). Our studies showed that miR-483 regulated OS-induced endothelial inflammation and EndMT. Treatment with a miR-483 mimic in OS conditions decreased inflammation and EndMT; in contrast, silencing of miR-483 in LS conditions by anti-miR-483 lead to increased inflammation and EndMT in HAVECs. We conducted an *in silico* analysis to determine shear-sensitive targets of miR-483 and identified UBE2C and ASH2L. Although both UBE2C and ASH2L are likely to play major roles in CAVD, they are potentially involved in two very complex and different pathways (UBE2C on ubiquitin-dependent pathways and ASH2L on epigenetic regulation through histone modifications). Studying both simultaneously would interfere with focused studies; therefore, we decided to concentrate on UBE2C for this dissertation and we will conduct an independent study on ASH2L to determine its novel functional role in AV endothelial biology and CAVD. We further validated that miR-483 regulated mRNA and protein levels of UBE2C via miR-483 modulation studies in static and shear conditions in HAVECs.

Functional studies showed that the protective role of miR-483 is controlled by UBE2C. These studies were conducted by co-transfecting HAVECs with anti-miR-483 and siUBE2C and assessing endothelial inflammation. Silencing of UBE2C in HAVECs lead

to decreased inflammation and EndMT while overexpression of UBE2C lead to increased inflammation. UBE2C is an E2 ubiquitin ligase that ubiquitinates proteins, leading to degradation via the proteasome pathway. UBE2C is part of the E3 ligase complex APC/C and acts in conjunction with another E2 ligase, UBE2S. UBE2C is an initiating E2 ligase responsible for monoubiquitinating substrates while UBE2S recognizes monoubiquitinated substrates and extends the ubiquitin chain so that the proteasome recognized the ubiquitin chain and degrades the substrate. APC/C and UBE2S are both known to degrade pVHL, a major regulator of HIF1 α . Here, we showed that UBE2C binds and ubiquitinates pVHL, leading to its degradation. Interestingly, our studies showed that for UBE2C to degrade pVHL, it requires at least one lysine site in pVHL. Mutation of all the lysine residues in pVHL prevents UBE2C-dependent ubiquitination and proteasomal degradation. Silencing of UBE2C reduced HIF1 α protein levels in a pVHL-dependent manner. Additionally, we studied the function of pVHL and HIF1 α in HAVECs and found that pVHL acted as an anti-inflammatory and anti-EndMT gene while HIF1 α was a pro-inflammatory, pro-EndMT gene.

We conducted therapeutic studies to test whether miR-483 or HIF1 α could be used to prevent and treat CAVD. To this end, we cultured static porcine AVs *ex vivo* in osteogenic media (DMEM media supplemented with phosphates, dexamethasone, β -glycerophosphate and TGF- β) and treated with either miR-483 mimic or a HIF1 α inhibitor (PX478) every three days for two weeks. We observed that both treatments significantly decreased calcification, as shown in our Alizarin Red staining and Arsenazo assay. Overexpression of miR-483 lead to decreased levels of UBE2C and HIF1 α while pVHL levels increased. Furthermore, HIF1 α levels were significantly upregulated by osteogenic media and significantly decreased by treatment with PX478. These studies demonstrate that the UBE2C-HIF1 α pathway is important for AV calcification and provides preliminary

evidence of the therapeutic potential of miR-483 mimic and PX478 as a CAVD medical therapy.

Last, we are developing an accelerated animal model for CAVD. We used GATA5 knockout mice, known to develop bicuspid AV (BAV) phenotype, increased AV velocity and thickened AV leaflets. We induced hypercholesterolemia in this mouse strain via an AAV-PCSK9 injection along with high-fat diet. At eight weeks of age (prior to PCSK9-injection), ultrasound imaging was conducted on these mice to determine if their AV was bicuspid or tricuspid morphologically (if feasible) and by measuring AV velocity. After the mice were sorted according to valve phenotype, we injected AAV-PCSK9 and started feeding high-fat diet. Monthly ultrasound imaging to assess AV velocity was conducted and after four months, the mice were sacrificed. AVs were excised, and we conducted immunohistochemical stainings on the valves. We observed that the BAV group had developed mild sclerosis and microcalcification nodules while the tricuspid aortic valve (TAV) groups had not. Additionally, we showed that subcutaneous injection of fluorescently labeled siRNA in mice can be used to deliver oligonucleotide therapies to mice AVs.

7.2 Conclusions

We have discovered two novel, shear-sensitive miRNAs in AVs: miR-181b and miR-483. We showed that miR-181b, which is upregulated in OS conditions, plays a critical role in ECM degradation in AV endothelium by silencing TIMP3; which we found to inhibit MMP activity in HAVECs. On the other hand, miR-483 is upregulated in LS conditions and targets a novel shear-sensitive gene UBE2C. We identified a novel function of UBE2C by targeting and degrading pVHL which in turn leads to the stabilization and activation of HIF1 α . Through therapeutic studies in porcine AVs using miR-483 mimics or HIF1 α inhibitors, such as PX478 which is used currently used in clinical trials for cancer treatments, we demonstrated their potential as medical therapies for CAVD. Last, we are developing an accelerated animal model for CAVD by combining bicuspid AV mice,

induced by GATA5 knockdown, with hypercholesterolemia. These mice developed mild AV sclerosis, AV stenosis, and microcalcification in the AV leaflets.

7.3 Future Directions

From Aim 1, we identified two additional novel shear-sensitive target genes of miR-181b; GATA6 and SIRT1. GATA6 and SIRT1 are known to have a protective role in atherosclerosis disease. SIRT1 induces EC relaxation in an angiotensin-induced model of atherosclerosis, and it has been shown to inhibit foam cells formation in the vasculature [336]. GATA6 inhibits VCAM-1 expression in the endothelium and protects smooth muscle cell differentiation [337]. We intend to validate whether miR-181b directly regulates GATA6 and SIRT1 via additional miR-181b modulation studies as well as 3'UTR validation studies. These studies will help us better understand the functional role of both miR-181b in valvular endothelial biology and CAVD. Additionally, we are interested in studying the role of miR-181b not only in endothelial cells but also in whole AV leaflets as well as in valvular interstitial cells. miR-181b plays a role in ECM degradation, and we would like to examine its potential in preventing increased ECM degradation and sclerosis in porcine AVs treated with osteogenic media as well as in our novel GATA5 knockout CAVD model. We are also considering the use of TIMP3 overexpression in *in vitro*, *ex vivo* and *in vivo* studies to inhibit MMP activity and reduce AV calcification. TIMP3 has been shown to play a critical role in atherosclerosis and we want to demonstrate whether it is also a critical player in the pathogenesis of CAVD.

For Aim 2, we have conducted static *ex vivo* therapeutic studies which have shown the potential of both the miR-483 mimic and HIF1 α inhibitor PX478 in significantly reducing AV calcification. These studies were done in static cultures of porcine AVs and we are interested in validating these results in shear conditions. To this end, we will conduct shear stress experiments using the cone-and-plate bioreactors developed by our collaborators, Dr. Yoganathan and Dr. Nerem, to study whether miR-483 mimic and PX478 can prevent OS-induced porcine AV calcification. These studies will provide

further evidence of the therapeutic potential of miR-483 and the HIF1 α pathway in treating CAVD. Additionally, to better understand the role of these two treatments in the pathogenesis of AV calcification, we would like to study the effect of these therapies in interstitial cells as well as in our accelerated model of CAVD to determine if treatment with miR-483 mimic or PX478 can be used to decrease AV calcification in a more clinically relevant model of CAVD.

Moreover, we identified pVHL as a shear-sensitive target regulated by UBE2C via the ubiquitin-proteasome pathway. UBE2C is an E2 ubiquitin ligase, and its role is to ubiquitinate other proteins to induce its degradation via the proteasome. Because there may be other proteins that are regulated in a shear-dependent manner by UBE2C we are planning on exposing HAVECs to LS or OS conditions followed by immunoprecipitation using UBE2C antibodies. The immunoprecipitated proteins will be sent for identification via mass spectrometry. *In silico* studies will be conducted comparing proteins identified via mass spectrometry with our HAVEC array data to identify potential shear-sensitive targets regulated by UBE2C. Validation of the identified targets will be conducted to better understand the role of UBE2C-dependent ubiquitination in HAVECs.

From our *in silico* studies and *in vitro* validation, we discovered another target of miR-483, ASH2L. ASH2L is a member of the COMPASS complex responsible for trimethylating histone 3 lysine (H3K4me3), an epigenetic modification which opens the chromatin structure allowing for gene transcription. In order to discover the main target genes regulated in OS conditions by ASH2L, we will first expose HAVECs to LS or OS conditions followed by chromatin immunoprecipitation (CHIP) studies using ASH2L antibodies. The pulled down protein-DNA complex will be sequenced and matched to their genomic location via *in silico* analysis. We will further validate the results from our sequencing data by conducting CHIP on sheared HAVECs, followed by qPCR amplification of the promoter region of the genes identified in our CHIP studies. These

studies will be one of the first to study the role of flow-sensitive epigenetic gene regulation in the valvular endothelium.

We are currently working in translating the findings from our studies to other cardiovascular diseases such as atherosclerosis. To this end, we will try using HIF1 α inhibitors to treat atherosclerosis. We want to test these therapeutics in two models of atherosclerosis commonly used in the Jo lab; partial carotid ligation model as an acute model, and long-term high-fat diet chronic study. By repurposing HIF1 α inhibitors currently in clinical trials for cancer diseases, we expect to accelerate the translation of these therapies to the clinic for use in cardiovascular diseases.

Furthermore, we want to test our therapeutics findings in our hypercholesterolemic GATA5 knockout animal model. We are currently working in testing the role of the HIF1 α inhibitor, PX478, in this model. We will start PX478 injections in these mice two months after hypercholesterolemia induction in order to mimic a more realistic clinical situation where the patient will start the treatment not before CAVD has developed but when the first signs of the disease can be observed. We will inject biweekly PX478 (or saline control) for two more months and then harvest the AV and determine whether PX478 has any effect in AV sclerosis and calcification. We are interested in expanding these therapeutic studies to study the role of miR-181b and miR-483 in CAVD by injecting either anti-miR-181b or miR-483 mimic via subcutaneous injection in a similar experimental design as the PX478 study. Completion of these studies will be invaluable in accelerating the transition from our discoveries to clinical trials.

Lastly, even though our subcutaneous injection showed promising results in delivering fluorescently labeled siRNAs to the AV, this delivery technique might present side-effects due to the non-specific delivery. To address this problem, development of targeted delivery to the AV need to be conducted. The fibrosa side is known to have increased expression of pro-inflammatory proteins, such as VCAM-1 or ICAM-1, which might be used for targeted delivery. Nanoparticles might be functionalized to target these

proteins to improve specificity and decrease side-effects. Additional AV markers might be needed in order to further increase specificity and will be a challenge for us and other researchers in the road to developing medical therapies for CAVD.

REFERENCES

1. Li R, Mittelstein D, Lee J, Fang K, Majumdar R, Tintut Y, Demer LL, Hsiai TK: **A dynamic model of calcific nodule destabilization in response to monocyte- and oxidized lipid-induced matrix metalloproteinases.** *Am J Physiol Cell Physiol* 2012;**302**:C658-665.
2. Yu T, Tang B, Sun X: **Development of inhibitors targeting hypoxia-inducible factor 1 and 2 for cancer therapy.** *Yonsei Medical Journal* 2017;**58**:489-496.
3. Wilson GK, Tennant DA, McKeating JA: **Hypoxia inducible factors in liver disease and hepatocellular carcinoma: Current understanding and future directions.** *Journal of Hepatology* 2014;**61**:1397-1406.
4. Lu R, Barca O: **Fine-tuning oligodendrocyte development by micrornas.** *Frontiers in Neuroscience* 2012;**6**.
5. Fernandez Esmerats J, Heath JM, Jo H: **Shear-sensitive genes in aortic valve endothelium.** *Antioxid Redox Signal* 2015.
6. Otto CM, Lind BK, Kitzman DW, Gersh BJ, Siscovick DS, Cardiovascular Hlth S: **Association of aortic-valve sclerosis with cardiovascular mortality and morbidity in the elderly.** *New England Journal of Medicine* 1999;**341**:142-147.
7. Hsu SY, Hsieh IC, Chang SH, Wen MS, Hung KC: **Aortic valve sclerosis is an echocardiographic indicator of significant coronary disease in patients undergoing diagnostic coronary angiography.** *International Journal of Clinical Practice* 2005;**59**:72-77.
8. Mohler ER, Sheridan MJ, Nichols R, Harvey WP, Waller BF: **Development and progression of aortic-valve stenosis - atherosclerosis risk-factors - a causal relationship - a clinical morphological-study.** *Clinical Cardiology* 1991;**14**:995-999.
9. Muneretto C, Alfieri O, Cesana BM, Bisleri G, De Bonis M, Di Bartolomeo R, Savini C, Folesani G, Di Bacco L, Rambaldini M, Maureira JP, Laborde F, Tespili M, Repossini A, Folliguet T: **A comparison of conventional surgery, transcatheter aortic valve replacement, and sutureless valves in "real-world" patients with aortic stenosis and intermediate- to high-risk profile.** *J Thorac Cardiovasc Surg* 2015;**150**:1570-1577; discussion 1577-1579.
10. Dasi LP, Hatoum H, Kheradvar A, Zareian R, Alavi SH, Sun W, Martin C, Pham T, Wang Q, Midha PA, Raghav V, Yoganathan AP: **On the mechanics of transcatheter aortic valve replacement.** *Ann Biomed Eng* 2017;**45**:310-331.
11. Mohler ER, Gannon F, Reynolds C, Zimmerman R, Keane MG, Kaplan FS: **Bone formation and inflammation in cardiac valves.** *Circulation* 2001;**103**:1522-1528.
12. Otto CM, Kuusisto J, Reichenbach DD, Gown AM, O'Brien KD: **Characterization of the early lesion of degenerative valvular aortic-stenosis - histological and immunohistochemical studies.** *Circulation* 1994;**90**:844-853.
13. Rajamannan NM, Evans FJ, Aikawa E, Grande-Allen KJ, Demer LL, Heistad DD, Simmons CA, Masters KS, Mathieu P, O'Brien KD, Schoen FJ, Towler DA, Yoganathan AP, Otto CM: **Calcific aortic valve disease: Not simply a**

- degenerative process: A review and agenda for research from the national heart and lung and blood institute aortic stenosis working group executive summary: Calcific aortic valve disease – 2011 update.** *Circulation* 2011;**124**:1783-1791.
14. Holliday CJ, Ankeny RF, Jo H, Nerem RM: **Discovery of shear- and side-specific mrnas and mirnas in human aortic valvular endothelial cells.** *Am J Physiol Heart Circ Physiol* 2011;**301**:H856-867.
 15. Rathan S, Ankeny CJ, Arjunon S, Ferdous Z, Kumar S, Fernandez Esmerats J, Heath JM, Nerem RM, Yoganathan AP, Jo H: **Identification of side- and shear-dependent micrnas regulating porcine aortic valve pathogenesis.** *Scientific Reports* 2016;**6**:25397.
 16. Sacks MS, Schoen FJ, Mayer JE: **Bioengineering challenges for heart valve tissue engineering.** *Annual review of biomedical engineering* 2009;**11**:289-313.
 17. Vesely I, Lozon A: **Natural preload of aortic valve leaflet components during glutaraldehyde fixation: Effects on tissue mechanics.** *Journal of biomechanics* 1993;**26**:121-131.
 18. Wiltz D, Arevalos CA, Balaoing LR, Blancas AA, Sapp MC, Zhang X, Grande-Allen KJ: **Extracellular matrix organization, structure, and function;** 2013.
 19. Schoen FJ: **Aortic valve structure-function correlations: Role of elastic fibers no longer a stretch of the imagination.** *The Journal of heart valve disease* 1997;**6**:1-6.
 20. Leopold JA: **Cellular mechanisms of aortic valve calcification.** *Circulation Cardiovascular interventions* 2012;**5**:605-614.
 21. Chen JH, Simmons CA: **Cell-matrix interactions in the pathobiology of calcific aortic valve disease: Critical roles for matricellular, matricrine, and matrix mechanics cues.** *Circ Res* 2011;**108**:1510-1524.
 22. Bashey RI, Torii S, Angrist A: **Age-related collagen and elastin content of human heart valves.** *Journal of gerontology* 1967;**22**:203-208.
 23. Kastelic J, Baer E: **Deformation in tendon collagen.** *Symposia of the Society for Experimental Biology* 1980;**34**:397-435.
 24. Scott M, Vesely I: **Aortic valve cusp microstructure: The role of elastin.** *Ann Thorac Surg* 1995;**60**:S391-394.
 25. Tseng H, Grande-Allen KJ: **Elastic fibers in the aortic valve spongiosa: A fresh perspective on its structure and role in overall tissue function.** *Acta Biomater* 2011;**7**:2101-2108.
 26. Petrovic D, Obrenovic R, Stojimirovic B: **Risk factors for aortic valve calcification in patients on regular hemodialysis.** *Int J Artif Organs* 2009;**32**:173-179.
 27. Baumgartner H: **Hemodynamic assessment of aortic stenosis: Are there still lessons to learn?** *J Am Coll Cardiol* 2006;**47**:138-140.
 28. Ward C: **Clinical significance of the bicuspid aortic valve.** *Heart* 2000;**83**:81-85.
 29. Barker AJ, Markl M, Burk J, Lorenz R, Bock J, Bauer S, Schulz-Menger J, von Knobelsdorff-Brenkenhoff F: **Bicuspid aortic valve is associated with altered wall shear stress in the ascending aorta.** *Circ Cardiovasc Imaging* 2012;**5**:457-466.

30. Lewin MB, Otto CM: **The bicuspid aortic valve: Adverse outcomes from infancy to old age.** *Circulation* 2005;**111**:832-834.
31. Mohler ER, 3rd: **Mechanisms of aortic valve calcification.** *The American journal of cardiology* 2004;**94**:1396-1402, A1396.
32. Rajamannan NM, Gersh B, Bonow RO: **Calcific aortic stenosis: From bench to the bedside--emerging clinical and cellular concepts.** *Heart* 2003;**89**:801-805.
33. Yacoub MH, Takkenberg JJ: **Will heart valve tissue engineering change the world?** *Nat Clin Pract Cardiovasc Med* 2005;**2**:60-61.
34. Bäck M, Gasser TC, Michel J-B, Caligiuri G: **Biomechanical factors in the biology of aortic wall and aortic valve diseases,** vol. 99; 2013.
35. Then KL, Rankin JA: **Hypertension: A review for clinicians.** *Nursing Clinics of North America* 2004;**39**:793-814.
36. Takx RAP, Zanen P, Leiner T, van der Graaf Y, de Jong PA: **The interdependence between cardiovascular calcifications in different arterial beds and vascular risk factors in patients at high cardiovascular risk.** *Atherosclerosis* 2015;**238**:140-146.
37. Iwata S, Russo C, Jin Z, Schwartz JE, Homma S, Elkind MSV, Rundek T, Sacco RL, Di Tullio MR: **Higher ambulatory blood pressure is associated with aortic valve calcification in the elderly: A population-based study.** *Hypertension* 2013;**61**:55-60.
38. Bermejo J: **The effects of hypertension on aortic valve stenosis.** *Heart* 2005;**91**:280-282.
39. Kaden JJ, Haghgi D: **Hypertension in aortic valve stenosis--a trojan horse.** *Eur Heart J* 2008;**29**:1934-1935.
40. Ivanovic B, Tadic M, Dincic D: **The effects of arterial hypertension on aortic valve stenosis.** *Vojnosanitetski pregled Military-medical and pharmaceutical review* 2010;**67**:588-592.
41. Chester AH, El-Hamamsy I, Butcher JT, Latif N, Bertazzo S, Yacoub MH: **The living aortic valve: From molecules to function.** *Global Cardiology Science & Practice* 2014;**2014**:52-77.
42. Corden J, David T, Fisher J: **Determination of the curvatures and bending strains in open trileaflet heart valves.** *Proceedings of the Institution of Mechanical Engineers Part H, Journal of engineering in medicine* 1995;**209**:121-128.
43. Siu SC, Silversides CK: **Bicuspid aortic valve disease.** *J Am Coll Cardiol* 2010;**55**:2789-2800.
44. Beppu S, Suzuki S, Matsuda H, Ohmori F, Nagata S, Miyatake K: **Rapidity of progression of aortic stenosis in patients with congenital bicuspid aortic valves.** *The American journal of cardiology* 1993;**71**:322-327.
45. Stewart BF, Siscovick D, Lind BK, Gardin JM, Gottdiener JS, Smith VE, Kitzman DW, Otto CM: **Clinical factors associated with calcific aortic valve disease. Cardiovascular health study.** *J Am Coll Cardiol* 1997;**29**:630-634.
46. Boon A, Cheriex E, Lodder J, Kessels F: **Cardiac valve calcification: Characteristics of patients with calcification of the mitral annulus or aortic valve.** *Heart* 1997;**78**:472-474.

47. Katayama S, Umetani N, Hisada T, Sugiura S: **Bicuspid aortic valves undergo excessive strain during opening: A simulation study.** *The Journal of Thoracic and Cardiovascular Surgery* 2013;**145**:1570-1576.
48. Conti CA, Della Corte A, Votta E, Del Viscovo L, Bancone C, De Santo LS, Redaelli A: **Biomechanical implications of the congenital bicuspid aortic valve: A finite element study of aortic root function from in vivo data.** *The Journal of Thoracic and Cardiovascular Surgery* 2010;**140**:890-896.e892.
49. Martin C, Sun W: **Biomechanical characterization of aortic valve tissue in humans and common animal models.** *Journal of biomedical materials research Part A* 2012;**100**:10.1002/jbm.a.34099.
50. Abrams J: **The aortic valve by mano thubrikar crc press, inc., boca raton (1990) 221 pages, illustrated, \$97.50 isbn: 0-8493-4771-8.** *Clinical Cardiology* 1991;**14**:364a-365.
51. Singh R, Strom JA, Ondrovic L, Joseph B, VanAuker MD: **Age-related changes in the aortic valve affect leaflet stress distributions: Implications for aortic valve degeneration.** *The Journal of heart valve disease* 2008;**17**:290-298; discussion 299.
52. Freeman RV, Otto CM: **Spectrum of calcific aortic valve disease: Pathogenesis, disease progression, and treatment strategies.** *Circulation* 2005;**111**:3316-3326.
53. Richards J, El-Hamamsy I, Chen S, Sarang Z, Sarathchandra P, Yacoub MH, Chester AH, Butcher JT: **Side-specific endothelial-dependent regulation of aortic valve calcification: Interplay of hemodynamics and nitric oxide signaling.** *The American journal of pathology* 2013;**182**:1922-1931.
54. Ankeny RF, Thourani VH, Weiss D, Vega JD, Taylor WR, Nerem RM, Jo H: **Preferential activation of smad1/5/8 on the fibrosa endothelium in calcified human aortic valves - association with low bmp antagonists and smad6.** *PLoS ONE* 2011;**6**:e20969.
55. Keele KD: **Leonardo da vinci on movement of the heart and blood,,81.** 1952.
56. Bellhouse BJ, Bellhouse FH: **Mechanism of closure of the aortic valve.** *Nature* 1968;**217**:86.
57. Aboelkassem Y, Savic D, Campbell SG: **Mathematical modeling of aortic valve dynamics during systole.** *Journal of Theoretical Biology* 2015;**365**:280-288.
58. Weston MW, LaBorde DV, Yoganathan AP: **Estimation of the shear stress on the surface of an aortic valve leaflet.** *Ann Biomed Eng* 1999;**27**:572-579.
59. Agmon Y, Khandheria BK, Meissner I, Sicks JD, O'Fallon WM, Wiebers DO, Whisnant JP, Seward JB, Tajik AJ: **Aortic valve sclerosis and aortic atherosclerosis: Different manifestations of the same disease? Insights from a population-based study.** *Journal of the American College of Cardiology* 2001;**38**:827-834.
60. Ku DN, Giddens DP, Zarins CK, Glagov S: **Pulsatile flow and atherosclerosis in the human carotid bifurcation. Positive correlation between plaque location and low oscillating shear stress.** *Arteriosclerosis* 1985;**5**:293-302.
61. Cunningham KS, Gotlieb AI: **The role of shear stress in the pathogenesis of atherosclerosis.** *Lab Invest* 2005;**85**:9-23.

62. Malek AM, Izumo S: **Mechanism of endothelial cell shape change and cytoskeletal remodeling in response to fluid shear stress.** *J Cell Sci* 1996;**109** (Pt 4):713-726.
63. Saikrishnan N, Mirabella L, Yoganathan AP: **Bicuspid aortic valves are associated with increased wall and turbulence shear stress levels compared to trileaflet aortic valves.** *Biomechanics and modeling in mechanobiology* 2014.
64. Chandra S, Rajamannan NM, Sucosky P: **Computational assessment of bicuspid aortic valve wall-shear stress: Implications for calcific aortic valve disease.** *Biomechanics and modeling in mechanobiology* 2012;**11**:1085-1096.
65. Sucosky P, Balachandran K, Elhammali A, Jo H, Yoganathan A: **Altered shear stress stimulates upregulation of endothelial vcam-1 and icam-1 in a bmp-4- and tgfbeta1-dependent pathway.** *Arterioscler Thromb Vasc Biol* 2009;**29**:254 - 260.
66. Tarbell JM, Shi ZD, Dunn J, Jo H: **Fluid mechanics, arterial disease, and gene expression.** *Annual review of fluid mechanics* 2014;**46**:591-614.
67. Yang B, Rizzo V: **Shear stress activates enos at the endothelial apical surface through 1 containing integrins and caveolae.** *Cellular and molecular bioengineering* 2013;**6**:346-354.
68. Zhao F, Li L, Guan L, Yang H, Wu C, Liu Y: **Roles for gp iib/iiia and alphavbeta3 integrins in mda-mb-231 cell invasion and shear flow-induced cancer cell mechanotransduction.** *Cancer Lett* 2014;**344**:62-73.
69. Takada Y, Ye X, Simon S: **The integrins.** *Genome biology* 2007;**8**:215.
70. Ziegler WH, Gingras AR, Critchley DR, Emsley J: **Integrin connections to the cytoskeleton through talin and vinculin.** *Biochemical Society transactions* 2008;**36**:235-239.
71. Parsons JT, Martin KH, Slack JK, Taylor JM, Weed SA: **Focal adhesion kinase: A regulator of focal adhesion dynamics and cell movement.** *Oncogene* 2000;**19**:5606-5613.
72. Ciobanasu C, Faivre B, Le Clainche C: **Integrating actin dynamics, mechanotransduction and integrin activation: The multiple functions of actin binding proteins in focal adhesions.** *European journal of cell biology* 2013;**92**:339-348.
73. Zebda N, Dubrovskiy O, Birukov KG: **Focal adhesion kinase regulation of mechanotransduction and its impact on endothelial cell functions.** *Microvascular research* 2012;**83**:71-81.
74. Lehoux S, Esposito B, Merval R, Tedgui A: **Differential regulation of vascular focal adhesion kinase by steady stretch and pulsatility.** *Circulation* 2005;**111**:643-649.
75. Li S, Butler P, Wang Y, Hu Y, Han DC, Usami S, Guan JL, Chien S: **The role of the dynamics of focal adhesion kinase in the mechanotaxis of endothelial cells.** *Proc Natl Acad Sci U S A* 2002;**99**:3546-3551.
76. Hirakawa M, Oike M, Karashima Y, Ito Y: **Sequential activation of rhoa and fak/paxillin leads to atp release and actin reorganization in human endothelium.** *J Physiol* 2004;**558**:479-488.

77. Hsu HJ, Lee CF, Locke A, Vanderzyl SQ, Kaunas R: **Stretch-induced stress fiber remodeling and the activations of jnk and erk depend on mechanical strain rate, but not fak.** *PLoS One* 2010;**5**:e12470.
78. Sokabe M, Naruse K, Sai S, Yamada T, Kawakami K, Inoue M, Murase K, Miyazu M: **Mechanotransduction and intracellular signaling mechanisms of stretch-induced remodeling in endothelial cells.** *Heart and vessels* 1997;**Suppl 12**:191-193.
79. Wu CC, Li YS, Haga JH, Kaunas R, Chiu JJ, Su FC, Usami S, Chien S: **Directional shear flow and rho activation prevent the endothelial cell apoptosis induced by micropatterned anisotropic geometry.** *Proc Natl Acad Sci U S A* 2007;**104**:1254-1259.
80. Wang JG, Miyazu M, Matsushita E, Sokabe M, Naruse K: **Uniaxial cyclic stretch induces focal adhesion kinase (fak) tyrosine phosphorylation followed by mitogen-activated protein kinase (mapk) activation.** *Biochem Biophys Res Commun* 2001;**288**:356-361.
81. Katriitch V, Cherezov V, Stevens RC: **Structure-function of the g protein-coupled receptor superfamily.** *Annual review of pharmacology and toxicology* 2013;**53**:531-556.
82. Chachisvilis M, Zhang YL, Frangos JA: **G protein-coupled receptors sense fluid shear stress in endothelial cells.** *Proc Natl Acad Sci U S A* 2006;**103**:15463-15468.
83. Cuerrier CM, Gagner A, Lebel R, Gobeil F, Jr., Grandbois M: **Effect of thrombin and bradykinin on endothelial cell mechanical properties monitored through membrane deformation.** *Journal of molecular recognition : JMR* 2009;**22**:389-396.
84. Anger T, El-Chafchak J, Habib A, Stumpf C, Weyand M, Daniel WG, Hombach V, Hoehner M, Garlich CD: **Statins stimulate rgs-regulated erk 1/2 activation in human calcified and stenotic aortic valves.** *Experimental and molecular pathology* 2008;**85**:101-111.
85. Christopoulos A: **Advances in g protein-coupled receptor allostery: From function to structure.** *Mol Pharmacol* 2014;**86**:463-478.
86. Becker BF, Chappell D, Jacob M: **Endothelial glycocalyx and coronary vascular permeability: The fringe benefit.** *Basic Res Cardiol* 2010;**105**:687-701.
87. Alphonso CS, Rodseth RN: **The endothelial glycocalyx: A review of the vascular barrier.** *Anaesthesia* 2014;**69**:777-784.
88. Afratis N, Gialeli C, Nikitovic D, Tsegenidis T, Karousou E, Theocharis AD, Pavao MS, Tzanakakis GN, Karamanos NK: **Glycosaminoglycans: Key players in cancer cell biology and treatment.** *The FEBS journal* 2012;**279**:1177-1197.
89. Kolářová H, Ambrůzová B, Švihálková Šindlerová L, Klinke A, Kubala L: **Modulation of endothelial glycocalyx structure under inflammatory conditions.** *Mediators of Inflammation* 2014;**2014**:694312.
90. Chien S: **Molecular and mechanical bases of focal lipid accumulation in arterial wall.** *Progress in biophysics and molecular biology* 2003;**83**:131-151.
91. Sarphie TG: **Interactions of igg and beta-vldl with aortic valve endothelium from hypercholesterolemic rabbits.** *Atherosclerosis* 1987;**68**:199-212.

92. Sarphie TG: **A cytochemical study of the surface properties of aortic and mitral valve endothelium from hypercholesterolemic rabbits.** *Experimental and molecular pathology* 1986;**44**:281-296.
93. Chien S: **Mechanotransduction and endothelial cell homeostasis: The wisdom of the cell.** *Am J Physiol Heart Circ Physiol* 2007;**292**:H1209-1224.
94. Davies PF: **Multiple signaling pathways in flow-mediated endothelial mechanotransduction: Pyk-ing the right location.** *Arteriosclerosis, Thrombosis, and Vascular Biology* 2002;**22**:1755-1757.
95. Chrétien ML, Zhang M, Jackson MR, Kapus A, Langille BL: **Mechanotransduction by endothelial cells is locally generated, direction-dependent, and ligand-specific.** *Journal of Cellular Physiology* 2010;**224**:352-361.
96. Kubiczikova L, Sedlarikova L, Hajek R, Sevcikova S: **Tgf-beta - an excellent servant but a bad master.** *Journal of Translational Medicine* 2012;**10**:183.
97. Huang F, Chen YG: **Regulation of tgf-beta receptor activity.** *Cell & bioscience* 2012;**2**:9.
98. Ohno M, Cooke JP, Dzau VJ, Gibbons GH: **Fluid shear stress induces endothelial transforming growth factor beta-1 transcription and production. Modulation by potassium channel blockade.** *J Clin Invest* 1995;**95**:1363-1369.
99. Villar AV, Cobo M, Llano M, Montalvo C, Gonzalez-Vilchez F, Martin-Duran R, Hurle MA, Nistal JF: **Plasma levels of transforming growth factor-beta1 reflect left ventricular remodeling in aortic stenosis.** *PLoS One* 2009;**4**:e8476.
100. Yetkin E, Tchaikovski V, Erdil N, Alan S, Waltenberger J: **Increased expression of cystatin c and transforming growth factor beta-1 in calcific aortic valves.** *Int J Cardiol* 2014;**176**:1252-1254.
101. Candelieri GA, Rao Y, Floh A, Sandler SD, Aubin JE: **Cdna fingerprinting of osteoprogenitor cells to isolate differentiation stage-specific genes.** *Nucleic acids research* 1999;**27**:1079-1083.
102. Johansson L, Grubb A, Abrahamson M, Kasprzykowski F, Kasprzykowska R, Grzonka Z, Lerner UH: **A peptidyl derivative structurally based on the inhibitory center of cystatin c inhibits bone resorption in vitro.** *Bone* 2000;**26**:451-459.
103. Paranya G, Vineberg S, Dvorin E, Kaushal S, Roth SJ, Rabkin E, Schoen FJ, Bischoff J: **Aortic valve endothelial cells undergo transforming growth factor- β -mediated and non-transforming growth factor- β -mediated transdifferentiation in vitro.** *The American journal of pathology* 2001;**159**:1335-1343.
104. Chen D, Zhao M, Mundy GR: **Bone morphogenetic proteins.** *Growth factors* 2004;**22**:233-241.
105. Sorescu GP, Song H, Tressel SL, Hwang J, Dikalov S, Smith DA, Boyd NL, Platt MO, Lassegue B, Griendling KK, Jo H: **Bone morphogenic protein 4 produced in endothelial cells by oscillatory shear stress induces monocyte adhesion by stimulating reactive oxygen species production from a nox1-based nadph oxidase.** *Circ Res* 2004;**95**:773-779.
106. Chang K, Weiss D, Suo J, Vega JD, Giddens D, Taylor WR, Jo H: **Bone morphogenic protein antagonists are coexpressed with bone morphogenic**

- protein 4 in endothelial cells exposed to unstable flow in vitro in mouse aortas and in human coronary arteries: Role of bone morphogenic protein antagonists in inflammation and atherosclerosis.** *Circulation* 2007;**116**:1258-1266.
107. Sorescu GP, Sykes M, Weiss D, Platt MO, Saha A, Hwang J, Boyd N, Boo YC, Vega JD, Taylor WR, Jo H: **Bone morphogenic protein 4 produced in endothelial cells by oscillatory shear stress stimulates an inflammatory response.** *J Biol Chem* 2003;**278**:31128-31135.
 108. Dhore CR, Cleutjens JP, Lutgens E, Cleutjens KB, Geusens PP, Kitslaar PJ, Tordoir JH, Spronk HM, Vermeer C, Daemen MJ: **Differential expression of bone matrix regulatory proteins in human atherosclerotic plaques.** *Arteriosclerosis, thrombosis, and vascular biology* 2001;**21**:1998-2003.
 109. Miriyala S, Gongora Nieto MC, Mingone C, Smith D, Dikalov S, Harrison DG, Jo H: **Bone morphogenic protein-4 induces hypertension in mice: Role of noggin, vascular nadph oxidases, and impaired vasorelaxation.** *Circulation* 2006;**113**:2818-2825.
 110. Yao Y, Bennett BJ, Wang X, Rosenfeld ME, Giachelli C, Lusis AJ, Bostrom KI: **Inhibition of bone morphogenetic proteins protects against atherosclerosis and vascular calcification.** *Circulation research* 2010;**107**:485-494.
 111. Derwall M, Malhotra R, Lai CS, Beppu Y, Aikawa E, Seehra JS, Zapol WM, Bloch KD, Yu PB: **Inhibition of bone morphogenetic protein signaling reduces vascular calcification and atherosclerosis.** *Arteriosclerosis, thrombosis, and vascular biology* 2012;**32**:613-622.
 112. Seya K, Yu Z, Kanemaru K, Daitoku K, Akemoto Y, Shibuya H, Fukuda I, Okumura K, Motomura S, Furukawa K: **Contribution of bone morphogenetic protein-2 to aortic valve calcification in aged rat.** *Journal of pharmacological sciences* 2011;**115**:8-14.
 113. Yu Z, Seya K, Daitoku K, Motomura S, Fukuda I, Furukawa K-I: **Tumor necrosis factor- α accelerates the calcification of human aortic valve interstitial cells obtained from patients with calcific aortic valve stenosis via the bmp2-dlx5 pathway.** *Journal of Pharmacology and Experimental Therapeutics* 2011;**337**:16-23.
 114. MacDonald BT, Tamai K, He X: **Wnt/ β -catenin signaling: Components, mechanisms, and diseases.** *Developmental cell* 2009;**17**:9-26.
 115. Rao TP, Kühn M: **An updated overview on wnt signaling pathways: A prelude for more.** *Circulation Research* 2010;**106**:1798-1806.
 116. Komiyama Y, Habas R: **Wnt signal transduction pathways.** *Organogenesis* 2008;**4**:68-75.
 117. Hurlstone AFL, Haramis A-PG, Wienholds E, Begthel H, Korving J, van Eeden F, Cuppen E, Zivkovic D, Plasterk RHA, Clevers H: **The wnt/ β -catenin pathway regulates cardiac valve formation.** *Nature* 2003;**425**:633-637.
 118. Aberle H, Bauer A, Stappert J, Kispert A, Kemler R: **Beta-catenin is a target for the ubiquitin-proteasome pathway.** *EMBO J* 1997;**16**:3797-3804.
 119. Li R, Beebe T, Jen N, Yu F, Takabe W, Harrison M, Cao H, Lee J, Yang H, Han P, Wang K, Shimizu H, Chen J, Lien C-L, Chi NC, Hsiai TK: **Shear stress–**

- activated wnt-angiopoietin-2 signaling recapitulated vascular repair in zebrafish embryos.** *Arteriosclerosis, Thrombosis, and Vascular Biology* 2014.
120. Askevold ET, Gullestad L, Aakhus S, Ranheim T, Tonnessen T, Solberg OG, Aukrust P, Ueland T: **Secreted wnt modulators in symptomatic aortic stenosis.** *Journal of the American Heart Association* 2012;**1**:e002261.
 121. Caira FC, Stock SR, Gleason TG, McGee EC, Huang J, Bonow RO, Spelsberg TC, McCarthy PM, Rahimtoola SH, Rajamannan NM: **Human degenerative valve disease is associated with up-regulation of low-density lipoprotein receptor-related protein 5 receptor-mediated bone formation.** *Journal of the American College of Cardiology* 2006;**47**:1707-1712.
 122. Rajamannan NM, Subramaniam M, Stock SR, Stone NJ, Springett M, Ignatiev KI, McConnell JP, Singh RJ, Bonow RO, Spelsberg TC: **Atorvastatin inhibits calcification and enhances nitric oxide synthase production in the hypercholesterolaemic aortic valve.** *Heart* 2005;**91**:806-810.
 123. Miller JD, Weiss RM, Serrano KM, Castaneda LE, Brooks RM, Zimmerman K, Heistad DD: **Evidence for active regulation of pro-osteogenic signaling in advanced aortic valve disease.** *Arterioscler Thromb Vasc Biol* 2010;**30**:2482-2486.
 124. Fortini ME: **Notch signaling: The core pathway and its posttranslational regulation.** *Developmental Cell* 2009;**16**:633-647.
 125. Baron M: **An overview of the notch signalling pathway.** *Seminars in Cell & Developmental Biology* 2003;**14**:113-119.
 126. Hofmann JJ, Iruela-Arispe ML: **Notch signaling in blood vessels: Who is talking to whom about what?** *Circulation Research* 2007;**100**:1556-1568.
 127. Theodoris CV, Li M, White MP, Liu L, He D, Pollard KS, Bruneau BG, Srivastava D: **Human disease modeling reveals integrated transcriptional and epigenetic mechanisms of notch1 haploinsufficiency.** *Cell* 2015;**160**:1072-1086.
 128. McKellar SH, Tester DJ, Yagubyan M, Majumdar R, Ackerman MJ, Sundt TM, 3rd: **Novel notch1 mutations in patients with bicuspid aortic valve disease and thoracic aortic aneurysms.** *J Thorac Cardiovasc Surg* 2007;**134**:290-296.
 129. Garg V, Muth AN, Ransom JF, Schluterman MK, Barnes R, King IN, Grossfeld PD, Srivastava D: **Mutations in notch1 cause aortic valve disease.** *Nature* 2005;**437**:270-274.
 130. Palmer RM, Ashton DS, Moncada S: **Vascular endothelial cells synthesize nitric oxide from l-arginine.** *Nature* 1988;**333**:664-666.
 131. Ying L, Hofseth LJ: **An emerging role for endothelial nitric oxide synthase in chronic inflammation and cancer.** *Cancer Research* 2007;**67**:1407-1410.
 132. Tousoulis D, Kampoli AM, Tentolouris C, Papageorgiou N, Stefanadis C: **The role of nitric oxide on endothelial function.** *Current vascular pharmacology* 2012;**10**:4-18.
 133. Ozawa N, Shichiri M, Iwashina M, Fukai N, Yoshimoto T, Hirata Y: **Laminar shear stress up-regulates inducible nitric oxide synthase in the endothelium.** *Hypertension research : official journal of the Japanese Society of Hypertension* 2004;**27**:93-99.

134. Bosse AK, Hans CP, Zhao N, Koenig SN, Huang N, Guggilam A, LaHaye S, Tao G, Lucchesi PA, Lincoln J, Lilly B, Garg V: **Endothelial nitric oxide signaling regulates notch1 in aortic valve disease.** *Journal of molecular and cellular cardiology* 2013;**60**:27-35.
135. El Accaoui RN, Gould ST, Hajj GP, Chu Y, Davis MK, Kraft DC, Lund DD, Brooks RM, Doshi H, Zimmerman KA, Kutschke W, Anseth KS, Heistad DD, Weiss RM: **Aortic valve sclerosis in mice deficient in endothelial nitric oxide synthase.** *Am J Physiol Heart Circ Physiol* 2014;**306**:H1302-1313.
136. Mittal M, Siddiqui MR, Tran K, Reddy SP, Malik AB: **Reactive oxygen species in inflammation and tissue injury.** *Antioxidants & Redox Signaling* 2014;**20**:1126-1167.
137. Thannickal VJ, Fanburg BL: **Reactive oxygen species in cell signaling.** *Am J Physiol Lung Cell Mol Physiol* 2000;**279**:L1005-1028.
138. Griffith B, Pendyala S, Hecker L, Lee PJ, Natarajan V, Thannickal VJ: **Nox enzymes and pulmonary disease.** *Antioxid Redox Signal* 2009;**11**:2505-2516.
139. Bedard K, Krause KH: **The nox family of ros-generating nadph oxidases: Physiology and pathophysiology.** *Physiol Rev* 2007;**87**:245-313.
140. Hwang J, Ing MH, Salazar A, Lassegue B, Griendling K, Navab M, Sevanian A, Hsiai TK: **Pulsatile versus oscillatory shear stress regulates nadph oxidase subunit expression: Implication for native ldl oxidation.** *Circ Res* 2003;**93**:1225-1232.
141. Chiu JJ, Wung BS, Shyy JYJ, Hsieh HJ, Wang DL: **Reactive oxygen species are involved in shear stress-induced intercellular adhesion molecule-1 expression in endothelial cells.** *Arteriosclerosis, Thrombosis, and Vascular Biology* 1997;**17**:3570-3577.
142. Miller JD, Chu Y, Brooks RM, Richenbacher WE, Pena-Silva R, Heistad DD: **Dysregulation of antioxidant mechanisms contributes to increased oxidative stress in calcific aortic valvular stenosis in humans.** *J Am Coll Cardiol* 2008;**52**:843-850.
143. Mody N, Parhami F, Sarafian TA, Demer LL: **Oxidative stress modulates osteoblastic differentiation of vascular and bone cells.** *Free Radic Biol Med* 2001;**31**:509-519.
144. Yip CY, Simmons CA: **The aortic valve microenvironment and its role in calcific aortic valve disease.** *Cardiovascular pathology : the official journal of the Society for Cardiovascular Pathology* 2011;**20**:177-182.
145. Sage AP, Tintut Y, Demer LL: **Regulatory mechanisms in vascular calcification.** *Nat Rev Cardiol* 2010;**7**:528-536.
146. Branchetti E, Sainger R, Poggio P, Grau JB, Patterson-Fortin J, Bavaria JE, Chorny M, Lai E, Gorman RC, Levy RJ, Ferrari G: **Antioxidant enzymes reduce DNA damage and early activation of valvular interstitial cells in aortic valve sclerosis.** *Arterioscler Thromb Vasc Biol* 2013;**33**:e66-74.
147. Das D, Holmes A, Murphy GA, Mishra K, Rosenkranz AC, Horowitz JD, Kennedy JA: **Tgf-beta1-induced mapk activation promotes collagen synthesis, nodule formation, redox stress and cellular senescence in porcine aortic valve interstitial cells.** *The Journal of heart valve disease* 2013;**22**:621-630.

148. Akdis M, Burgler S, Cramer R, Eiwegger T, Fujita H, Gomez E, Klunker S, Meyer N, O'Mahony L, Palomares O, Rhyner C, Quaked N, Schaffartzik A, Van De Veen W, Zeller S, Zimmermann M, Akdis CA: **Interleukins, from 1 to 37, and interferon- γ : Receptors, functions, and roles in diseases.** *Journal of Allergy and Clinical Immunology* 2011;**127**:701-721.e770.
149. Kanda T, Takahashi T: **Interleukin-6 and cardiovascular diseases.** *Jpn Heart J* 2004;**45**:183-193.
150. Weisman D, Hakimian E, Ho GJ: **Interleukins, inflammation, and mechanisms of alzheimer's disease.** In: *Vitamins & hormones. Volume Volume 74*, edn. Edited by Gerald L: Academic Press; 2006: 505-530.
151. Sterpetti AV, Cucina A, Morena AR, Di Donna S, D'Angelo LS, Cavalarro A, Stipa S: **Shear stress increases the release of interleukin-1 and interleukin-6 by aortic endothelial cells.** *Surgery* 1993;**114**:911-914.
152. Towler DA: **Molecular and cellular aspects of calcific aortic valve disease.** *Circulation Research* 2013;**113**:198-208.
153. Mahler GJ, Farrar EJ, Butcher JT: **Inflammatory cytokines promote mesenchymal transformation in embryonic and adult valve endothelial cells.** *Arteriosclerosis, Thrombosis, and Vascular Biology* 2013;**33**:121-130.
154. Wirrig EE, Yutzey KE: **Conserved transcriptional regulatory mechanisms in aortic valve development and disease.** *Arteriosclerosis, Thrombosis, and Vascular Biology* 2014;**34**:737-741.
155. Moura LM, Ramos SF, Zamorano JL, Barros IM, Azevedo LF, Rocha-Gonçalves F, Rajamannan NM: **Rosuvastatin affecting aortic valve endothelium to slow the progression of aortic stenosis.** *Journal of the American College of Cardiology* 2007;**49**:554-561.
156. Luvai A, Mbagaya W, Hall AS, Barth JH: **Rosuvastatin: A review of the pharmacology and clinical effectiveness in cardiovascular disease.** *Clinical Medicine Insights Cardiology* 2012;**6**:17-33.
157. Merhi-Soussi F, Kwak BR, Magne D, Chadjichristos C, Berti M, Pelli G, James RW, Mach F, Gabay C: **Interleukin-1 plays a major role in vascular inflammation and atherosclerosis in male apolipoprotein e-knockout mice,** vol. 66; 2005.
158. Isoda K, Matsuki T, Kondo H, Iwakura Y, Ohsuzu F: **Deficiency of interleukin-1 receptor antagonist induces aortic valve disease in balb/c mice.** *Arteriosclerosis, Thrombosis, and Vascular Biology* 2010;**30**:708-715.
159. Prosdocimo DA, Sabeh MK, Jain MK: **Kruppel-like factors in muscle health and disease.** *Trends in cardiovascular medicine* 2014.
160. Yamamoto K, Protack CD, Kuwahara G, Tsuneki M, Hashimoto T, Hall MR, Assi R, Brownson KE, Foster TR, Bai H, Wang M, Madri JA, Dardik A: **Disturbed shear stress reduces klf2 expression in arterial-venous fistulae in vivo.** *Physiological reports* 2015;**3**.
161. Dekker R, van Soest S, Fontijn R, Salamanca S, de Groot P, VanBavel E, Pannekoek H, Horrevoets A: **Prolonged fluid shear stress induces a distinct set of endothelial cell genes, most specifically lung kruppel-like factor (klf2).** *Blood* 2002;**100**:1689 - 1698.

162. Wang N, Miao H, Li Y-S, Zhang P, Haga JH, Hu Y, Young A, Yuan S, Nguyen P, Wu C-C, Chien S: **Shear stress regulation of krüppel-like factor 2 expression is flow pattern-specific.** *Biochemical and Biophysical Research Communications* 2006;**341**:1244-1251.
163. Weinberg EJ, Mack PJ, Schoen FJ, García-Cardena G, Kaazempur Mofrad MR: **Hemodynamic environments from opposing sides of human aortic valve leaflets evoke distinct endothelial phenotypes in vitro.** *Cardiovascular Engineering (Dordrecht, Netherlands)* 2010;**10**:5-11.
164. Hamik A, Lin Z, Kumar A, Balcells M, Sinha S, Katz J, Feinberg MW, Gerszten RE, Edelman ER, Jain MK: **Kruppel-like factor 4 regulates endothelial inflammation.** *Journal of Biological Chemistry* 2007;**282**:13769-13779.
165. Zhou G, Hamik A, Nayak L, Tian H, Shi H, Lu Y, Sharma N, Liao X, Hale A, Boerboom L, Feaver RE, Gao H, Desai A, Schmaier A, Gerson SL, Wang Y, Atkins GB, Blackman BR, Simon DI, Jain MK: **Endothelial kruppel-like factor 4 protects against atherothrombosis in mice.** *J Clin Invest* 2012;**122**:4727-4731.
166. White S, Hayes E, Lehoux S, Jeremy J, Horrevoets A, Newby A: **Characterization of the differential response of endothelial cells exposed to normal and elevated laminar shear stress.** *J Cell Physiol* 2011;**226**:2841 - 2848.
167. Villarreal Jr G, Zhang Y, Larman HB, Gracia-Sancho J, Koo A, García-Cardena G: **Defining the regulation of klf4 expression and its downstream transcriptional targets in vascular endothelial cells.** *Biochemical and Biophysical Research Communications* 2010;**391**:984-989.
168. Maleki S, Bjorck HM, Folkersen L, Nilsson R, Renner J, Caidahl K, Franco-Cereceda A, Lanne T, Eriksson P: **Identification of a novel flow-mediated gene expression signature in patients with bicuspid aortic valve.** *Journal of molecular medicine* 2013;**91**:129-139.
169. Panciera T, Azzolin L, Cordenonsi M, Piccolo S: **Mechanobiology of yap and taz in physiology and disease.** *Nature Reviews Molecular Cell Biology* 2017;**18**:758.
170. Witt W, Selle A, Jannasch A, Matschke K, Waldow T: **Expression of the hippo effectors yap and taz in valvular interstitial cells from porcine aortic valves.** *Thorac cardiovasc Surg* 2014;**62**:SC130.
171. Santoro R, Scaini D, Severino LU, Amadeo F, Ferrari S, Bernava G, Garoffolo G, Agrifoglio M, Casalis L, Pesce M: **Activation of human aortic valve interstitial cells by local stiffness involves yap-dependent transcriptional signaling.** *Biomaterials* 2018;**181**:268-279.
172. Wang K-C, Yeh Y-T, Nguyen P, Limqueco E, Lopez J, Thorossian S, Guan K-L, Li Y-SJ, Chien S: **Flow-dependent yap/taz activities regulate endothelial phenotypes and atherosclerosis.** *Proc Natl Acad Sci U S A* 2016;**113**:11525-11530.
173. Nakajima H, Yamamoto K, Agarwala S, Terai K, Fukui H, Fukuhara S, Ando K, Miyazaki T, Yokota Y, Schmelzer E, Belting HG, Affolter M, Lecaudey V, Mochizuki N: **Flow-dependent endothelial yap regulation contributes to vessel maintenance.** *Dev Cell* 2017;**40**:523-536 e526.

174. Hong L, Du X, Li W, Mao Y, Sun L, Li X: **Endmt: A promising and controversial field.** *European journal of cell biology* 2018.
175. Souilhol C, Harmsen MC, Evans PC, Krenning G: **Endothelial-mesenchymal transition in atherosclerosis.** *Cardiovasc Res* 2018;**114**:565-577.
176. Dahal S, Huang P, Murray BT, Mahler GJ: **Endothelial to mesenchymal transformation is induced by altered extracellular matrix in aortic valve endothelial cells.** *Journal of Biomedical Materials Research Part A* 2017;**105**:2729-2741.
177. Farrar E, Butcher J: **Heterogeneous susceptibility of valve endothelial cells to mesenchymal transformation in response to tnfa.** *Ann Biomed Eng* 2014;**42**:149-161.
178. Hjortnaes J, Shapero K, Goettsch C, Hutcheson JD, Keegan J, Kluin J, Mayer JE, Bischoff J, Aikawa E: **Valvular interstitial cells suppress calcification of valvular endothelial cells.** *Atherosclerosis* 2015;**242**:251-260.
179. Mahler GJ, Frendl CM, Cao Q, Butcher JT: **Effects of shear stress pattern and magnitude on mesenchymal transformation and invasion of aortic valve endothelial cells.** *Biotechnology and bioengineering* 2014;**111**:2326-2337.
180. Dewey CF, Jr., Bussolari SR, Gimbrone MA, Jr., Davies PF: **The dynamic response of vascular endothelial cells to fluid shear stress.** *J Biomech Eng* 1981;**103**:177-185.
181. Bussolari SR, Dewey CF, Jr., Gimbrone MA, Jr.: **Apparatus for subjecting living cells to fluid shear stress.** *The Review of scientific instruments* 1982;**53**:1851-1854.
182. Franke RP, Grafe M, Schnittler H, Seiffge D, Mittermayer C, Drenckhahn D: **Induction of human vascular endothelial stress fibres by fluid shear stress.** *Nature* 1984;**307**:648-649.
183. Go YM, Boo YC, Park H, Maland MC, Patel R, Pritchard KA, Jr., Fujio Y, Walsh K, Darley-Usmar V, Jo H: **Protein kinase b/akt activates c-jun nh(2)-terminal kinase by increasing no production in response to shear stress.** *J Appl Physiol (1985)* 2001;**91**:1574-1581.
184. Jo H, Song H, Mowbray A: **Role of nadph oxidases in disturbed flow- and bmp4- induced inflammation and atherosclerosis.** *Antioxid Redox Signal* 2006;**8**:1609-1619.
185. Sucusky P, Padala M, Elhammali A, Balachandran K, Jo H, Yoganathan AP: **Design of an ex vivo culture system to investigate the effects of shear stress on cardiovascular tissue.** *Journal of Biomechanical Engineering* 2008;**130**:035001-035001.
186. Frangos JA, Eskin SG, McIntire LV, Ives CL: **Flow effects on prostacyclin production by cultured human endothelial cells.** *Science* 1985;**227**:1477-1479.
187. Frangos JA, McIntire LV, Eskin SG: **Shear stress induced stimulation of mammalian cell metabolism.** *Biotechnol Bioeng* 1988;**32**:1053-1060.
188. Schaff UY, Xing MM, Lin KK, Pan N, Jeon NL, Simon SI: **Vascular mimetics based on microfluidics for imaging the leukocyte--endothelial inflammatory response.** *Lab Chip* 2007;**7**:448-456.

189. Ashpole NE, Overby DR, Ethier CR, Stamer WD: **Shear stress-triggered nitric oxide release from schlemm's canal cells.** *Investigative ophthalmology & visual science* 2014;**55**:8067-8076.
190. Ganguly A, Zhang H, Sharma R, Parsons S, Patel KD: **Isolation of human umbilical vein endothelial cells and their use in the study of neutrophil transmigration under flow conditions.** *Journal of visualized experiments : JoVE* 2012:e4032.
191. Li F, Cai Z, Chen F, Shi X, Zhang Q, Chen S, Shi J, Wang DW, Dong N: **Pioglitazone attenuates progression of aortic valve calcification via down-regulating receptor for advanced glycation end products.** *Basic Res Cardiol* 2012;**107**:306.
192. Sider KL, Blaser MC, Simmons CA: **Animal models of calcific aortic valve disease.** *Int J Inflam* 2011;**2011**:364310.
193. Weiss RM, Ohashi M, Miller JD, Young SG, Heistad DD: **Calcific aortic valve stenosis in old hypercholesterolemic mice.** *Circulation* 2006;**114**:2065-2069.
194. Emini Veseli B, Perrotta P, De Meyer GRA, Roth L, Van der Donckt C, Martinet W, De Meyer GRY: **Animal models of atherosclerosis.** *European Journal of Pharmacology* 2017;**816**:3-13.
195. Towler DA, Bidder M, Latifi T, Coleman T, Semenkovich CF: **Diet-induced diabetes activates an osteogenic gene regulatory program in the aortas of low density lipoprotein receptor-deficient mice.** *J Biol Chem* 1998;**273**:30427-30434.
196. Matsumoto Y, Adams V, Jacob S, Mangner N, Schuler G, Linke A: **Regular exercise training prevents aortic valve disease in low-density lipoprotein-receptor-deficient mice.** *Circulation* 2010;**121**:759-767.
197. Scatena M, Jackson MF, Speer MY, Leaf EM, Wallingford MC, Giachelli CM: **Increased calcific aortic valve disease in response to a diabetogenic, procalcific diet in the ldlr^{-/-}apob^{100/100} mouse model.** *Cardiovascular Pathology* 2018;**34**:28-37.
198. Mehrabian M, Demer LL, Lusic AJ: **Differential accumulation of intimal monocyte-macrophages relative to lipoproteins and lipofuscin corresponds to hemodynamic forces on cardiac valves in mice.** *Arterioscler Thromb* 1991;**11**:947-957.
199. Daugherty A, Rateri DL: **Development of experimental designs for atherosclerosis studies in mice.** *Methods* 2005;**36**:129-138.
200. Aikawa E, Aikawa M, Libby P, Figueiredo JL, Rusanescu G, Iwamoto Y, Fukuda D, Kohler RH, Shi GP, Jaffer FA, Weissleder R: **Arterial and aortic valve calcification abolished by elastolytic cathepsin s deficiency in chronic renal disease.** *Circulation* 2009;**119**:1785-1794.
201. Hjortnaes J, Butcher J, Figueiredo JL, Riccio M, Kohler RH, Kozloff KM, Weissleder R, Aikawa E: **Arterial and aortic valve calcification inversely correlates with osteoporotic bone remodelling: A role for inflammation.** *Eur Heart J* 2010;**31**:1975-1984.
202. Zhang HL, Wu J, Zhu J: **The role of apolipoprotein e in guillain-barre syndrome and experimental autoimmune neuritis.** *J Biomed Biotechnol* 2010;**2010**:357412.

203. Plump AS, Smith JD, Hayek T, Aalto-Setälä K, Walsh A, Verstuyft JG, Rubin EM, Breslow JL: **Severe hypercholesterolemia and atherosclerosis in apolipoprotein e-deficient mice created by homologous recombination in es cells.** *Cell* 1992;**71**:343-353.
204. Tanaka K, Sata M, Fukuda D, Suematsu Y, Motomura N, Takamoto S, Hirata Y, Nagai R: **Age-associated aortic stenosis in apolipoprotein e-deficient mice.** *J Am Coll Cardiol* 2005;**46**:134-141.
205. Aikawa E, Nahrendorf M, Figueiredo JL, Swirski FK, Shtatland T, Kohler RH, Jaffer FA, Aikawa M, Weissleder R: **Osteogenesis associates with inflammation in early-stage atherosclerosis evaluated by molecular imaging in vivo.** *Circulation* 2007;**116**:2841-2850.
206. Aikawa E, Nahrendorf M, Sosnovik D, Lok VM, Jaffer FA, Aikawa M, Weissleder R: **Multimodality molecular imaging identifies proteolytic and osteogenic activities in early aortic valve disease.** *Circulation* 2007;**115**:377-386.
207. Luo G, Ducey P, McKee MD, Pinero GJ, Loyer E, Behringer RR, Karsenty G: **Spontaneous calcification of arteries and cartilage in mice lacking matrix gla protein.** *Nature* 1997;**386**:78-81.
208. Hinton RB, Adelman-Brown J, Witt S, Krishnamurthy VK, Osinska H, Sakthivel B, James JF, Li DY, Narboneva DA, Mecham RP, Benson DW: **Elastin haploinsufficiency results in progressive aortic valve malformation and latent valve disease in a mouse model.** *Circ Res* 2010;**107**:549-557.
209. Hanada K, Vermeij M, Garinis GA, de Waard MC, Kunen MG, Myers L, Maas A, Duncker DJ, Meijers C, Dietz HC, Kanaar R, Essers J: **Perturbations of vascular homeostasis and aortic valve abnormalities in fibulin-4 deficient mice.** *Circ Res* 2007;**100**:738-746.
210. Choi B, Lee S, Kim SM, Lee EJ, Lee SR, Kim DH, Jang JY, Kang SW, Lee KU, Chang EJ, Song JK: **Dipeptidyl peptidase-4 induces aortic valve calcification by inhibiting insulin-like growth factor-1 signaling in valvular interstitial cells.** *Circulation* 2017;**135**:1935-1950.
211. Laforest B, Andelfinger G, Nemer M: **Loss of gata5 in mice leads to bicuspid aortic valve.** *The Journal of Clinical Investigation* 2011;**121**:2876-2887.
212. Bartel DP: **MicRNAs: Genomics, biogenesis, mechanism, and function.** *Cell* 2004;**116**:281-297.
213. Bartel DP: **MicRNAs: Target recognition and regulatory functions.** *Cell* 2009;**136**:215-233.
214. van Rooij E: **The art of microRNA research.** *Circ Res* 2011;**108**:219-234.
215. van Rooij E, Marshall WS, Olson EN: **Toward microRNA-based therapeutics for heart disease: The sense in antisense.** *Circ Res* 2008;**103**:919-928.
216. van Rooij E, Purcell AL, Levin AA: **Developing microRNA therapeutics.** *Circ Res* 2012;**110**:496-507.
217. van Rooij E, Sutherland LB, Qi X, Richardson JA, Hill J, Olson EN: **Control of stress-dependent cardiac growth and gene expression by a microRNA.** *Science* 2007;**316**:575-579.

218. Kumar S, Kim CW, Simmons RD, Jo H: **Role of flow-sensitive micrnas in endothelial dysfunction and atherosclerosis mechanosensitive athero-mirs.** *Arteriosclerosis, thrombosis, and vascular biology* 2014;**34**:2206-2216.
219. Goettsch C, Hutcheson JD, Aikawa E: **Micrnas in cardiovascular calcification focus on targets and extracellular vesicle delivery mechanisms.** *Circulation Research* 2013;**112**:1073-1084.
220. Rathan S, Ankeny CJ, Arjunon S, Ferdous Z, Kumar S, Fernandez Esmerats J, Heath JM, Nerem RM, Yoganathan AP, Jo H: **Identification of side- and shear-dependent micrnas regulating porcine aortic valve pathogenesis.** *Sci Rep* 2016;**6**:25397.
221. Kumar S, Jang IH, Kim CW, Kang DW, Lee WJ, Jo H: **Functional screening of mammalian mechanosensitive genes using drosophila rnai library-smarcd3/bap60 is a mechanosensitive pro-inflammatory gene.** *Sci Rep* 2016;**6**:36461.
222. Li XF, Wang Y, Zheng DD, Xu HX, Wang T, Pan M, Shi JH, Zhu JH: **M1 macrophages promote aortic valve calcification mediated by micrnas-214/twist1 pathway in valvular interstitial cells.** *Am J Transl Res* 2016;**8**:5773-5783.
223. Ohukainen P, Syvaranta S, Napankangas J, Rajamaki K, Taskinen P, Peltonen T, Helske-Suihko S, Kovanen PT, Ruskoaho H, Rysa J: **Micrnas-125b and chemokine ccl4 expression are associated with calcific aortic valve disease.** *Ann Med* 2015;**47**:423-429.
224. Nigam V, Sievers HH, Jensen BC, Sier HA, Simpson PC, Srivastava D, Mohamed SA: **Altered micrnas in bicuspid aortic valve: A comparison between stenotic and insufficient valves.** *Journal of Heart Valve Disease* 2010;**19**:459-465.
225. Wang H, Shi J, Li B, Zhou Q, Kong X, Bei Y: **Micrnas expression signature in human calcific aortic valve disease.** *BioMed Research International* 2017;**2017**:4820275.
226. Yanagawa B, Lovren F, Pan Y, Garg V, Quan A, Tang G, Singh KK, Shukla PC, Kalra NP, Peterson MD, Verma S: **Mirna-141 is a novel regulator of bmp-2-mediated calcification in aortic stenosis.** *The Journal of Thoracic and Cardiovascular Surgery* 2012;**144**:256-262.e252.
227. Xiao X, Zhou T, Guo S, Guo C, Zhang Q, Dong N, Wang Y: **Lncrna malat1 sponges mir-204 to promote osteoblast differentiation of human aortic valve interstitial cells through up-regulating smad4.** *International Journal of Cardiology.*
228. Wang Y, Chen S, Deng C, Li F, Wang Y, Hu X, Shi F, Dong N: **Micrnas-204 targets runx2 to attenuate bmp-2-induced osteoblast differentiation of human aortic valve interstitial cells.** *J Cardiovasc Pharmacol* 2015;**66**:63-71.
229. Song R, Fullerton DA, Ao L, Zhao KS, Meng X: **An epigenetic regulatory loop controls pro-osteogenic activation by tgf-beta1 or bone morphogenetic protein 2 in human aortic valve interstitial cells.** *J Biol Chem* 2017;**292**:8657-8666.
230. Fang M, Wang CG, Zheng C, Luo J, Hou S, Liu K, Li X: **Mir-29b promotes human aortic valve interstitial cell calcification via inhibiting tgf-beta3**

- through activation of wnt3/beta-catenin/smad3 signaling. *J Cell Biochem* 2017.
231. Yu C, Li L, Xie F, Guo S, Liu F, Dong N, Wang Y: **Lncrna tug1 sponges mir-204-5p to promote osteoblast differentiation through upregulating runx2 in aortic valve calcification.** *Cardiovasc Res* 2018;**114**:168-179.
232. Xu R, Zhao M, Yang Y, Huang Z, Shi C, Hou X, Zhao Y, Chen B, Xiao Z, Liu J, Miao Q, Dai J: **Microrna-449c-5p inhibits osteogenic differentiation of human vics through smad4-mediated pathway.** *Sci Rep* 2017;**7**:8740.
233. Wang Z, Chen S, Zhu M, Zhang W, Zhang H, Li H, Zou C: **Functional snp in the 3'utr of pon1 is associated with the risk of calcific aortic valve stenosis via mir-616.** *Cell Physiol Biochem* 2018;**45**:1390-1398.
234. Ming F, Cheng-Guang W, Changzhu Z, Jun L, Shiqiang H, Kangyong L, Xinming L: **Mir-29b promotes human aortic valve interstitial cell calcification via inhibiting tgf-β3 through activation of wnt3/β-catenin/smad3 signaling.** *Journal of Cellular Biochemistry* 2018;**119**:5175-5185.
235. Nader J, Metzinger-Le Meuth V, Maitrias P, Humbert JR, Brigant B, Tribouilloy C, Metzinger L, Caus T: **Mir-92a: A novel potential biomarker of rapid aortic valve calcification.** *The Journal of heart valve disease* 2017;**26**:327-333.
236. Du J, Zheng R, Xiao F, Zhang S, He K, Zhang J, Shao Y: **Downregulated microrna-195 in the bicuspid aortic valve promotes calcification of valve interstitial cells via targeting smad7.** *Cell Physiol Biochem* 2017;**44**:884-896.
237. Rupaimoole R, Slack FJ: **Microrna therapeutics: Towards a new era for the management of cancer and other diseases.** *Nat Rev Drug Discov* 2017;**16**:203-222.
238. van Rooij E, Kauppinen S: **Development of microrna therapeutics is coming of age.** *EMBO Mol Med* 2014;**6**:851-864.
239. Elmen J, Lindow M, Schutz S, Lawrence M, Petri A, Obad S, Lindholm M, Hedtjarn M, Hansen HF, Berger U, Gullans S, Kearney P, Sarnow P, Straarup EM, Kauppinen S: **Lna-mediated microrna silencing in non-human primates.** *Nature* 2008;**452**:896-899.
240. Elmen J, Lindow M, Silahtaroglu A, Bak M, Christensen M, Lind-Thomsen A, Hedtjarn M, Hansen JB, Hansen HF, Straarup EM, McCullagh K, Kearney P, Kauppinen S: **Antagonism of microrna-122 in mice by systemically administered lna-antimir leads to up-regulation of a large set of predicted target mrnas in the liver.** *Nucleic acids research* 2008;**36**:1153-1162.
241. Janssen HL, Reesink HW, Lawitz EJ, Zeuzem S, Rodriguez-Torres M, Patel K, van der Meer AJ, Patick AK, Chen A, Zhou Y, Persson R, King BD, Kauppinen S, Levin AA, Hodges MR: **Treatment of hcv infection by targeting microrna.** *The New England journal of medicine* 2013;**368**:1685-1694.
242. Ottosen S, Parsley TB, Yang L, Zeh K, van Doorn LJ, van der Veer E, Raney AK, Hodges MR, Patick AK: **In vitro antiviral activity and preclinical and clinical resistance profile of miravirsin, a novel anti-hepatitis c virus therapeutic targeting the human factor mir-122.** *Antimicrob Agents Chemother* 2015;**59**:599-608.

243. Trajkovski M, Hausser J, Soutschek J, Bhat B, Akin A, Zavolan M, Heim MH, Stoffel M: **Micrnas 103 and 107 regulate insulin sensitivity.** *Nature* 2011;**474**:649-653.
244. Bader AG: **Mir-34 - a microRNA replacement therapy is headed to the clinic.** *Front Genet* 2012;**3**:120.
245. Misso G, Di Martino MT, De Rosa G, Farooqi AA, Lombardi A, Campani V, Zarone MR, Gulla A, Tagliaferri P, Tassone P, Caraglia M: **Mir-34: A new weapon against cancer?** *Mol Ther Nucleic Acids* 2014;**3**:e194.
246. Cortez MA, Ivan C, Valdecanas D, Wang X, Peltier HJ, Ye Y, Araujo L, Carbone DP, Shilo K, Giri DK, Kelnar K, Martin D, Komaki R, Gomez DR, Krishnan S, Calin GA, Bader AG, Welsh JW: **Pd11 regulation by p53 via mir-34.** *J Natl Cancer Inst* 2016;**108**.
247. Stahlhut C, Slack FJ: **Combinatorial action of microRNAs let-7 and mir-34 effectively synergizes with erlotinib to suppress non-small cell lung cancer cell proliferation.** *Cell Cycle* 2015;**14**:2171-2180.
248. Reid G, Kao SC, Pavlakis N, Brahmabhatt H, MacDiarmid J, Clarke S, Boyer M, van Zandwijk N: **Clinical development of targomirs, a mirna mimic-based treatment for patients with recurrent thoracic cancer.** *Epigenomics* 2016;**8**:1079-1085.
249. van Zandwijk N, Fong KM: **Update in lung cancer: Prologue to a modern review series.** *Respirology* 2015;**20**:183-184.
250. Liu J, Shi W, Wu C, Ju J, Jiang J: **Mir-181b as a key regulator of the oncogenic process and its clinical implications in cancer (review).** *Biomedical Reports* 2014;**2**:7-11.
251. Sun X, Icli B, Wara AK, Belkin N, He S, Kobzik L, Hunninghake GM, Vera MP, Registry M, Blackwell TS, Baron RM, Feinberg MW: **Microrna-181b regulates nf-kb-mediated vascular inflammation.** *The Journal of Clinical Investigation* 2012;**122**:1973-1990.
252. Sun X, Lin J, Zhang Y, Kang S, Belkin N, Wara AK, Icli B, Hamburg NM, Li D, Feinberg MW: **Microrna-181b improves glucose homeostasis and insulin sensitivity by regulating endothelial function in white adipose tissue.** *Circulation research* 2016;**118**:810-821.
253. Goldbarg SH, Elmariah S, Miller MA, Fuster V: **Insights into degenerative aortic valve disease.** *Journal of the American College of Cardiology* 2007;**50**:1205-1213.
254. Murphy G, Nagase H: **Progress in matrix metalloproteinase research.** *Molecular aspects of medicine* 2008;**29**:290-308.
255. Porter S, Clark Ian M, Kevorkian L, Edwards Dylan R: **The adamts metalloproteinases.** *Biochemical Journal* 2005;**386**:15-27.
256. Weiss RM, Miller JD, Heistad DD: **Fibrocalcific aortic valve disease: Opportunity to understand disease mechanisms using mouse models.** *Circulation Research* 2013;**113**:209-222.
257. Kaden JJ, Dempfle C-E, Grobholz R, Fischer CS, Vocke DC, Kılıç R, Sarıkoç A, Piñol R, Hagl S, Lang S, Brueckmann M, Borggreffe M: **Inflammatory regulation of extracellular matrix remodeling in calcific aortic valve stenosis.** *Cardiovascular Pathology* 2005;**14**:80-87.

258. Nagy E, Eriksson P, Yousry M, Caidahl K, Ingelsson E, Hansson GK, Franco-Cereceda A, Bäck M: **Valvular osteoclasts in calcification and aortic valve stenosis severity.** *International Journal of Cardiology* 2013;**168**:2264-2271.
259. Jung J-J, Razavian M, Challa AA, Nie L, Golestani R, Zhang J, Ye Y, Russell KS, Robinson SP, Heistad DD, Sadeghi MM: **Multimodality and molecular imaging of matrix metalloproteinase activation in calcific aortic valve disease.** *Journal of Nuclear Medicine* 2015;**56**:933-938.
260. Perrotta I, Sciangula A, Aquila S, Mazzulla S: **Matrix metalloproteinase-9 expression in calcified human aortic valves: A histopathologic, immunohistochemical, and ultrastructural study.** *Applied Immunohistochemistry & Molecular Morphology* 2016;**24**:128-137.
261. Wang Y, Wu B, Dong L, Wang C, Wang X, Shu X: **Circulating matrix metalloproteinase patterns in association with aortic dilatation in bicuspid aortic valve patients with isolated severe aortic stenosis.** *Heart and vessels* 2016;**31**:189-197.
262. Platt MO, Xing Y, Jo H, Yoganathan AP: **Cyclic pressure and shear stress regulate matrix metalloproteinases and cathepsin activity in porcine aortic valves.** *The Journal of heart valve disease* 2006;**15**:622-629.
263. Son DJ, Kumar S, Takabe W, Kim CW, Ni CW, Alberts-Grill N, Jang IH, Kim S, Kim W, Won Kang S, Baker AH, Woong Seo J, Ferrara KW, Jo H: **The atypical mechanosensitive microRNA-712 derived from pre-ribosomal rna induces endothelial inflammation and atherosclerosis.** *Nat Commun* 2013;**4**:3000.
264. Qi JH, Ebrahim Q, Moore N, Murphy G, Claesson-Welsh L, Bond M, Baker A, Anand-Apte B: **A novel function for tissue inhibitor of metalloproteinases-3 (timp3): Inhibition of angiogenesis by blockage of vegf binding to vegf receptor-2.** *Nature medicine* 2003;**9**:407-415.
265. Heath JM, Fernandez Esmerats J, Khambouneheuang L, Kumar S, Simmons RD, Jo H: **Mechanosensitive microRNA-181b regulates aortic valve endothelial matrix degradation by targeting timp3.** *Cardiovascular Engineering and Technology* 2017.
266. Constancia M, Hemberger M, Hughes J, Dean W, Ferguson-Smith A, Fundele R, Stewart F, Kelsey G, Fowden A, Sibley C, Reik W: **Placental-specific igf-ii is a major modulator of placental and fetal growth.** *Nature* 2002;**417**:945-948.
267. Abue M, Yokoyama M, Shibuya R, Tamai K, Yamaguchi K, Sato I, Tanaka N, Hamada S, Shimosegawa T, Sugamura K, Satoh K: **Circulating mir-483-3p and mir-21 is highly expressed in plasma of pancreatic cancer.** *Int J Oncol* 2015;**46**:539-547.
268. Bertero T, Bourget-Ponzio I, Puissant A, Loubat A, Mari B, Meneguzzi G, Auberger P, Barbry P, Ponzio G, Rezzonico R: **Tumor suppressor function of mir-483-3p on squamous cell carcinomas due to its pro-apoptotic properties.** *Cell Cycle* 2013;**12**:2183-2193.
269. Lupini L, Pepe F, Ferracin M, Braconi C, Callegari E, Pagotto S, Spizzo R, Zagatti B, Lanuti P, Fornari F, Ghasemi R, Mariani-Costantini R, Bolondi L, Gramantieri L, Calin GA, Sabbioni S, Visone R, Veronese A, Negrini M: **Over-expression of the mir-483-3p overcomes the mir-145/tp53 pro-apoptotic loop in hepatocellular carcinoma.** *Oncotarget* 2016.

270. Ma J, Hong L, Xu G, Hao J, Wang R, Guo H, Liu J, Zhang Y, Nie Y, Fan D: **Mir-483-3p plays an oncogenic role in esophageal squamous cell carcinoma by targeting tumor suppressor ei24.** *Cell Biol Int* 2016;**40**:448-455.
271. Kemp JR, Unal H, Desnoyer R, Yue H, Bhatnagar A, Karnik SS: **Angiotensin ii-regulated microrna 483-3p directly targets multiple components of the renin-angiotensin system.** *Journal of molecular and cellular cardiology* 2014;**75**:25-39.
272. Morley-Smith AC, Mills A, Jacobs S, Meyns B, Rega F, Simon AR, Pepper JR, Lyon AR, Thum T: **Circulating micrornas for predicting and monitoring response to mechanical circulatory support from a left ventricular assist device.** *European Journal of Heart Failure* 2014;**16**:871-879.
273. He M, Chen Z, Martin M, Zhang J, Sangwung P, Woo B, Tremoulet AH, Shimizu C, Jain MK, Burns JC, Shyy JY: **Mir-483 targeting of ctgf suppresses endothelial-to-mesenchymal transition: Therapeutic implications in kawasaki disease.** *Circ Res* 2017;**120**:354-365.
274. Kong L, Hu N, Du X, Wang W, Chen H, Li W, Wei S, Zhuang H, Li X, Li C: **Upregulation of mir-483-3p contributes to endothelial progenitor cells dysfunction in deep vein thrombosis patients via srf.** *J Transl Med* 2016;**14**:23.
275. Ciechanover A: **The ubiquitin-proteasome proteolytic pathway.** *Cell* 1994;**79**:13-21.
276. Stewart MD, Ritterhoff T, Klevit RE, Brzovic PS: **E2 enzymes: More than just middle men.** *Cell Research* 2016;**26**:423-440.
277. Hao Z, Zhang H, Cowell J: **Ubiquitin-conjugating enzyme ube2c: Molecular biology, role in tumorigenesis, and potential as a biomarker.** *Tumor Biology* 2012;**33**:723-730.
278. Alfieri C, Zhang S, Barford D: **Visualizing the complex functions and mechanisms of the anaphase promoting complex/cyclosome (apc/c).** *Open Biol* 2017;**7**.
279. Liu W, Xin H, Eckert DT, Brown JA, Gnarr JR: **Hypoxia and cell cycle regulation of the von hippel-lindau tumor suppressor.** *Oncogene* 2011;**30**:21-31.
280. Harley ME, Allan LA, Sanderson HS, Clarke PR: **Phosphorylation of mcl-1 by cdk1-cyclin b1 initiates its cdc20-dependent destruction during mitotic arrest.** *EMBO J* 2010;**29**:2407-2420.
281. Takahashi A, Imai Y, Yamakoshi K, Kuninaka S, Ohtani N, Yoshimoto S, Hori S, Tachibana M, Anderton E, Takeuchi T, Shinkai Y, Peters G, Saya H, Hara E: **DNA damage signaling triggers degradation of histone methyltransferases through apc/c(cdh1) in senescent cells.** *Mol Cell* 2012;**45**:123-131.
282. Garcia-Cao I, Song MS, Hobbs RM, Laurent G, Giorgi C, de Boer VCJ, Anastasiou D, Ito K, Sasaki AT, Rameh L, Carracedo A, Vander Heiden MG, Cantley LC, Pinton P, Haigis MC, Pandolfi PP: **Systemic elevation of pten induces a tumor suppressive metabolic state.** *Cell* 2012;**149**:49-62.
283. Garcia-Nogales P, Almeida A, Bolanos JP: **Peroxynitrite protects neurons against nitric oxide-mediated apoptosis. A key role for glucose-6-phosphate dehydrogenase activity in neuroprotection.** *J Biol Chem* 2003;**278**:864-874.

284. Maxwell PH, Pugh CW, Ratcliffe PJ: **The pvh1-hif-1 system. A key mediator of oxygen homeostasis.** *Adv Exp Med Biol* 2001;**502**:365-376.
285. Majmundar AJ, Wong WJ, Simon MC: **Hypoxia-inducible factors and the response to hypoxic stress.** *Mol Cell* 2010;**40**:294-309.
286. Masoud GN, Li W: **Hif-1 α pathway: Role, regulation and intervention for cancer therapy.** *Acta Pharmaceutica Sinica B* 2015;**5**:378-389.
287. Akhtar S, Hartmann P, Karshovska E, Rinderknecht F-A, Subramanian P, Gremse F, Grommes J, Jacobs M, Kiessling F, Weber C, Steffens S, Schober A: **Endothelial hypoxia-inducible factor-1 α promotes atherosclerosis and monocyte recruitment by upregulating microRNA-19a.** *Hypertension* 2015;**66**:1220-1226.
288. Liu W, Shen S-M, Zhao X-Y, Chen G-Q: **Targeted genes and interacting proteins of hypoxia inducible factor-1.** *International Journal of Biochemistry and Molecular Biology* 2012;**3**:165-178.
289. Demidenko ZN, Blagosklonny MV: **The purpose of the hif-1/phd feedback loop: To limit mtor-induced hif-1 α .** *Cell Cycle* 2011;**10**:1557-1562.
290. Chou C-P, Huang N-C, Jhuang S-J, Pan H-B, Peng N-J, Cheng J-T, Chen C-F, Chen J-J, Chang T-H: **Ubiquitin-conjugating enzyme ube2c is highly expressed in breast microcalcification lesions.** *PLOS ONE* 2014;**9**:e93934.
291. Schwab LP, Peacock DL, Majumdar D, Ingels JF, Jensen LC, Smith KD, Cushing RC, Seagroves TN: **Hypoxia-inducible factor 1 α promotes primary tumor growth and tumor-initiating cell activity in breast cancer.** *Breast Cancer Research : BCR* 2012;**14**:R6-R6.
292. Morikawa T, Kawai T, Abe H, Kume H, Homma Y, Fukayama M: **Ube2c is a marker of unfavorable prognosis in bladder cancer after radical cystectomy.** *International Journal of Clinical and Experimental Pathology* 2013;**6**:1367-1374.
293. Hunter BA, Eustace A, Irlam JJ, Valentine HR, Denley H, Oguejiofor KK, Swindell R, Hoskin PJ, Choudhury A, West CM: **Expression of hypoxia-inducible factor-1[alpha] predicts benefit from hypoxia modification in invasive bladder cancer.** *Br J Cancer* 2014;**111**:437-443.
294. Takahashi Y, Ishii Y, Nishida Y, Ikarashi M, Nagata T, Nakamura T, Yamamori S, Asai S: **Detection of aberrations of ubiquitin-conjugating enzyme e2c gene (ube2c) in advanced colon cancer with liver metastases by DNA microarray and two-color fish.** *Cancer Genetics and Cytogenetics*; **168**:30-35.
295. Baba Y, Noshio K, Shima K, Irahara N, Chan AT, Meyerhardt JA, Chung DC, Giovannucci EL, Fuchs CS, Ogino S: **Hif1 α overexpression is associated with poor prognosis in a cohort of 731 colorectal cancers.** *The American journal of pathology* 2010;**176**:2292-2301.
296. Perrotta I, Moraca FM, Sciangula A, Aquila S, Mazzulla S: **Hif-1 α and vegf: Immunohistochemical profile and possible function in human aortic valve stenosis.** *Ultrastructural Pathology* 2015;**39**:198-206.
297. Palazon A, Goldrath AW, Nizet V, Johnson RS: **Hif transcription factors, inflammation, and immunity.** *Immunity* 2014;**41**:518-528.
298. Xu X, Tan X, Tampe B, Sanchez E, Zeisberg M, Zeisberg EM: **Snail is a direct target of hypoxia-inducible factor 1alpha (hif1alpha) in hypoxia-induced**

- endothelial to mesenchymal transition of human coronary endothelial cells. *J Biol Chem* 2015;**290**:16653-16664.
299. Jeong W, Rapisarda A, Park SR, Kinders RJ, Chen A, Melillo G, Turkbey B, Steinberg SM, Choyke P, Doroshow JH, Kummar S: **Pilot trial of ezn-2968, an antisense oligonucleotide inhibitor of hypoxia-inducible factor-1 alpha (hif-1 α), in patients with refractory solid tumors.** *Cancer Chemotherapy and Pharmacology* 2014;**73**:343-348.
300. Zhu Y, Zang Y, Zhao F, Li Z, Zhang J, Fang L, Li M, Xing L, Xu Z, Yu J: **Inhibition of hif-1 α by px-478 suppresses tumor growth of esophageal squamous cell cancer in vitro and in vivo.** *American Journal of Cancer Research* 2017;**7**:1198-1212.
301. Tibes R, Falchook GS, Von Hoff DD, Weiss GJ, Iyengar T, Kurzrock R, Pestano L, Lowe AM, Herbst RS: **Results from a phase i, dose-escalation study of px-478, an orally available inhibitor of hif-1 α .** *Journal of Clinical Oncology* 2010;**28**:3076-3076.
302. Czarny MJ, Resar JR: **Diagnosis and management of valvular aortic stenosis.** *Clinical Medicine Insights: Cardiology* 2014:15-24.
303. Sun X, Icli B, Wara AK, Belkin N, He S, Kobzik L, Hunninghake GM, Vera MP, Registry M, Blackwell TS, Baron RM, Feinberg MW: **Microrna-181b regulates nf-kappab-mediated vascular inflammation.** *The Journal of clinical investigation* 2012;**122**:1973-1990.
304. Lin J, He S, Sun X, Franck G, Deng Y, Yang D, Haemmig S, Wara AK, Icli B, Li D, Feinberg MW: **Microrna-181b inhibits thrombin-mediated endothelial activation and arterial thrombosis by targeting caspase recruitment domain family member 10.** *FASEB journal : official publication of the Federation of American Societies for Experimental Biology* 2016.
305. Zhou Q, Zheng X, Chen L, Xu B, Yang X, Jiang J, Wu C: **Smad2/3/4 pathway contributes to tgf-beta-induced mirna-181b expression to promote gastric cancer metastasis by targeting timp3.** *Cellular physiology and biochemistry : international journal of experimental cellular physiology, biochemistry, and pharmacology* 2016;**39**:453-466.
306. Simmons RD, Kumar S, Jo H: **The role of endothelial mechanosensitive genes in atherosclerosis and omics approaches.** *Arch Biochem Biophys* 2016;**591**:111-131.
307. Kumar S, Kang D-W, Rezvan A, Jo H: **Accelerated atherosclerosis development in c57bl6 mice by overexpressing aav-mediated pcsk9 and partial carotid ligation.** *Lab Invest* 2017.
308. Mohler ER, Sheridan MJ, Nichols R, Harvey WP, Waller BF: **Development and progression of aortic valve stenosis: Atherosclerosis risk factors--a causal relationship? A clinical morphologic study.** *Clin Cardiol* 1991;**14**:995-999.
309. Honda S, Miyamoto T, Watanabe T, Narumi T, Kadowaki S, Honda Y, Otaki Y, Hasegawa H, Netsu S, Funayama A, Ishino M, Nishiyama S, Takahashi H, Arimoto T, Shishido T, Miyashita T, Kubota I: **A novel mouse model of aortic valve stenosis induced by direct wire injury.** *Arteriosclerosis, Thrombosis, and Vascular Biology* 2014;**34**:270-278.

310. Miller JD, Weiss RM, Heistad DD: **Calcific aortic valve stenosis: Methods, models, and mechanisms.** *Circ Res* 2011;**108**:1392-1412.
311. Cheek JD, Wirrig EE, Alfieri CM, James JF, Yutzey KE: **Differential activation of valvulogenic, chondrogenic, and osteogenic pathways in mouse models of myxomatous and calcific aortic valve disease.** *Journal of Molecular and Cellular Cardiology*;52:689-700.
312. Rajamannan NM: **Oxidative-mechanical stress signals stem cell niche mediated lrp5 osteogenesis in enos(-/-) null mice.** *J Cell Biochem* 2012;**113**:1623-1634.
313. Schmittgen TD: **Regulation of microRNA processing in development, differentiation and cancer.** *Journal of cellular and molecular medicine* 2008;**12**:1811-1819.
314. Metcalf JL, Bradshaw PS, Komosa M, Greer SN, Stephen Meyn M, Ohh M: **K63-ubiquitylation of vhl by socs1 mediates DNA double-strand break repair.** *Oncogene* 2014;**33**:1055-1065.
315. Stickle NH, Chung J, Klco JM, Hill RP, Kaelin WG, Jr., Ohh M: **Pvhl modification by nedd8 is required for fibronectin matrix assembly and suppression of tumor development.** *Mol Cell Biol* 2004;**24**:3251-3261.
316. Sun L, Rajamannan NM, Sucosky P: **Defining the role of fluid shear stress in the expression of early signaling markers for calcific aortic valve disease.** *PLoS One* 2013;**8**:e84433.
317. Cappelli S, Epistolato MC, Vianello A, Mazzone A, Glauber M, Franzini M, Ottaviano V, Pompella A, Paolicchi A, Tanganelli P: **Aortic valve disease and gamma-glutamyltransferase: Accumulation in tissue and relationships with calcific degeneration.** *Atherosclerosis* 2010;**213**:385-391.
318. Kumar S, Kim CW, Simmons RD, Jo H: **Role of flow-sensitive microRNAs in endothelial dysfunction and atherosclerosis: Mechanosensitive athero-mirs.** *Arteriosclerosis, Thrombosis, and Vascular Biology* 2014;**34**:2206-2216.
319. Guo HL, Ingolia NT, Weissman JS, Bartel DP: **Mammalian microRNAs predominantly act to decrease target mrna levels.** *Nature* 2010;**466**:835-U866.
320. Zhang M, Liu X, Zhang X, Song Z, Han L, He Y, Xu Z: **Microrna-30b is a multifunctional regulator of aortic valve interstitial cells.** *The Journal of Thoracic and Cardiovascular Surgery* 2014;**147**:1073-1080.e1072.
321. Vandooren J, Geurts N, Martens E, Van den Steen PE, Jonghe SD, Herdewijn P, Opdenakker G: **Gelatin degradation assay reveals mmp-9 inhibitors and function of o-glycosylated domain.** *World J Biol Chem* 2011;**2**:14-24.
322. Balachandran K, Sucosky P, Jo H, Yoganathan AP: **Elevated cyclic stretch alters matrix remodeling in aortic valve cusps: Implications for degenerative aortic valve disease.** *American journal of physiology Heart and circulatory physiology* 2009;**296**:H756-764.
323. Stephens EH, Grande-Allen KJ: **Age-related changes in collagen synthesis and turnover in porcine heart valves.** *The Journal of heart valve disease* 2007;**16**:672-682.
324. Schonbeck U, Mach F, Sukhova GK, Atkinson E, Levesque E, Herman M, Graber P, Basset P, Libby P: **Expression of stromelysin-3 in atherosclerotic lesions:**

- Regulation via cd40-cd40 ligand signaling in vitro and in vivo.** *The Journal of experimental medicine* 1999;**189**:843-853.
325. Soumyarani VS, Jayakumari N: **Oxidatively modified high density lipoprotein promotes inflammatory response in human monocytes-macrophages by enhanced production of ros, tnf-alpha, mmp-9, and mmp-2.** *Molecular and cellular biochemistry* 2012;**366**:277-285.
326. Uzui H, Harpf A, Liu M, Doherty TM, Shukla A, Chai NN, Tripathi PV, Jovinge S, Wilkin DJ, Asotra K, Shah PK, Rajavashisth TB: **Increased expression of membrane type 3-matrix metalloproteinase in human atherosclerotic plaque: Role of activated macrophages and inflammatory cytokines.** *Circulation* 2002;**106**:3024-3030.
327. Cheung PY, Sawicki G, Wozniak M, Wang W, Radomski MW, Schulz R: **Matrix metalloproteinase-2 contributes to ischemia-reperfusion injury in the heart.** *Circulation* 2000;**101**:1833-1839.
328. Alfonso-Jaume MA, Bergman MR, Mahimkar R, Cheng S, Jin ZQ, Karliner JS, Lovett DH: **Cardiac ischemia-reperfusion injury induces matrix metalloproteinase-2 expression through the ap-1 components fosb and junb.** *American journal of physiology Heart and circulatory physiology* 2006;**291**:H1838-1846.
329. Perrotta I, Russo E, Camastra C, Filice G, Di Mizio G, Colosimo F, Ricci P, Tripepi S, Amorosi A, Triumbari F, Donato G: **New evidence for a critical role of elastin in calcification of native heart valves: Immunohistochemical and ultrastructural study with literature review.** *Histopathology* 2011;**59**:504-513.
330. Yip CY, Chen JH, Zhao R, Simmons CA: **Calcification by valve interstitial cells is regulated by the stiffness of the extracellular matrix.** *Arteriosclerosis, thrombosis, and vascular biology* 2009;**29**:936-942.
331. Fan D, Takawale A, Basu R, Patel V, Lee J, Kandalam V, Wang X, Oudit GY, Kassiri Z: **Differential role of timp2 and timp3 in cardiac hypertrophy, fibrosis, and diastolic dysfunction.** *Cardiovascular research* 2014;**103**:268-280.
332. Wang B, Hsu SH, Majumder S, Kutay H, Huang W, Jacob ST, Ghoshal K: **Tgfbeta-mediated upregulation of hepatic mir-181b promotes hepatocarcinogenesis by targeting timp3.** *Oncogene* 2010;**29**:1787-1797.
333. Feinberg MW, Moore KJ: **Microrna regulation of atherosclerosis.** *Circulation research* 2016;**118**:703-720.
334. Sun X, Lin J, Zhang Y, Kang S, Belkin N, Wara AK, Icli B, Hamburg NM, Li D, Feinberg MW: **Microrna-181b improves glucose homeostasis and insulin sensitivity by regulating endothelial function in white adipose tissue.** *Circulation research* 2016;**118**:810-821.
335. Cao Q, Li YY, He WF, Zhang ZZ, Zhou Q, Liu X, Shen Y, Huang TT: **Interplay between micrornas and the stat3 signaling pathway in human cancers.** *Physiological genomics* 2013;**45**:1206-1214.
336. Chen YX, Zhang M, Cai Y, Zhao Q, Dai W: **The sirt1 activator srt1720 attenuates angiotensin ii-induced atherosclerosis in apoe(-)/(-) mice through inhibiting vascular inflammatory response.** *Biochemical and biophysical research communications* 2015;**465**:732-738.

337. Tsoyi K, Jang HJ, Nizamutdinova IT, Park K, Kim YM, Kim HJ, Seo HG, Lee JH, Chang KC: **Pten differentially regulates expressions of icam-1 and vcam-1 through pi3k/akt/gsk-3beta/gata-6 signaling pathways in tnf-alpha-activated human endothelial cells.** *Atherosclerosis* 2010;**213**:115-121.
338. Garbacki N, Di Valentin E, Huynh-Thu VA, Geurts P, Irrthum A, Crahay C, Arnould T, Deroanne C, Piette J, Cataldo D, Colige A: **Micrnas profiling in murine models of acute and chronic asthma: A relationship with mrnas targets.** *PLOS ONE* 2011;**6**:e16509.
339. Kim WT, Jeong P, Yan C, Kim YH, Lee I-S, Kang H-W, Kim Y-J, Lee S-C, Kim SJ, Kim YT, Moon S-K, Choi Y-H, Kim IY, Yun SJ, Kim W-J: **Ube2c cell-free rna in urine can discriminate between bladder cancer and hematuria.** *Oncotarget* 2016;**7**:58193-58202.
340. Somers P, Knaapen M, Kockx M, van Cauwelaert P, Bortier H, Mistiaen W: **Histological evaluation of autophagic cell death in calcified aortic valve stenosis.** *The Journal of heart valve disease* 2006;**15**:43-47; discussion 48.
341. Semenza GL: **Targeting hif-1 for cancer therapy.** *Nature reviews Cancer* 2003;**3**:721-732.
342. Gao L, Chen Q, Zhou X, Fan L: **The role of hypoxia-inducible factor 1 in atherosclerosis.** *J Clin Pathol* 2012;**65**:872-876.
343. Feng S, Bowden N, Fragiadaki M, Souilhol C, Hsiao S, Mahmoud M, Allen S, Pirri D, Ayllon BT, Akhtar S, Thompson AAR, Jo H, Weber C, Ridger V, Schober A, Evans PC: **Mechanical activation of hypoxia-inducible factor 1 α drives endothelial dysfunction at atheroprone sites.** *Arteriosclerosis, Thrombosis, and Vascular Biology* 2017;**37**:2087-2101.
344. Sudip D, Peter H, T. MB, J. MG: **Endothelial to mesenchymal transformation is induced by altered extracellular matrix in aortic valve endothelial cells.** *Journal of Biomedical Materials Research Part A* 2017;**105**:2729-2741.
345. Smeringaiova I, Reinstein Merjava S, Stranak Z, Studeny P, Bednar J, Jirsova K: **Endothelial wound repair of the organ-cultured porcine corneas.** *Current Eye Research* 2018;**43**:856-865.
346. Dekker RJ, Boon RA, Rondaij MG, Kragt A, Volger OL, Elderkamp YW, Meijers JCM, Voorberg J, Pannekoek H, Horrevoets AJG: **Klf2 provokes a gene expression pattern that establishes functional quiescent differentiation of the endothelium.** *Blood* 2006;**107**:4354-4363.
347. Meeks JJ, Shilatifard A: **Multiple roles for the mll/compass family in the epigenetic regulation of gene expression and in cancer.** *Annual Review of Cancer Biology* 2017;**1**:425-446.
348. Lee HJ, Diaz MF, Price KM, Ozuna JA, Zhang S, Sevic-Muraca EM, Hagan JP, Wenzel PL: **Fluid shear stress activates yap1 to promote cancer cell motility.** *Nat Commun* 2017;**8**:14122.
349. Gošev I, Zeljko M, Đurić Ž, Nikolić I, Gošev M, Ivčević S, Bešić D, Legčević Z, Paić F: **Epigenome alterations in aortic valve stenosis and its related left ventricular hypertrophy.** *Clinical Epigenetics* 2017;**9**:106.
350. Garnett MJ, Mansfeld J, Godwin C, Matsusaka T, Wu J, Russell P, Pines J, Venkitaraman AR: **Ube2s elongates ubiquitin chains on apc/c substrates to promote mitotic exit.** *Nature cell biology* 2009;**11**:1363-1369.

351. Lee J-W, Bae S-H, Jeong J-W, Kim S-H, Kim K-W: **Hypoxia-inducible factor (hif-1)[alpha]: Its protein stability and biological functions.** *Exp Mol Med* 0000;**36**:1-12.
352. Balachandran K, Sucosky P, Jo H, Yoganathan AP: **Elevated cyclic stretch induces aortic valve calcification in a bone morphogenic protein-dependent manner.** *The American journal of pathology* 2010;**177**:49-57.
353. Bertero T, Gastaldi C, Bourget-Ponzio I, Mari B, Meneguzzi G, Barbry P, Ponzio G, Rezzonico R: **Cdc25a targeting by mir-483-3p decreases ccnd-cdk4/6 assembly and contributes to cell cycle arrest.** *Cell Death Differ* 2013;**20**:800-811.
354. Pepe F, Pagotto S, Soliman S, Rossi C, Lanuti P, Braconi C, Mariani-Costantini R, Visone R, Veronese A: **Regulation of mir-483-3p by the o-linked n-acetylglucosamine transferase links chemosensitivity to glucose metabolism in liver cancer cells.** *Oncogenesis* 2017;**6**:e328.
355. Penas C, Ramachandran V, Ayad N: **The apc/c ubiquitin ligase: From cell biology to tumorigenesis.** *Frontiers in Oncology* 2012;**1**.
356. Zhou Z, He M, Shah AA, Wan Y: **Insights into apc/c: From cellular function to diseases and therapeutics.** *Cell Division* 2016;**11**:9.
357. McLean JR, Chaix D, Ohi MD, Gould KL: **State of the apc/c: Organization, function, and structure.** *Critical reviews in biochemistry and molecular biology* 2011;**46**:118-136.
358. Bavi P, Uddin S, Ahmed M, Jehan Z, Bu R, Abubaker J, Sultana M, Al-Sanea N, Abduljabbar A, Ashari LH, Alhomoud S, Al-Dayel F, Prabhakaran S, Hussain AR, Al-Kuraya KS: **Bortezomib stabilizes mitotic cyclins and prevents cell cycle progression via inhibition of ube2c in colorectal carcinoma.** *The American journal of pathology* 2011;**178**:2109-2120.
359. Lin J, Raof DA, Wang Z, Lin MY, Thomas DG, Greenson JK, Giordano TJ, Orringer MB, Chang AC, Beer DG, Lin L: **Expression and effect of inhibition of the ubiquitin-conjugating enzyme e2c on esophageal adenocarcinoma.** *Neoplasia* 2006;**8**:1062-1071.
360. Jung C-R, Hwang K-S, Yoo J, Cho W-K, Kim J-M, Kim WH, Im D-S: **E2-epf ucp targets pvhl for degradation and associates with tumor growth and metastasis.** *Nature medicine* 2006;**12**:809-816.
361. Park K-S, Kim JH, Shin HW, Chung K-S, Im D-S, Lim JH, Jung C-R: **E2-epf ucp regulates stability and functions of missense mutant pvhl via ubiquitin mediated proteolysis.** *BMC Cancer* 2015;**15**:800.
362. Eltzschig HK, Bratton DL, Colgan SP: **Targeting hypoxia signalling for the treatment of ischaemic and inflammatory diseases.** *Nature reviews Drug discovery* 2014;**13**:852-869.
363. Diaz-Gonzalez JA, Russell J, Rouzaut A, Gil-Bazo I, Montuenga L: **Targeting hypoxia and angiogenesis through hif-1alpha inhibition.** *Cancer Biol Ther* 2005;**4**:1055-1062.
364. Bonachea EM, Chang S-W, Zender G, LaHaye S, Fitzgerald-Butt S, McBride KL, Garg V: **Gata5 sequence variants identified in individuals with bicuspid aortic valve.** *Pediatric research* 2014;**76**:211-216.

365. Bonachea EM, Chang S-W, Zender G, LaHaye S, Fitzgerald-Butt S, McBride KL, Garg V: **Rare gata5 sequence variants identified in individuals with bicuspid aortic valve.** *Pediatric research* 2014;**76**:211.
366. Giusti B, Sticchi E, De Cario R, Magi A, Nistri S, Pepe G: **Genetic bases of bicuspid aortic valve: The contribution of traditional and high-throughput sequencing approaches on research and diagnosis.** *Frontiers in Physiology* 2017;**8**:612.
367. Messaoudi S, He Y, Gutsol A, Wight A, Hébert RL, Vilmundarson RO, Makrigiannis AP, Chalmers J, Hamet P, Tremblay J, McPherson R, Stewart AFR, Touyz RM, Nemer M: **Endothelial gata5 transcription factor regulates blood pressure.** *Nature Communications* 2015;**6**:8835.
368. van Ree JH, Jeganathan KB, Malureanu L, van Deursen JM: **Overexpression of the e2 ubiquitin–conjugating enzyme ubch10 causes chromosome missegregation and tumor formation.** *The Journal of cell biology* 2010;**188**:83-100.